UCLouvain

epl

École polytechnique de Louvain

Polymerisation of Glycidyl Methacrylate Resin Modified with Unsaturated Polyester from Recycled PET

Analysis and optimisation of the resin and its curing process

Author: **Célia FORET**
Supervisor: **Thomas PARDOEN**
Readers: **Christian BAILLY, Bernard NYSTEN, Martial KUETE**
Academic year 2021–2022
Master [120] in Chemical and Materials Engineering

Acknowledgments

I would like to thank the various people involved with this thesis. Initially, I would like to thank Professor Thomas Pardoen and Professor Christian Bailly for supervising this thesis. A special thank to Professor Bailly for following my work and for his expertise, ideas and advisement. I would also like to thank Professor Bernard Nysten for welcoming me into the Bio and Soft Matter Department and providing me access to all the equipments and resources.

I would like to thank Mr. Martial Kuete for his continuous guidance and help, especially for the traction and compression tests and for all the time spent on this work. Thank you to Mr. Wael Ballout and Mr. Pascal Van Lethem for their help for the SEM analysis, but also for their ideas, feedback, and for their warm welcome into the lab. Thank you to Mr Baptiste Lambert for the collaborative help during this semester.

I would also like to address my gratitude to Mrs. Colette Douchamps for her precious help with the orders, to Mrs Sabine Bebelman for her valuable assistance with the FTIR and Raman analysis, to Mr. Alban Maton and the IMMC department for the preparation of the samples for the mechanical tests.

Finally, I would like to thank my family and friends for their help and support. Thank you to Clémence Vanhal and to my dear grandma Carol Thompson for their feedback on my writing. A special thank to my parents. This thesis marks the end of six years of study that would not have been possible without their constant support, patience and encouragements.

Abstract

Environmental concerns regarding the increase in solid waste and its impact on greenhouse gas emissions have been growing in the recent years. The improvement of recycling and the production of biosourced materials are well-known solutions in the research industry. Glycidyl methacrylate (GMA) in particular, is a bifunctional epoxy resins that can be biosourced. Modification of GMA with unsaturated polyester (UP) from recycled PET is used to form a denser network and increase the mechanical properties of GMA resins. Bottle grade PET is recycled via glycolysis with diol (1,3-propanediol or 2-methyl-1,3-propanediol). UP is synthesised from recycled PET, citraconic anhydride and diol. Semi-crystalline UP (UPsc) is obtained from 1,3-propanediol and amorphous UP (UPam) from 2-methyl-1,3-propanediol. Both UPs are characterised by a double C=C bond and -OH and -COOH end chains. The first curing step forms a 2D-network by radical polymerisation of the ethylene bonds of GMA and UP. The second step is the opening of the oxirane group via ring-opening mechanism with the UP end chains. Polymerisation is initiated with benzoyl peroxide and accelerated with N,N-dimethylaniline. Characterisation methods used in this work were thermal (DSC, TGA), spectroscopic (FTIR, Raman), surface (microscopy) and mechanical (traction) analysis. These methods were used to analyse UPsc, UPam and GMA, to understand the polymerisation mechanism, to establish a suitable curing cycle and to optimise the system. The optimised curing cycle of the resin was evaluated to be a first step of gelation at 45℃ for 6 hours, a cure at 100℃ for 2 hours and a post-cure at 180℃ for 1 hour. Amorphous UP manifested better thermal and mechanical properties than semi-crystalline UP. The system shows environmental and economic interest by valorising the POST-C PET and producing a biosourced material.

Contents

Introduction **1**

1 Literature review **3**
1.1 Polymerisation mechanisms . . . 3
1.1.1 Chain polymerisation . . . 3
1.1.2 Step-growth polymerisation . . . 14
1.1.3 Ring-Opening Polymerisation . . . 17
1.2 Polyethylene terephthalate (PET) . . . 18
1.2.1 Synthesis of PET . . . 18
1.2.2 Processing methods . . . 20
1.2.3 Properties of PET . . . 20
1.3 Recycling of PET . . . 23
1.3.1 Categories of recycling . . . 23
1.3.2 Unsaturated polyester from recycled PET . . . 29
1.4 Epoxy resins . . . 32
1.4.1 Properties and applications . . . 32
1.4.2 Synthesis . . . 32
1.4.3 Curing . . . 33
1.4.4 Physical phenomenon during curing . . . 35
1.5 Glycidyl methacrylate (GMA) . . . 36
1.5.1 Synthesis . . . 36
1.5.2 Properties . . . 37
1.5.3 Reactivity of GMA . . . 37

2 Materials and methods **44**
2.1 Materials . . . 44
2.2 Methods . . . 45
2.2.1 Preparation of PET . . . 45
2.2.2 Depolymerisation by glycolysis . . . 49
2.2.3 Repolymerisation . . . 51
2.2.4 Curing of resins . . . 53

2.3 Characterisation methods 56
2.3.1 Thermal analysis 56
2.3.2 Spectroscopic methods of analysis 60
2.3.3 Characterisation and analysis of polymer surface 62
2.3.4 Mechanical properties 63

3 Results and discussion **65**
3.1 Chemical modification of PET 65
3.1.1 Extrusion and grinding 66
3.1.2 Depolymerisation by glycolysis and repolymerisation into unsaturated polyester (UP) 68
3.2 Polymerisation and thermal degradation mechanism of glycidyl methacrylate 72
3.2.1 Spectroscopic characterisation 72
3.2.2 Thermal characterisation 73
3.3 Polymerisation mechanism of UP/GMA resin 75
3.3.1 Influence of benzoyl peroxide content on polymerisation kinetic 75
3.3.2 Influence of heating rate on the kinetic of polymerisation . . 77
3.3.3 Evaluation of polymerisation mechanism 79
3.4 Determination of curing cycle of the resin 85
3.4.1 Study of gelation conditions 86
3.4.2 Analysis of the thermal stability during curing 87
3.4.3 Modifications of curing cycle 89
3.5 Optimisation of the curing 91
3.5.1 Modification of the mixing during preparation of the samples to cure 91
3.5.2 Use of an accelerator 92
3.5.3 Utilisation of amorphous UP 94
3.6 Evaluation of mechanical properties of the resins 96

4 Conclusion and perspectives **98**

Appendix **111**
A Experiments 111
A.1 Depolymerisation of PET 111
A.2 Repolymerization of GPET into UP 112
A.3 Cured resins 113
A.4 SEM images of GMA and UP/GMA resins with UPsc and UPam 113

List of Tables

1.1 Chemical formula and characteristics of a) N,N-dimethylaniline b) N,N-diethylaniline c) N,N-dimethyl-*p*-toluidine [17] 11
1.2 Physical and mechanical properties of PET [25, 27]. 22
1.3 Parameters of the different chemical recycling methods [24, 32]. . . 28
1.4 Main properties of GMA [52]. 37

2.1 Parameters of the Process 11 Parallel Twin-screw Extruder used for the extrusion of synthetic PET pellets 47
2.2 Parameters for the chemicals used in the glycolysis reaction 49
2.3 Masses of the chemicals used in the repolymerisation reaction . . . 51
2.4 Wavelengths associated to chemical functions in polymers [43, 47, 55, 59, 63, 86, 87, 88] 61

3.1 Results from the DSC curve in Figure 3.3. The values are averaged over three analysis. 67
3.2 Results from the DSC curves in Figure 3.6. The values are averaged over three analysis. 70
3.3 Mass concentrations of the two systems used for the experiments. *Proportions of BPO are given in % of the weight of the UP/GMA mixture 75
3.4 Results from the DSC curves in Figure 3.11. 76
3.5 Results from the DSC curves in Figure 3.13 78
3.6 Summary of the different mechanisms in the UP/GMA reaction with temperature. 85
3.7 Loss of mass of UP/GMA sample for different gel temperatures . . 88
3.8 Results from the DSC curve in Figure 3.35. 95
3.9 Modulus at 30°C of each sample. 97

List of Figures

1.1 Chemical formula of benzoyl peroxide 8
1.2 Reduction–oxidation process of benzoylperoxide (BPO) caused by N,N-dimethylaniline, adapted from [19]. 12
1.3 PET repeating unit (with the ester function represented in purple) . 18
1.4 Reactions occurring in the synthesis of PET. 1a: esterification, 1b: trans-esterification, 2: polycondensation. 19
1.5 Conventional DSC curve of PET [31] 21
1.6 Resin symbol of polyethylene terephthalate 23
1.7 Categories of polymers recycling 24
1.8 Solvolysis methods for PET depolymerisation. 1: hydrolysis (neutral, basic, acidic), 2: methanolysis, 3: glycolysis, 4: ammonolysis and 5: aminolysis. 27
1.9 (a) Epoxide and (bà oxirane groups 32
1.10 Chemical structure of glycidyl methacrylate 36
1.11 Homopolymerisation of GMA into pGMA 38
1.12 FTIR spectra of (a) virgin PP, (b) GMA-soaked PP (step 1, sample A), (c) PP-g-GMA (step 2, sample A, 1 h thermal treatment), (d) PP-g-GMA (step 2, sample A, 4 h thermal treatment), and (e) PP-g-GMA (sample B, 4 h thermal treatment) from GMA grafting on PP studied by Kunita et al. [59] 39
1.13 Synthesis methodology of dual-curing polymer network systems implemented by Zhang and coworkers [65] 40
1.14 Schematic representation of reaction between PET end-groups and GMA grafted onto PP backbone, as studied by Jazani and coworkers [55] 41
1.15 Autoacceleration in benzoyl peroxide–initiated polymerisation of methyl methacrylate in benzene at 50℃. [14] 42
1.16 Grafting of GMA onto PET sheet with UV radiation time [54]. . . . 43

2.1 Samples of (a) synthetic PET (b) extruded and pelletised PET (c) grinded PET 45
2.2 Cross section of a single screw extruder [71] 46

2.3 Thermo Scientific^{TM} Process 11 Parallel Twin-screw Extruder. . . . 47
2.4 Thermo Scientific^{TM} VariCut Pelletizer 47
2.5 Variable Speed Rotor Mill Pulverisette 14 48
2.6 Operating principles of the grinding process (a) feeding (b) powdering (adapted from [72]). 49
2.7 Reaction of glycolysis: transesterification with 1,3-propanediol . . . 50
2.8 Reaction of repolymerisation from PET oligomers with citraconic anhydride as crosslinker and 1,3-propanediol. 52
2.9 Vaccuum pump chamber 53
2.10 Polymerisation of GMA resin with UP using benzoyl peroxide as initiator 54
2.11 Summary of the recycling process of a bottle of PET into a UP/GMA resin. 55
2.12 Schematic representation of a DSC device. Adaptated from [75]. . . 56
2.13 Conventional DSC curve of semicrystalline polymer showing the typical steps: (1) Initial deflection proportional to the heat capacity of the sample, (2) change of c_p with no other thermal effect, (3) glass transition of amorphous fraction, (4) cold crystallisation and (5) melting of the crystalline fraction [76]. 57
2.14 Schematic representation of a TGA device [79]. 59
2.15 Conventional TGA curve of a polymer showing the typical mass loss steps: (1) volatile compounds, (2) polymer decomposition, (3) change of atmosphere, (4) burning step of carbon and (5) residues [80]. 59
2.16 Schematic representation of a FTIR device [85] 61
2.17 Schematic representation of a SEM device [82] 63

3.1 First POST-C bottle analysed. 66
3.2 Second POST-C bottle analysed. 66
3.3 Normalised DSC second heating curves of PET after its modification through extrusion and grinding. PET lighter C88 is the industrial and synthetic PET. PET ext-grind is the PET after extrusion and grinding. POST-C PET (1) and (2) are waste PET from used bottle. 67
3.4 Chemical formula of (a) semi-crystalline UP synthesised with citraconic anhydride and 1,3-propanediol (b) amorphous UP synthesised with citraconic anhydride and 2-methylpropane-1,3-diol. 68
3.5 Samples of (a) semi-crystalline (b) amorphous unsaturated polyester. 69

3.6 Normalised DSC curves of PET during the different stages leading to unsaturated polyester. PET extruded is the PET after extrusion and grinding. GPET is the PET depolymerised through glycolysis. UPam and UPsc are the repolymerised PET through esterification with citraconic anhydride and 1,3-propanediol (PD) or 2-methyl-1,3-propanediol (MPD) respectively. 69
3.7 FTIR spectra of PET, PET depolymerized with PD (GPET1), PET depolymerised with MPD (GPET2), semi-crystalline UP (UP sc) and amorphous UP (UP am), normalised at 1951 cm^{-1}. 71
3.8 Raman spectra of crude and cured glycidyl methacrylate containing 1 wt% of benzoyl peroxide, normalised with the peak in 1726 cm^{-1}. 72
3.9 Normalised DSC curve of GMA initiated by benzoyl peroxide. A)s start of the reaction B) acceleration of the reaction C) Peak temperature D) Effet Trommsdorf. 73
3.10 TGA curve curve of GMA initiated by benzoyl peroxide. 74
3.11 Normalised DSC curves for UP/GMA resins with 0.2 and 1 wt% of benzoyl peroxide heated from room temperature to 280℃ at 10$Kmin^{-1}$. 76
3.12 Kinetic of polymerisation for resin containing 0.2 and 1 wt% of benzoyl peroxide. 77
3.13 Normalised DSC curves for UP/GMA resins heated at different rates: 2.5, 5, 10 and 20K/min^{-1} 78
3.14 Conversion of reaction for different heating rates: 2.5, 5, 10 and 20$Kmin^{-1}$ 79
3.15 Reaction mechanism of epoxy opening with -OH end chains of UP, producing (a) ether and (b) ester groups. 80
3.16 Raman spectra of UP/GMA resins heated to temperatures ranging from 80 to 150℃, normalised with the aromatic peak in 1610 cm^{-1}. 80
3.17 Conversion of the ethylenic function of glycidyl methacrylate (at 1640 cm^{-1}) with temperature. 81
3.18 FTIR spectra of UP/GMA resins heated to temperatures ranging from 80 to 250℃ normalised with the peak in 1953 cm^{-1} 82
3.18 FTIR spectra of (a) the hydroxyl end groups -OH at 3550 cm^{-1} (b) the acid end groups -COOH at 3270 cm^{-1} (c) the ether -R-C-O-O-R' group around 1015 cm^{-1} and ester -C-O-H group at 1040 cm^{-1} (d) the epoxy functions between 845 and 910 cm^{-1} 83
3.19 Evolution with temperature of hydroxyl (-OH) and carboxyl (-COOH) groups and epoxy rings 84
3.20 Curing cycle 1. 86
3.21 Resin cured with different gel temperatures. 87
3.22 TGA curves of GMA and the mixture UP/GMA 87

3.23 TGA curves of UP/GMA mixture showing different gel temperatures and the resulting mass loss. 88
3.24 Curing cycle 2. 89
3.25 Resins curing with cycle 2 and with 5 wt% and 10 wt% of UP. B = phase change, C = cavities/bubbles. 89
3.26 Curing cycle 3. 90
3.27 Resins curing with cycle 3 and with 0, 5 and 10 wt% of UP. B = phase change, C = cavities/voids. 90
3.28 UP/GMA mixture containing 1wt% of UP and 1 wt% of BPO after mixing at 80℃ for 90 minutes. 91
3.29 UP/GMA mixture containing 1wt% of UP and 1 wt% of BPO after degassing. 91
3.30 UP/GMA resins containing (a) 100wt% GMA, (b) 1wt% UP, (c) 5wt% UP and (d) 10wt% UP. B = phase change, C= cavities/voids 92
3.31 Curing cycle 4 93
3.32 Resins 1-2-5% UP with 0,1% dimethlaniline 93
3.33 Resin with 5% UP amorphous - 0.1% dimethylaniline 94
3.34 Resin with 10% UP amorphous - 0.1% dimethylaniline 94
3.35 Normalised DSC curves of the second heating of different sample of UP/GMA resins. 95
3.36 Evolution of the resins T_g with UP mass proportion 95
3.37 (a) Storage and (b) loss modulus for different resins of UP and GMA. 96
3.38 Complex modulus E^* of the different resins at 30℃. 97

4.1 Slurring with methanol 111
4.2 Glycolysis of PET and PD 111
4.3 Grinding of depolymerised PET 111
4.4 Solubilisation of BHET in hot water. 111
4.5 Decantation of GPET. 111
4.6 Filtration of BHET. 111
4.7 Polycondensation reaction with CA and PD. 112
4.8 Solubilisation in dichloromethane. 112
4.9 Precipitation in methanol. 112
4.10 Curing of resin with 40% of UP, 60% of GMA and 0.2% of BPO as initiator 113
4.11 Images obtained from SEM analysis on GMA samples. (a) sample surface (polished) (b) side of the sample (non-polished) 113
4.12 Images obtained from SEM analysis on UP/GMA samples. (a) 5 wt% UPsc (b) 10 wt% UPsc. 114

4.13 Images obtained from SEM analysis on resin samples with 5 wt% of UPam. (a) sample surface (polished) (b) side of the sample (non-polished) 114

List of Acronyms

ATRP	Atom Transfer Radical Polymerization
BHET	Bis(hydroxyethyl) Terephtalate
BPO	Benzoyl Peroxide
CRP	Controlled Radical Polymerization
DSC	Differential Scanning Calorimetry
DEG	Diethylene glycol
DMA	Dynamic Mechanical Analysis
DMT	Dimethyl Terephtalate
DP	Degree of Polymerisation
EG	Ethylene Glycol
FRP	Free-radical polymerization
FTIR	Fourier-Transform Infrared Spectroscopy
GMA	Glycidyl Methacrylate
GPET	Glycolysed oligomers of PET
HDPE	High-Density Polyethylene
LDPE	Low-Density Polyethylene
LHV	Low heating value
LLDPE	Linear Low-Density Polyethylene
MA	Maleic anhydride
MPD	2-methylpropane-1,3-diol
NIR	Near-Infrared
PE	Polyethylene
PET(E)	Polyethylene Terephtalate
PG	Propylene glycol
pGMA	Poly(glycidyl methacrylate)

POST-C	Post-consumer
PP	Polypropylene
PVC	Polyvinylchloride
ROP	Ring-opening Polymerisation
r-PET	Recycled PET
r.u.	repeating unit
SEM	Scanning Electron Microscopy
SSP	Solid state polymerization
TEG	Triethylene glycol
TGA	Thermogravimetric analysis
TLV	Threshold Limit Value
TPA	Terephtalic acid
UM	Unsaturated Monomer
UP	Unsaturated Polyester
UPR	Unsaturated Polyester Resin
UV	Ultra-violet
VMS VOC's	Volatiles Organic Compounds

List of Symbols

Thermal properties

ΔH	Enthalpy
ΔH_c	Enthalpy of crystallisation
ΔH_m	Latent heat of melting (enthalpy of fusion)
ΔH_r	Enthalpy of reaction
ΔH_f^o	Melting enthalpy of a pure crystalline sample
c_p	Heat capacity
T	Temperature
T_g	Glass transition temperature
T_m	Melting temperature
T_c	Cold crystallisation temperature

Mechanical and physical properties

ρ	(Bulk) Density
σ	Tensile strength
$\tan\delta$	Damping factor
E	Tensile modulus
E'	Storage modulus
E''	Loss modulus

Other symbols

M_w	Molecular weight
m	Mass
p	Pressure
χ_c	Degree of crystallinity

Introduction

Climate change is an everyday challenge faced by our society. The waste sector in particular is climbing the environmental agenda. Waste contributes directly to greenhouse gas emissions such as CO_2, CH_4 and N_2O emissions [1]. About 1.6 billion tonnes of CO_{2eq} emissions were produced from solid waste in 2016, representing 5% of global emissions. Despite recent legislations, its generation has been constantly increasing and is expected to rise up to 2.6 billion tonnes of CO_{2eq} by 2050 [2].

Plastic largely contributes to these emissions as it represents about 12% of the global solid waste [2]. There is an urgent need to promote plastic circularity by increasing and improving recycling. Plastic recyclates are valuable raw materials and can optimise the use of resources. In 2021 in Europe, 34.6% of post-consumer plastic was sent to recycling. More than 99.8% of this fraction was recycled through mechanical methods while only 0.2% was sent for chemical recycling [3]. If mechanical recycling has proved effective in producing reused materials, it has limitations in terms of use, quality and durability of the recycled material [4]. Chemical recycling, and especially solvolysis, is a great alternative as it recovers clean and useful monomers and oligomers.

Polyethylene terephtalate (PET) is one of the five most important plastics in terms of plastic demand [3]. It is mainly used in the packaging industry, such as beverage bottles and containers. Post-consumer PET (POST-C PET) can be chemically recycled by solvolysis using different techniques depending on the solvent used. The recovered products can be used to synthesise other materials, such as unsaturated polyesters. These are produced by polycondensation with a diol and an acid (or anhydride) to introduce an unsaturated bond. This bond can further react with other species via radical polymerisation to produce harder materials.

Following the need to decrease materials impact on the environment, researches have been conducted regarding the development of bio-based materials such as biosourced resins. In particular, glycidyl methacrylate is a dual-functional monomer

with both epoxy and methacrylate functionalities and can be biosourced. The advantage of such system is the possibility of polymerisation via reactive sites on the ethylenic bond and of network formation via epoxy ring-opening [5]. Glycidyl methacrylate is used in coating, adhesive and dental applications [6]. It polymerises quickly into pGMA via its ethylenic bond, but necessitates specific functional groups (nucleophilic, acid or basic) to open its epoxy rings [7].

The objective of this master thesis is to produce a biosourced materials with good mechanical properties. The curing of GMA is optimised by synthesis of a GMA resin modified with unsaturated polyester from recycled polyethylene terephtalate (PET). The ethylenic bond of unsaturated polyester can react with those of GMA to form a 2D network. The hydroxyl (-OH) and carboxylic (-COOH) end groups of UP can then open the epoxy rings to form a 3D network. Synthesis of the resin starts by the recycling of PET into unsaturated polyester. PET is depolymerised with diols and zinc acetate dehydrate as catalyst. The glycolysed oligomers of PET (GPET) are repolymerised into UP with citraconic anhydride as crosslinker, diols as homogeniser and antimony oxide (Zb_2O_3) as catalyst. These monomers were chosen to reach specific properties for UP, such as T_g and crystallinity, and for their potential to be biosourced [8, 9, 10]. GPET and UP were analysed with thermal and spectroscopic methods to determine their structure and thermal properties.

The second step is to cure glycidyl methacrylate with unsaturated polyester, acting as a modifier and crosslinker, and with benzoyl peroxide and N-N,dimethylaniline as catalyst and accelerator. The cured system forms a 3D network. Different steps of curing were established. At moderate temperature, a radical polymerisation takes places, linking both ethylenic functions of GMA and UP. A gel is formed. At higher temperature, the epoxy group of GMA are opened with the hydroxyl and carboxyl group of UP to form a 3D network.

This work is separated in four sections. First, it introduces the main theoretical concepts used in the work and presents a literature review on UP resins and GMA polymerisation. The second section explains the materials, processing and characterisation methods covered in the study. The third part presents and discusses the results obtained from the thermal (DSC, TGA), spectroscopic (FTIR, Raman), surface (SEM, microscopy) and mechanical (DMA) analysis done to characterise the UPs and GMA, understand the polymerisation mechanism and find the best curing conditions for the resins. Finally, the fourth part summarises the main results of this study and the possible future prospects.

Chapter 1

Literature review

This first chapter has the purpose of presenting the main theoretical points addressed in this thesis. It explains the main different polymerisation mechanisms with their kinetic and some of their characteristics. It presents polyethylene terephtalate (PET) and its different methods of recycling, including its synthesis into unsaturated polyester resins. Epoxy resins and their curing mechanism, and glycidyl methacrylate (GMA) and its different methods of polymerisation are also described.

1.1 Polymerisation mechanisms

Polymerisation is "the process of converting a monomer or a mixture of monomers into a polymer" [11]. Different structures of molecules (linear, branched) can be obtained at the end of polymerisation reactions. These can be classified following their mechanism. The two fundamental ones are polyaddition and polycondensation. The main differences between the two processes are their kinetics and the production of by-products during the polycondensation. Addition polymerisation is referred as chain polymerisation since it consists in successive addition of saturated monomers units on an active centre through a chain reaction. Condensation reaction is referred as step(-growth) polymerisation because the polymer chain is formed progressively by random union of monomer molecules [12, 13].

1.1.1 Chain polymerisation

Chain-reaction polymerisation methods involve distinct kinetic steps : 1) initiation, where an active centre (R*) is created from a stable, non radical precursor, 2) propagation and growth, consisting in a successive addition of a mono or multifunctional monomer on the active centre at the chain end, and 3) termination

of the chain by deactivation. The monomers involved in the reaction can be unsaturated (vinyl or cyclic) monomers. Different types of chain reaction exist: free-radical polymerisation (FRP), copolymerisation, coordination polymerisation and ionic polymerisation. Free-radical polymerisation will be used to illustrate the mechanism of chain polymerisation. The three other types of reactions will be briefly introduced [12, 13, 14].

1.1.1.1 Free-radical polymerisation

Free-radical polymerisation is a type of chain-reaction polymerisation initiated by free-radicals in the presence of monomer. They are used to polymerise unsaturated monomers such as ethylene, α-olefins or vinyl compounds [12]. With more than 50% of all polymers produced in the world through FRP processes, it is a very important industrial polymerisation process in volume and in polymer variety. Different techniques are used for free-radical polymerisation : bulk, solution, suspension or emulsion polymerisation [13, 15].

a) Mechanism of polymerisation

As previously stated, chain polymerisation consists of three steps.

a.1) Initiation A pair of radicals (2 R·) is formed by the homolytic dissociation of an initiator (I) (most commonly a thermolabile compound). The initiator radical (R·) is added to an unsaturated monomer (M) by opening the π-bond. It is fixed at one end of the growing chain and forms a new radical (RM·) [12, 13].

$$\mathrm{I} \xrightarrow{\mathrm{k}_d} 2\mathrm{R}\cdot \tag{1.1}$$

$$\mathrm{R}\cdot + \mathrm{M} \xrightarrow{\mathrm{k}_i} \mathrm{RM}\cdot \tag{1.2}$$

k_d is the rate constant for the initiator dissociation and k_i for the addition reaction.

a.2) Propagation The reaction propagates by successive additions of many more monomers on the active centre and the transfer of the radical centre to the end monomer unit. The size of the chain increases and the propagation continues until a termination reaction occurs. The reactivity of the monomer depends on the steric hindrance of the substituents and the stabilisation of the free radical by resonance [12, 13].

$$\mathrm{RM}_{n-1}\cdot + \mathrm{M} \xrightarrow{\mathrm{k}_p} \mathrm{R(M)}_n\cdot \tag{1.3}$$

k_p is the rate constant of the termination reaction (assuming the reactivity constant with the chain length).

a.3) Termination The reaction terminates when the active centre is destroyed, i.e. when the chain-ends are inactivated or the monomer completely consumed. The polymer will take the term *dead polymer* [14]. Two main mechanism of propagation can occur: radical coupling (or combination) or disproportionation , or a combination of both [12, 13] . k_{tc} and k_{td} are their respective rate constants.

- **Radical coupling** : the two radicals combine to form an electron-pair (covalent) bond and the propagating chains are terminated.

$$\mathrm{RM}_n\cdot + \mathrm{RM}_n\cdot \xrightarrow{\mathrm{k_{tc}}} \mathrm{RM}_{(n+m)}\mathrm{R} \tag{1.4}$$

- **Disproportionation** : an atom is transferred from one chain to the other and forms two new molecules.

$$\mathrm{RM}_n\cdot + \mathrm{RM}_n\cdot \xrightarrow{\mathrm{k_{td}}} \mathrm{RM}_n + \mathrm{RM}_m \tag{1.5}$$

Secondary reactions can occur during free-radical polymerisation: chain transfer reaction (represented by equations (1.6) and (1.7)), or inhibition and delaying. In chain transfer reaction the reactivity is transferred from the growing polymer chain (RM_n) to other species. This can occur with polymer chain (inter-molecular and intra-molecular transfer), initiator and/or monomer, solvent or transfer agent (TB). Inhibition and delaying happen during a transfer reaction and lead to the formation of an inactive radical towards a more stable monomer than the growing radical polymer chain [13].

$$\mathrm{RM}_n\cdot + \mathrm{TB} \rightarrow \mathrm{RM}_n\mathrm{T} + \mathrm{B}\cdot \tag{1.6}$$

$$\mathrm{B}\cdot + \mathrm{M} \rightarrow \mathrm{BM}\cdot \tag{1.7}$$

b) Radical initiators

Free radicals are atoms or group of atoms with no electric charge but one unpaired electron. They can be produced by many different methods: thermal decomposition of initiators, redox reactions, ultraviolet irradiation, high-energy irradiation or thermal activation of monomers [12]. The most common initiators are peroxides and hydroperoxides, azo compounds, redox initiators and photo initiators [15]. Since the research of this master thesis uses thermal decomposition of initiators, the other methods will only be briefly introduced.

b.1) Photochemical initiation In photochemical or photoinitiated polymerisation the free radicals are produced by exposure of some monomer to ultra-violet (UV) or visible light. Two pathways exist for the absorbed light to produce radicals: 1) direct photoinitiation and 2) photosentisation [12, 14].

- **Direct photoinitiation**: a monomer (M) is directly exposed to UV or visible light (hv), absorbs light photons of a specific wavelength (M$\star$) and decomposes into radicals (R$\cdot$ and R'$\cdot$), as in equation (1.8). The generated free radicals will initiate the polymerisation in the remaining monomer.

$$\mathrm{M} + hv \rightarrow \mathrm{M}^{\star} \rightarrow \mathrm{R}\cdot + \mathrm{R}'\cdot \tag{1.8}$$

- **Photosensitisation**: a photosensitiser (S) is exposed to UV or visible light (hv) and gets activated to the excited state (S*). As represented in equations 1.9 and 1.10, the photosensitiser either dissociates into radicals (R$\cdot$ and R'$\cdot$) or transfers energy to a monomer (M) or initiator (I) and forms excited species (M* or I*) that will undergo homolysis to produce radicals.

$$\mathrm{S}^{\star} \xrightarrow{\mathrm{hv}} \mathrm{R}\cdot + \mathrm{R}'\cdot \tag{1.9}$$

$$\mathrm{S}^{\star} + \mathrm{M}\ (\text{or I}) \rightarrow \mathrm{S} + \mathrm{M}^{\star}(\text{or I}^{\star}) \rightarrow \mathrm{S} + \mathrm{R}\cdot + \mathrm{R}'\cdot \tag{1.10}$$

Photopolymerisation has numerous technological and practical advantages. It is used for surface and thin-layer applications since the penetration of light energy lowers as the thickness of the material increases [12, 14].

b.2) Redox initiation Redox initiators are free-radicals generated by oxydation-reduction (or redox) reactions such as equation (1.11). The reducing agent X will be able to split the bond (preferably weak) between A and B if sufficiently strong.

$$\mathrm{A} - \mathrm{B} + \mathrm{X} \xrightarrow{\mathrm{k}_i} \mathrm{A}\cdot + \mathrm{B}^{\ominus} + \mathrm{X}^{\oplus} \tag{1.11}$$

The advantage of redox initiation is the large range of temperature suitable for the radical production to occur. These systems are commonly used in low temperature polymerisation [12].

b.3) High-energy radiation High-energy radiation involves particles or photons with energies much higher than visible or UV photons used in photochemical initiation. Typical examples are α-particles, β- and γ-rays or high-velocity particles from a particle accelerator. Any monomer able to polymerise by another free-radical mechanism can also by high-energy radiation. However, the substrate involved might ionise by injection of electrons during excitation, resulting in a further and undesired polymerisation by radiation or ionisation [12, 14].

b.4) Thermal activation of monomers Some monomers will self-initiate polymerisation, i.e. without the presence of any initiator or catalyst, when heated in an inert atmosphere. For most of these monomers, spontaneous polymerisation is due to the reaction with O_2 and the resulting presence of peroxides or hydroperoxides, producing thermal initiators. The rate of this type of polymerisation is slower but not negligible. Styrene and methyl methacrylate are common monomers able to polymerise by self-initiation [12, 14].

b.5) Thermal decomposition of initiators The most common method to produce radicals is the thermal decomposition of initiators. It consists of an unimolecular reaction in which a compound with a weak bond (i.e. with a bond dissipating energy in the range of 100 to 170 kJmol^{-1}) is thermally split into a pair of radicals. The compounds used are mainly organic peroxides

. These can be represented with the formula R-O-O-R', where O-O is the weak bond undergoing scission as in equation (1.12) [12]. Peroxides are "thermally unstable and decompose into radicals at a temperature and a rate dependent on structure" [15].

$$\mathrm{RO-OR'} \xrightarrow{k_d} \mathrm{RO\cdot + R'O\cdot} \tag{1.12}$$

Organic peroxides degrade and discolour due to the intrinsic instability of the free radicals. The solution will turn from a clear to a yellow liquid as a function of time and temperature. It will increase over longer periods of time and higher temperatures. This yellowing can cause colour matching problems with the different applications. Patel et al. created a method in which the organic peroxide solution is insulated from air and light. Until the mixing with adhesives, the solution is stored in a sealed container filled with inert gas (eg. nitrogen gas) and covered with an opaque material [16].

Peroxides are divided into six chemical types: acyl peroxides (eg. acetyl and benzoyl peroxides), ketone peroxides (eg. methyl ethyl ketone and cyclohexanone peroxides), hydroperoxides (eg. t-butyl and cumene hydroperoxides), alkyl peroxides (eg. cumyl and t-butyl peroxides), peroxyesters (t-Butyl peroxybenzoate) and perketals [17]. The most common peroxide is benzoyl peroxide (BPO) [15].

Benzoyl peroxide With the chemical formula $C_{14}H_{10}O_4$, (di)benzoyl peroxide is a peroxide-based agent in the class of acyl peroxides. As represented in Figure 1.1, its structure can be described as two benzoyl groups $C_6H_5C_6H_5$ interconnected with one peroxide $-O-O-$.

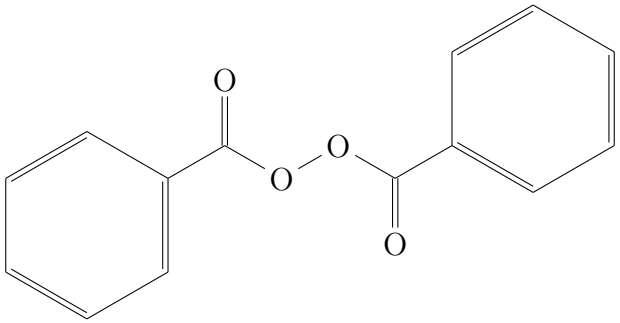

Figure 1.1: Chemical formula of benzoyl peroxide

During the initiation, BPO undergoes thermal homolysis and forms benzoyloxy radicals as in equation (1.13) [15].

$$\mathrm{Ph{-}\overset{\overset{\mathrm{O}}{\|}}{\mathrm{C}}{-}O{-}O{-}\overset{\overset{\mathrm{O}}{\|}}{\mathrm{C}}{-}Ph} \xrightarrow{\Delta} 2\ \mathrm{Ph{-}\overset{\overset{\mathrm{O}}{\|}}{\mathrm{C}}{-}O}\cdot \tag{1.13}$$

BPO is used in heat cured systems and room temperature systems if used with a tertiary amine accelerator (as explained later in this chapter) [17]. It has a critical temperature of about 75℃ [**shen**]. BPO will be the initiator used to cure unsaturated resins in this work.

Apart from peroxide compounds, azo compounds are another class finding extensive use as initiators, 2,2'-Azobisisobutyronitrile (AIBN) being the most important. Disulfides and tetrazenes are other commonly used thermo-initiators [12, 14, 15].

c) Kinetic of polymerisation

FRP processes have the advantage to grow long chains rapidly [14]. The reaction begins when the initiator starts decomposing and the concentration of radicals starts increasing. As radicals are formed and destroyed, their concentration becomes constant. This condition is described as "steady-state" and will be assumed for the following equations.

Kinetic of reaction depends on initiation, propagation and termination state. During the initiation step, the decomposition of the initiator will be the rate controlling step since it is much slower that the initiation reaction. According that there is no side reaction wasting primary radicals, the rate of the initiation R_i is similar to the rate of radicals generation. The equation will vary with the method

used. In the case of unimolecular thermal decomposition of radicals, it will be given by equation (1.14).

$$R_i = \left(\frac{d[\mathrm{M}\cdot]}{dt}\right) = 2fk_d[\mathrm{I}] \tag{1.14}$$

f is the initiator efficiency, k_d the rate constant for the initiator decomposition into radicals, and [I] the initiator concentration [12].

During propagation, the rate constant k_p is the same along the reaction since the radical reactivity is assumed to be independent of the chain length. The rate of propagation R_p is thus given by equation (1.15).

$$R_p = k_p[\mathrm{M}][\mathrm{M}\cdot] \tag{1.15}$$

k_p is the rate constant, [M] the monomer concentration and [M·] the total concentration of all chain radicals of size RM· and larger. k_p is usually much larger than other constants, resulting in a very rapid growth of the chain [12].

The rate of termination R_t is first zero and increases with the reaction. It is given by equation (1.16).

$$R_t = 2k_t[\mathrm{M}\cdot]^2 = 2(k_{tc} + k_{td})[\mathrm{M}\cdot]^2 \tag{1.16}$$

k_t is the overall termination rate constant, k_{tc} and k_{td} the rate constants for termination by coupling or disproportionation, and [M·] the total concentration of chain radicals of all sizes [12].

Under steady-state conditions, the overall rate of polymerisation is given by equation (1.17) (and by (1.18) in the case of thermal initiation) [12].

$$R_p = k_p[\mathrm{M}]\left(\frac{R_i}{2k_t}\right)^{1/2} \tag{1.17}$$

$$R_p = k_p[\mathrm{M}]\left(\frac{fk_d}{2k_t}\right)^{1/2} \tag{1.18}$$

These expressions apply to many vinyl polymers. However, deviations from the predicted kinetic behaviour can occur, such as the *gel effect*, also called *Trommsdorf effect*. It occurs in bulk or concentrated solutions polymerisation ($[\mathrm{M}_0] \geq 60\%$) due to the loss of the steady-state in the polymerisation kinetics. The viscosity increases so much that the mobility of the chain is reduced, as well as the probability of the chain ends to effect termination. Since the monomers can still diffuse to the active chain ends, the reaction autoaccelerates, the reaction exotherm increases and processing difficulties appear (especially in bulk polymerisation) [13, 15].

d) Accelerators and inhibitors

The kinetic of radical polymerisation can be altered by using accelerators or inhibitors [17].

d.1) Accelerators They are chemical substances that will activate peroxides and increase the rate at which these peroxides break down to produce radicals [17]. It is used for resin curing at ambient temperature or to lower the curing temperature of heat curing systems. With hydroperoxides and mixed peroxides, metal compounds will be used, and with pure peroxides, tertiary amines will be used. Systems with mixed metals and amine accelerators also exist. Accelerators must not be mixed directly with peroxides to avoid their decomposition [17].

d.1.1) Metal compounds Metal salts (cobalt or vanadium salt) and soaps (eg. manganese soap) are common metal accelerators. Cobalt accelerators are used in solution with concentrations from 0.5 to 10%. Vanadium and manganese accelerators are used with ketone peroxides and accelerate the curing of polyester resin at ambient and low temperatures respectively [17].

d.1.2). Tertiary amines accelerators Three tertiary amines are commonly used as accelerators: dimethylaniline, diethylaniline and dimethyl-*p*-toluidine. They activate the catalyst (such as benzoyl peroxide) through a reduction-oxidation process (represented in Figure 1.2). They also accelerate the production of free radicals and make curing at ambient temperature possible [18, 19, 20]. Their respective chemical structure, as well as their gel and cure time when used in benzoyl peroxide catalysed resin systems are given in Table 1.1.

In the literature, the proportion of these amines with benzol peroxide varies between 0.1 and 5wt%. According to Weatherhead, the proportion of one of these three tertiary amines in a polyester resin with benzoyl peroxide (50% paste) as inhibitor must be between 1 and 5% [17]. Other sources have found best rations with BPO/amine molar ratio of 1/1.57 BPO/amine molar ratio, with 1/4-12 BPO/amine mass ratio [21, 22]. The disadvantage of amines is their tendency to yellow during aging [17].

Table 1.1: Chemical formula and characteristics of a) N,N-dimethylaniline b) N,N-diethylaniline c) N,N-dimethyl-*p*-toluidine [17]

	(a)	**(b)**	**(c)**
	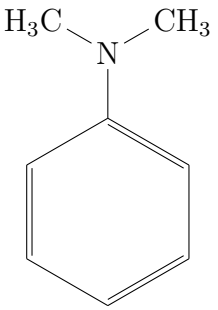	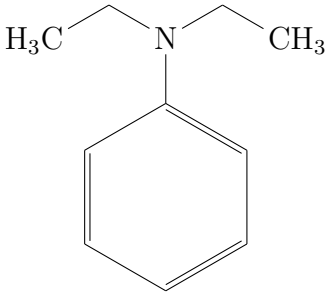	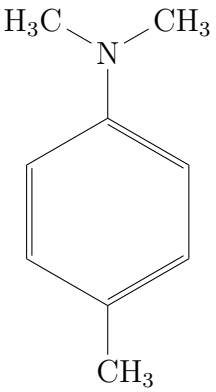
Gel time	Normal	Long	Short
Cure time	Quick	Fast (at room T)	Short

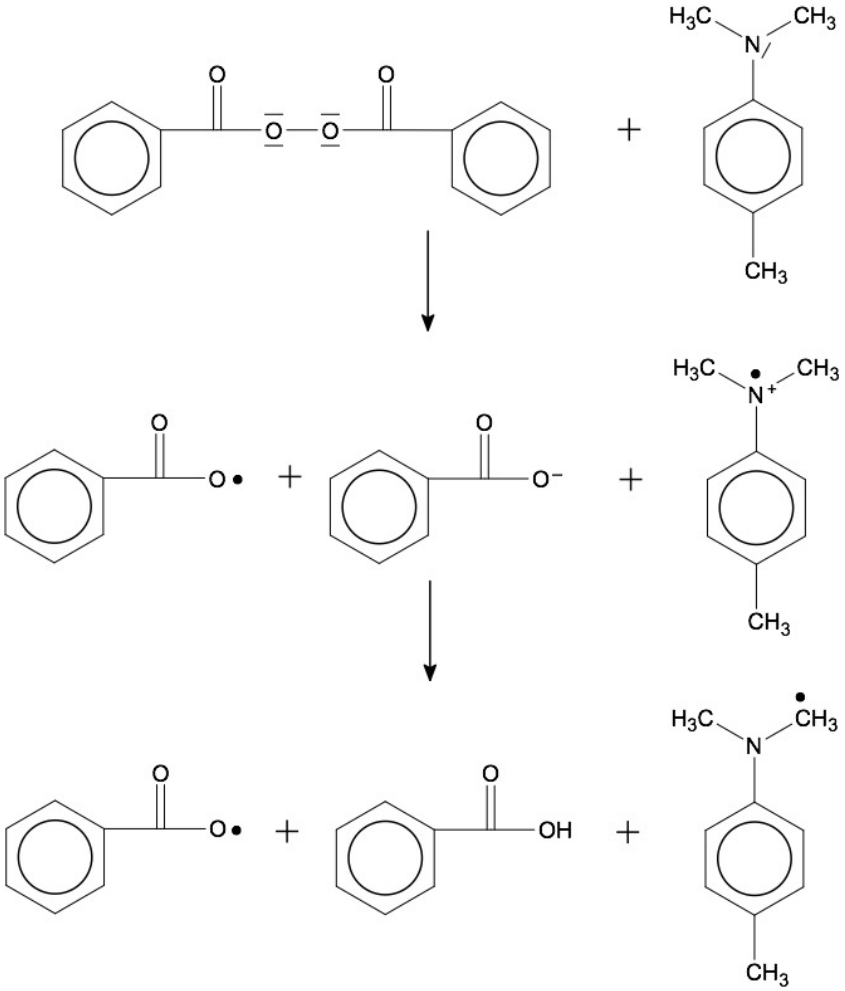

Figure 1.2: Reduction–oxidation process of benzoylperoxide (BPO) caused by N,N-dimethylaniline, adapted from [19].

d.2) Inhibitors They can be used to increase gel and cure time and guarantee adequate shelf-life of a resin [17]. They are typically added to monomers during shipment or storage. These substances react with primary or propagating chain radicals to produce nonradical products or products too low in reactivity to propagate. They will completely prevent polymerisation as long as they are present in the system. Equations (1.19) to (1.24) illustrate the case where the inhibitor Z reacts with primary radicals R· or propagating radicals M_n· [12].

$$\mathrm{I} \xrightarrow{\mathrm{k}_d} 2\mathrm{R}\cdot \tag{1.19}$$

$$\mathrm{R}\cdot + \mathrm{M} \xrightarrow{\mathrm{k}_i} \mathrm{RM}\cdot \tag{1.20}$$

$$\mathrm{R}\cdot + \mathrm{Z} \xrightarrow{\mathrm{k}_{zi}} \text{Inactive products} \tag{1.21}$$

$$\mathrm{M}_n\cdot + \mathrm{M} \xrightarrow{\mathrm{k}_p} (\mathrm{M})_{n+1}\cdot \tag{1.22}$$

$$\mathrm{M}_n\cdot + \mathrm{Z} \xrightarrow{\mathrm{k}_z} \text{Inactive products} \tag{1.23}$$

$$\mathrm{M}_n\cdot + \mathrm{M}_m\cdot \xrightarrow{\mathrm{k}_t} \text{Dead polymer} \tag{1.24}$$

1.1.1.2 Chain copolymerisation

Chain copolymerisation is the free-radical polymerisation of a mixture of at least two monomers with different chemical structure, called *comonomers*, to produce a *copolymer*, i.e. a polymer product containing at least two different mer units in the same polymer chain. "The relative proportions of the different mer units in the copolymer chain depend on the relative concentrations of the comonomers in the feed mixture and on their relative reactivities"[12]. The mechanism of copolymerisation is similar to homopolymerisation but the reactivity of the monomers towards the other monomers will vary.

1.1.1.3 Coordination polymerisation

Coordination polymerisation is the polymerisation with complex coordination catalysts. It was introduced in the 50s with the polymerisation of HDPE at low pressure and ambient temperature, and allowed to produce crystalline, stereoregular polypropylene. The main polymers synthesised by transition metal complex are polyolefins (eg. LDPE, HDPE, LLDPE), poly(1,3 dienes) and elastomers (by vulcanisation).

Two examples of coordination polymerisation are the heterogeneous and homogeneous Ziegler-Natta polymerisation. Heterogeneous Ziegler-natta polymerisation uses Ziegler-Natta catalyst, i.e. a catalyst combined with a co-cotalyst. The catalyst is a transition metal of an element from groups IV to VIII (Ti, V, Cr, Mo and Zr). The co-catalyst is an organometallic compound of a metal from groups I to III. The most common combination is $TiCl_3$ (or $TiCl_4$) and AlR_3. Homogeneous Ziegler-Natta polymerisation uses metallocene catalysts, a combination of a metallocene and a co-catalyst [13].

1.1.1.4 Ionic polymerisation

Ionic polymerisation can be anionic or cationic. It allows good control of the molecular structure and the synthesis of microstructure and more elaborated technical characteristics than for common polymers. However, it is less commercialised than free-radical polymerisation because of the high sensitivity to the presence of impurities, the high cost of the process and the much narrower choice of monomers. In cationic polymerisation, the initiation consists in additing an electrophile (I^+) to a monomer and the propagating specie is a carbocation (equation (1.25)). In anionic polymerisation, the initiation works by nucleophilic addition (I^-) to a vinyl monomer and the propagating chain is a carbanion (equation (1.26))[13].

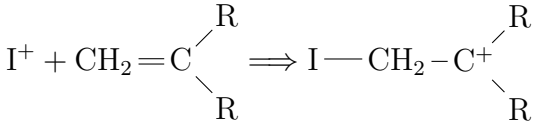

$$I^+ + CH_2{=}C(R)(R) \Longrightarrow I{-}CH_2{-}C^+(R)(R) \tag{1.25}$$

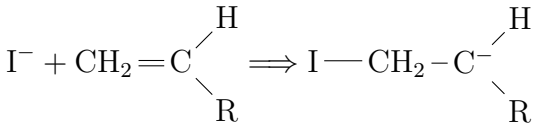

$$I^- + CH_2{=}C(H)(R) \Longrightarrow I{-}CH_2{-}C^-(H)(R) \tag{1.26}$$

Controlled radical polymerisation (CRP) is the third type of ionic polymerisation in which a dynamic equilibrium is established between propagating radicals and dormant species, introduced by a multi-valence metal catalyst [23]. The radicals are constantly activated and deactivated. Deactivation is reversible and can occur by coupling, such as in nitroxide-mediated polymerisation (NMP), or by atom transfer, as in atom transfer radical polymerisation (ATRP) [13].

1.1.2 Step-growth polymerisation

Step-growth polymerisation is the growth of linear polymers by step-wise intermolecular reaction of monomers. It requires the presence of bi- or multi-functional monomers with at least two chemical functions that can react together. Typical monomers present reactive functional groups such as -OH, -COOH, -NH_2, -NCO. These groups can react by esterification, amidification, or formation of urethanes. They are either present in the same molecule (equation (1.27)) or in two different bifunctionnal monomers (equation (1.28)) [12, 13].

$$\text{A-X-B} + \text{A-X-B} \rightarrow \text{A-X-X-B} + \text{A-B} \tag{1.27}$$

$$\text{A-Y-A} + \text{B-Y-B} \rightarrow \text{A-X-Y-B} + \text{A-B} \tag{1.28}$$

A and B are the reactive functional groups, and A-B is the by-product.

Four processing techniques are used for step-reaction polymers: homogeneous techniques such as bulk and solution (or solvent) polymerisations, and heterogeneous techniques, such as interfacial and phase-transfer catalysed polymerisations [13]. For example, bulk polymerisation is used to synthetise PET from EG and TA, where EG reacts like a nucleophilic agent.

1.1.2.1 Mechanism of reaction

The same reaction is responsible for all the steps of the polymer formation. Two monomers will start the reaction and form a dimer. The reaction continues with a dimer reacting with a monomer to form a trimer or with a dimer to form a tetramer,... until a polymer with a larger degree of polymerisation ($\overline{\mathrm{DP}}$) is formed. The reaction proceeds as long as molecules with the correct functionality and geometry, and necessary energy of activation interact. By-products (eg. H_2O, HCl, NH_3) are formed along the reaction. The general reaction is given by equation (1.29) [12, 13].

$$n\text{-mer} + m\text{-mer} \rightarrow (n+m)\text{-mer} \tag{1.29}$$

where n and m can have value from 1 to any number. Bifunctional and multifunctional monomers will form linear and network polymers respectively.

Reactions occur randomly between the intermediates and the monomer and the intermediates themselves. At any stage, the product is made of molecules of different sises and has a range of molecular weights. The average molecular weight will be high after a sufficiently long time of reaction (in contract with chain polymerisation where a long chain is formed as soon as the reaction starts) [12, 13].

1.1.2.2 Degree of polymerisation

For N_0 the initial number of molecules and N the total number of molecules after a given reaction time, the reaction conversion p is given by equation (1.30) [12, 15].

$$p = \frac{N_0 - N}{N_0} \tag{1.30}$$

DP, the degree of polymerisation, i.e. the average number of repeating units of all molecules present is given by the Carothers equation (1.31). It shows that even with high conversion (eg. 98%), high molecular weight are hard to obtain [15].

$$\overline{\mathrm{DP}} = \frac{N_0}{N} = \frac{1}{1-p} \tag{1.31}$$

High-molecular weight linear polymers will be obtained by high-yield reactions and an exact stoechiometric balance. The removal of by-products can drive the reaction to higher conversion [12, 15].

1.1.2.3 Kinetics of polymerisation

The rate constant in step-growth polymerisation is independent of the chain length. If the polymerisation reaction is first order with respect to each functional groups A and B, the rate expression will be given by equation (1.32), and by equation (1.33) assuming an exact stoechiometric balance [12].

$$\frac{-d[\mathrm{A}]}{dt} = k[\mathrm{A}][\mathrm{B}] \qquad (1.32) \qquad\qquad \frac{-d[\mathrm{A}]}{dt} = k[\mathrm{A}]^2 \qquad (1.33)$$

Using the Carother expression, equation (1.34) is obtained, and $\overline{\mathrm{DP}}$ can be expressed as equation (1.35).

$$\frac{1}{[\mathrm{A}_0](1-p)} - \frac{1}{[A_0]} = kt \qquad (1.34) \qquad\qquad \overline{\mathrm{DP}} = [\mathrm{A}_0]kt + 1 \qquad (1.35)$$

In specific cases the rate expression becomes second or third order and equation (1.32) becomes equation (1.36) (or equation (1.37) assuming an exact stoechiometric balance).

$$\frac{-d[\mathrm{A}]}{dt} = k[\mathrm{A}]^2[\mathrm{B}] \qquad (1.36) \qquad\qquad \frac{-d[\mathrm{A}]}{dt} = k[\mathrm{A}]^3 \qquad (1.37)$$

By integration and using Carothers equation, the expression of $\overline{\mathrm{DP}}$ is expressed as equation (1.38) [15].

$$\overline{\mathrm{DP}} = 2kt[\mathrm{A}_0]^2 + 1 \qquad (1.38)$$

1.1.2.4 Network Step Polymerisation

Step polymerisation using multifunctional polymers will form chain branching. The reaction consists in two steps: gelation and maturation. Gelation starts at the *gel point*, when the viscosity increases enough for the polymer to change from a liquid to a gel, and when bubbles are not able to rise and stirring becomes impossible. At this stage the polymer is a *network polymer*. The reaction will continue with the maturation to increase crosslink density and polymer rigidity. Gelation is not always desired and can be controlled by determining the critical reaction conversions at which gelation occurs [15].

1.1.3 Ring-Opening Polymerisation

Ring-opening polymerisation (ROP) is a third category of polymerisation that combines step-reaction and chain-reaction processes. It is used to polymerise cyclic compounds and prepare linear polymers. Examples are polyethers polymerised from three-membered ring cyclic ethers (epoxides), polyamides from cyclic amides (lactams), polyesters from cyclic esters (lactones) and polysiloxanes from cyclic siloxanes. However, not all cyclic monomers can be polymerised via ROP. Criteria of kinetic and thermodynamic feasibility must be satisfied. Moreover, the ceiling temperature is low and polymerisation will be less favourable with increase of temperature. It complicates the kinetics by the occurrence of polymerisation-depolymerisation equilibria [15].

Mechanism of polymerisation

The general process of ROP of cyclic compounds is represented by equation (1.39). It can be observed that in contrast with step polymerisation, there is no loss of small molecules and in contrast with chain polymerisation, there is no change in the type of bonding [15].

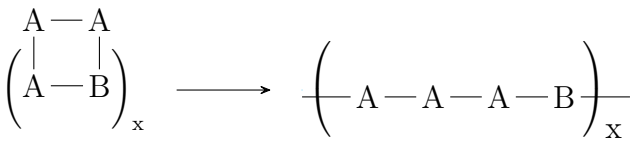

(1.39)

Depending on the monomer and initiator, the mechanism will vary between two forms :

1. some ionic or coordination species (X*) will attack the monomer at the functional group (G), the ring opened monomer will attack another cyclic unit, etc :

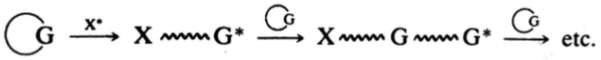

2. some ionic or coordination species (X*) will form a coordination specie, that will react with a second monomer, open the ring and continue as in 1 :

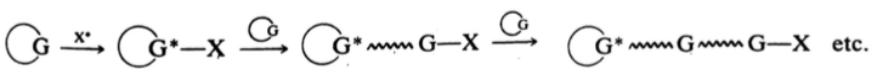

Depending on the initiator used, ring-opening polymerisation will show characteristics of step or chain polymerisation (or a combination of both). In general, the molecular weight increases slowly along the reaction as for step polymerisation, but as for chain polymerisation, only monomers are added to the growing chain during propagation [15].

1.2 Polyethylene terephthalate (PET)

Polyethylene terephthalate, generally abbreviated as PET (or PETE), is one of the most common thermoplastic resins. It is part of the polyester family, which groups polymers characterised by ester functions within their macromolecular main chains [24]. The PET repeating unit (r.u.) is shown in Figure 1.3 where the ester function is highlighted in purple. It consists of a short ethylene group (-CH_2CH_2-) and a *p*-phenylene group (R-aromatic cycle-R).

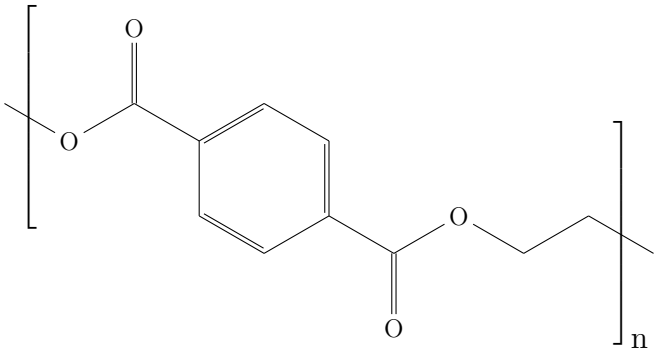

Figure 1.3: PET repeating unit (with the ester function represented in purple)

PET was first commercialised in 1941. In 2021, it was the fifth most demanded plastic in Europe with 8.5% of the yearly demand (4.14Mt over 49.1Mt) after polypropylene (PP), low-density polyethylene and linear low-density polyethylene (LDPE/LLPE), high-density polyethylene (HDPE) and polyvinylchloride (PVC). It is one of the most used polymers in Europe mainly in the packaging industry [3]. PET was originally used to produce fibres for clothing, but its use for blow-molded drinks and food containers increased significantly in the last three decades due to its good properties in such applications [25]. Low grade PET is still used for fibres.

1.2.1 Synthesis of PET

PET is synthetised by esterification and polycondensation of ethylene glycol (EG) and terepthalic acid (TPA) (or its dimethyl ester (DMT)). PET oligomers (and dimers) produced after esterification react by transesterification, increasing PET molecular weight. PET polymer is obtained by solid-state polymerisation (SSP). The polymerisation reaction is represented in Figure 1.4 and explained further below.

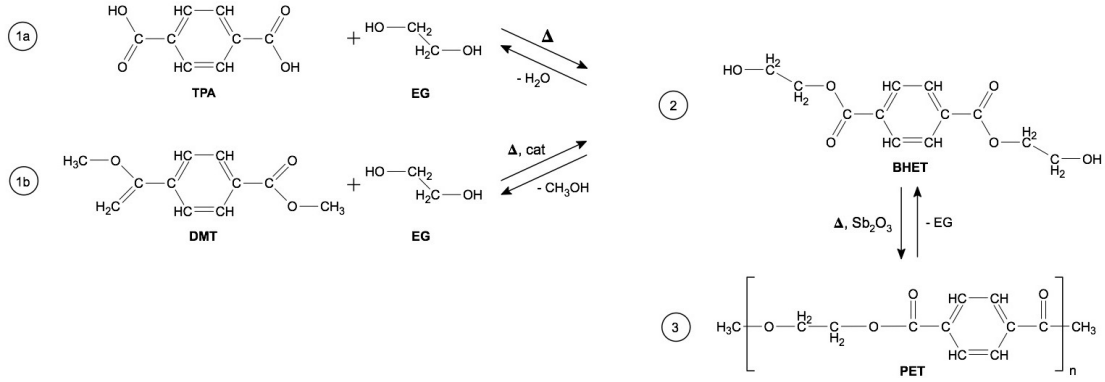

Figure 1.4: Reactions occurring in the synthesis of PET. 1a: esterification, 1b: trans-esterification, 2: polycondensation.

All the monomers involved in the reaction are generally derived from crude oil. Several alternative chemical routes exist to produce more sustainable EG and DMT but not many on an industrial scale [24, 26].

1.2.1.1 Pre-polymerisation step

Two reactions can start the synthesis of PET: a) an **esterification reaction** or b) a **trans-esterification reaction**:

a) Diacid terephtalic acid (TPA) is reacted with diol ethylene glycol (EG) at high temperature (240-260℃) and moderate pressure (300-500 kPa). Terephtalic acid is insoluble in ethylene glycol and high temperatures favour its solubilisation. No catalyst is needed since the diacid function of TPA self-catalyses the reaction with diol [24].

b) Dimethyl terephtalate (DMT) replaces TPA and is reacted at a lower temperature (140-220℃) and lower pressure (100 kPa) with EG in excess. A catalyst usually containing antimony (Sb) is used (below 0.5 wt%) [24].

Both reactions need the removal of the sub-product (water or methanol) with distillation to push the equilibrium forward. They produce the intermediate monomer bis(hydroxyethyl) terephtalate (BHET) which is polymerised to a degree of polymerisation up to 30 at a temperature of 250-280℃ and a pressure of 2-3 kPa [24, 27].

1.2.1.2 Polycondensation

The **polycondensation** of BHET happens at high temperature (about 300℃) and very low pressure (50-100 Pa) with the presence of antimony oxide (Sb_2O_3) as

catalyst. The mixture reacts further to increase the degree of polymerisation up to 100 (given that the equimolar ratio between the two monomers is maintained) and distils out the excess of EG during the reaction. PET is produced in a melt phase and is quenched with water [26, 28].

1.2.1.3 Solid-state polymerisation

The solid state polymerisation (SSP) increases DP to 150, and the physicochemical and mechanical properties of the polymer. The PET produced is heated for 5 to 25 hours in the presence of an inert gas at a temperature close to the melting point (200-240℃) and at 100 kPa. It removes volatile impurities such as acetaldehyde, free glycols and water [28]. This process obtains PET pellets with high molecular weight, melting point, crystallinity and viscosity [26].

1.2.2 Processing methods

PET can be processed by different techniques depending on the final application and product requirements. The main PET processes are extrusion, injection moulding and blow moulding.

a) Extrusion Extrusion is the oldest and simplest way to process PET. One of the most common extrusion processes is extrusion moulding, where the molten PET is forced into a mould with the required shape and is cut into moulding objects. It is generally used to produce large objects, as well as films, sheets, pipes and monofilaments [27].

b) Injection moulding In injection moulding the PET pellets are heated and softened in an extruder. The molten plastic is then injected under pressure into a cool mould to form a solid container. This technique is used to produce plastic tubs, cups, and lids [29].

c) Blow moulding Blow moulding is intensively used to produce bottles. The PET is injected into a cold mould to produce an amorphous preform, that is then transferred to an air-blowing unit to be stretched and blown into a bottle shape [27].

1.2.3 Properties of PET

PET is a low cost thermoplastic polymer with great and versatile properties [**santos**, 30]. It is produced at different specifications to satisfy the requirements of its many different applications [27]. For example, textile-fiber grade PET has a molecular

weight of 15000-20000 $gmol^{-1}$, while bottle-grade PET has a molecular weight of 24000 to 36000 $gmol^{-1}$ [28].

PET shows an improved thermal stability and a general stiffness due to its aromatic ring and polar groups.

1.2.3.1 Thermal properties

Virgin PET has a quite high melting temperature (T_m), which represents the transition from crystalline to solid-to-liquid. It varies between 255 and 260℃ (265℃ for more crystalline PET). Its glass transition temperature (T_g), which represents the glassy-to-rubbery transition, varies between 68 and 80℃ [25]. The higher the cristallinity (χ_c), i.e. the order degree within the structure, the higher T_g. The typical DSC curve of PET is shown in Figure 1.5.

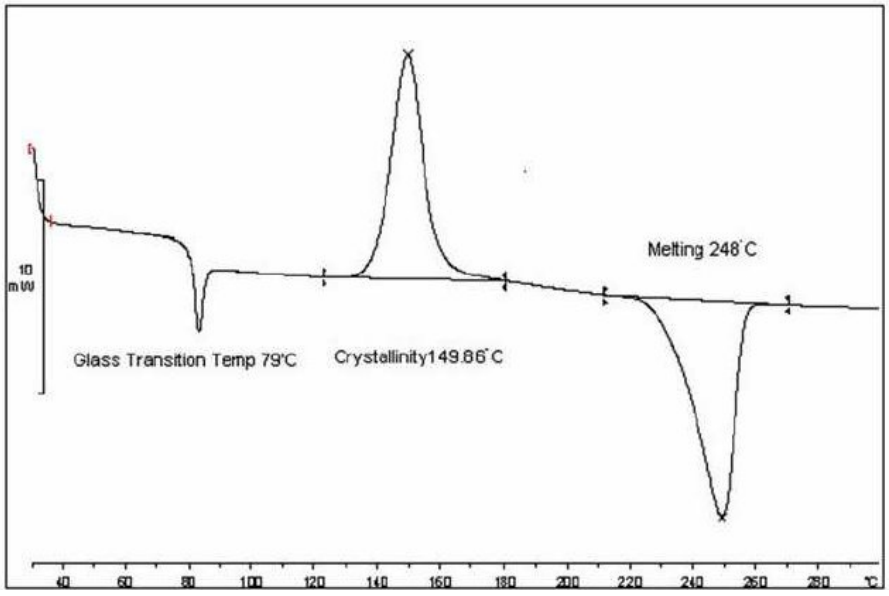

Figure 1.5: Conventional DSC curve of PET [31]

The necessary melting enthalpy to melt PET with higher degree of crystallinity (about 100%) is around 145 kJg^{-1}.

1.2.3.2 Crystallisation

PET is crystallisable because of its regular chemical and geometric structures. As other polymers, it can be in a semi-crystalline (where most of the polymer chains are parallel and closely packed) or amorphous (where the polymer chains are

disordered) state. Properties of PET will be affected by its crystallinity level and morphology. For example, crystallinity will increase T_g (about 67℃ for amorphous PET and 81℃ for crystalline PET), modulus, toughness, stiffness, tensile strength, hardness, resistance to solvents but will decrease the impact strength [31]. The rate of crystallisation of PET is slow. It depends on many factors, such as the cooling rate and the molecular weight, and is the highest around 170-190℃[27].

When heated above T_g (about 72℃ for semi-crystalline PET), the polymer shifts from a rigid glass-like state to a rubbery-elastic state. In this state, the molecular chains can be stretched in two directions to form films and bottles (or in one direction to form fibres). If the polymer is kept at this temperature, it will slowly shift back to a crystalline state and start to become opaque and less flexible. Meanwhile, PET will stay in an amorphous state if cooled rapidly from the melt to $T < T_g$ [27, 26].

1.2.3.3 Mechanical, physical and chemical properties

PET has a low density and good processability. It has higher mechanical strength and stiffness than most polymers. Its Young's modulus is about 3.0 GPa [24, 25]. It has excellent tensile and impact strength [32].

PET also has excellent transparency and clarity, and good low frequency electrical properties. It has excellent chemical resistance [32] and is a good water vapour, oxygen and CO_2 barrier [25]. It is insoluble in water and many common organic solvents, but can be dissolved by other type of solvents such as benzaldehyde, benzyl acetate, butyl and ethyl benzoate, trifluoroacetic acid and dichlomethane [33, 34]. Table 1.2 shows some of its standard mechanical and physical properties [24].

Table 1.2: Physical and mechanical properties of PET [25, 27].

Molecular weight of r.u.	192 ($gmol^{-1}$)
Density	1.21-1.41 (gcm^{-3})
Young's modulus	2.76-3.1 (GPa)
Impact strength	90 (Jm^{-1})
Yield strength (elastic limit)	50-55 MPa (%)

1.2.3.4 Degradation of PET

PET can be degraded by different types of processes or by a combination of them. These processes will often deteriorate the chemical structure of the polymer,

decrease its (thermo)mechanical stability and alter its morphology at a macro and microscopic level (eg. change of colour, molecular weight or degree of crystallinity, formation of cracks or debris). Degraded PET can release acetaldehyde (thermal degradation) or the residual antimony from the catalyst involved in its synthesis. [24]. Some of the main degradation processes are hydrolytic, thermal, radiative and biodegradation.

1.3 Recycling of PET

The recycling industry of PET started to grow with the environmental pressure to improve waste management. If recycling reduces plastic waste, it only reduces the necessary energy to produce virgin resin [35]. As previously said, PET is a non-degradable plastic due to is very slow rate of decomposition in natural conditions [27]. It is currently the most widely recycled thermoplastic with a recycling rate (fraction of what is recycled from the waste) of over 25% [36]. The resin code of PET is 1 (Figure1.6). It is a symbol placed on plastic items used to recognise the type of polymer they are made of and facilitate their recycling [37, 38].

Figure 1.6: Resin symbol of polyethylene terephthalate

1.3.1 Categories of recycling

Recycling of plastic can be defined as "the process of recovering scrap or waste plastics and reprocessing the material into useful products, sometimes completely different in form from their original state" [39]. These recovery processes can be divided into four categories: primary, secondary (or mechanical), tertiary (or chemical) and quaternary recycling. As represented in Figure 1.7 these categories will depend on the recyclate.

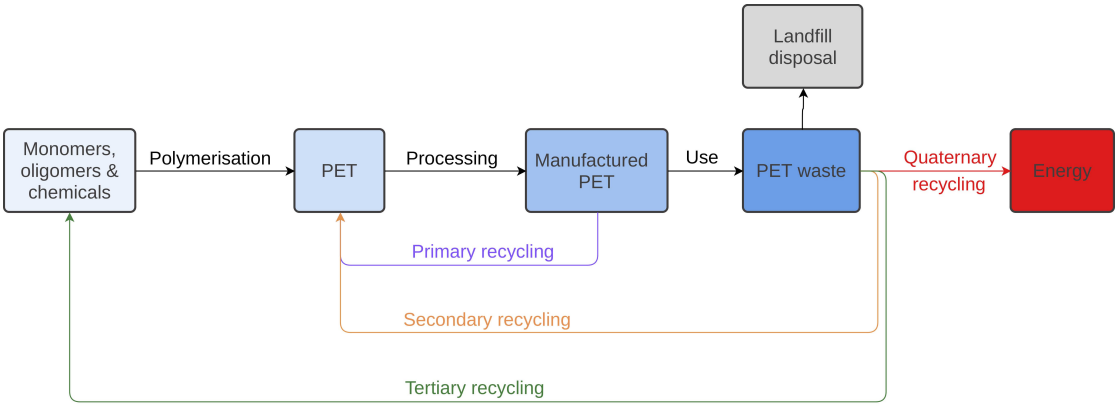

Figure 1.7: Categories of polymers recycling

1.3.1.1 Primary recycling

Also called **closed-loop recycling** or "**re-extrusion**", it refers to the "in-plant" recycling of clean and uncontaminated pre-consumer industrial scrap. The recycled material can be mixed with virgin material to ensure product quality. It is a simple and cheap process but is not very popular for recyclers since it only deals with single-type waste [26, 28, 39].

1.3.1.2 Secondary recycling

Secondary recycling, more commonly referred to as **mechanical recycling**, is the melt reprocessing of post-consumer (POST-C) plastic waste [24]. For PET, it leads to the production of granulates of recycled PET (r-PET). The process consists of three main steps : contaminants removal (1), drying (2) and melt reprocessing (3). These occur in a different order and at a different frequency depending on the origin and composition of the waste [40].

1. The **removal of contaminants** groups several processes. It starts with the sorting (manual, with NIR or colour sensors, or by density) of the waste and will separate the PET from other polymers (eg. PVC, PE) or other types of materials (eg. metals, ceramics). The waste is shredded to homogenise the distribution of the material and reduce the volume. The shredded particles are washed (aqueous washing or solvent washing) to eliminate remaining substances like glue, small metal parts, labels and fragments of other types of polymers. Grinding will then aim at reducing further the size of the material and ease the reprocessing [24, 28, 40].

2. The flakes are **dried** at 140-170℃ for 3 to 7 hours to minimise the moisture content, reduce any hydrolytic degradation effect [28] and increase the r-PET melt strength [41].

3. **Melt reprocessing** consists of using heat to convert the flakes into granules. The flakes are sent to an extruder (or an injection moulding machine), heated to the desired melting temperature (about 280℃), and sliced in the form of 2-4 mm granules. The granules can then be processed into any desired product using the same processing methods as virgin PET [24].

Mechanical recycling is the most common method to recycle PET as it is a simple and inexpensive process. It can work with established equipment and is flexible in terms of feedstock volume. However, this process is a form of downgrading as it tends to generate undesired reactions (eg. colouring, (photo-)oxidation or cross-linking reactions) as well as mechanical stresses that will change the material at a macromolecular scale. These changes will affect the mechanical and rheological properties of the recycled material [28, 42]. It will also produce high content of volatiles organic compounds (VOC's, most acethaldehydes) [24]. The more complex, heterogeneous and contaminated the waste is, the higher the deterioration of POSTC-PET during processing will be [26, 27, 41]. For these reasons, mechanical recycling limits the potential purpose of r-PET. It will be used for applications with less demanding performance requirements, such as fibres or non-food containers. It is a form of downgrading [24, 36, 39, 41].

1.3.1.3 Tertiary recycling

It is the chemical recycling of the polymers and is also called feedstock recycling. It can be differentiated into thermal or chemical processing [39].

Chemical recycling is the conversion of POST-C PET chains through depolymerisation, i.e. high molecular weight polymers into low molecular weight substances [43]. Total depolymerisation will recover monomers, and partial depolymerisation (i.e. random chain scission) will recover oligomers, or other industrial chemical substances. Both processes will form gaseous products [26, 32, 4]. Chemical recycling is carried out by pyrolysis (degradation by heat in the absence of O_2, air or vacuum) or solvolysis (degradation by solvents) [28].

Solvolysis The functional ester groups of PET can be cleaved by reagents, i.e. solvents, and opened within the macromolecular chains [24]. The process consists of three irreversible reactions, described by Al-Sabagh et al. [26]:

1. The carbonyl carbon (C=O) of the polymer chain undergoes rapid protonation where the carbonyl oxygen (C=O) is converted to a second hydroxyl group (-OH);

2. the hydroxyl oxygen (-OH) of the added hydroxyl-bearing molecule slowly attacks the protonated carboxyl carbon atom(C^{+}-O);

3. the converted carbonyl and a proton are rapidly removed to form water or a simple alcohol and the catalytic proton.

Solvolysis is "the most established and only acceptable one (type of recycling) according to the principles of 'sustainable development', defined as development that meets the needs of present generation without compromising the ability of future generations to their needs" [26]. The advantages of chemical recycling are numerous. The recovered monomers and oligomers can be purified before repolymerisation through decontamination processes (distillation/crystallisation steps or surface/vacuum treatments) and then repolymerised with condensation product through polycondensation reactions. By removing the possible post-consumer contaminants, the rPET will have acceptable properties for food applications [24]. One of the main disadvantage of the process is the high cost and the environmental impact using solvents.

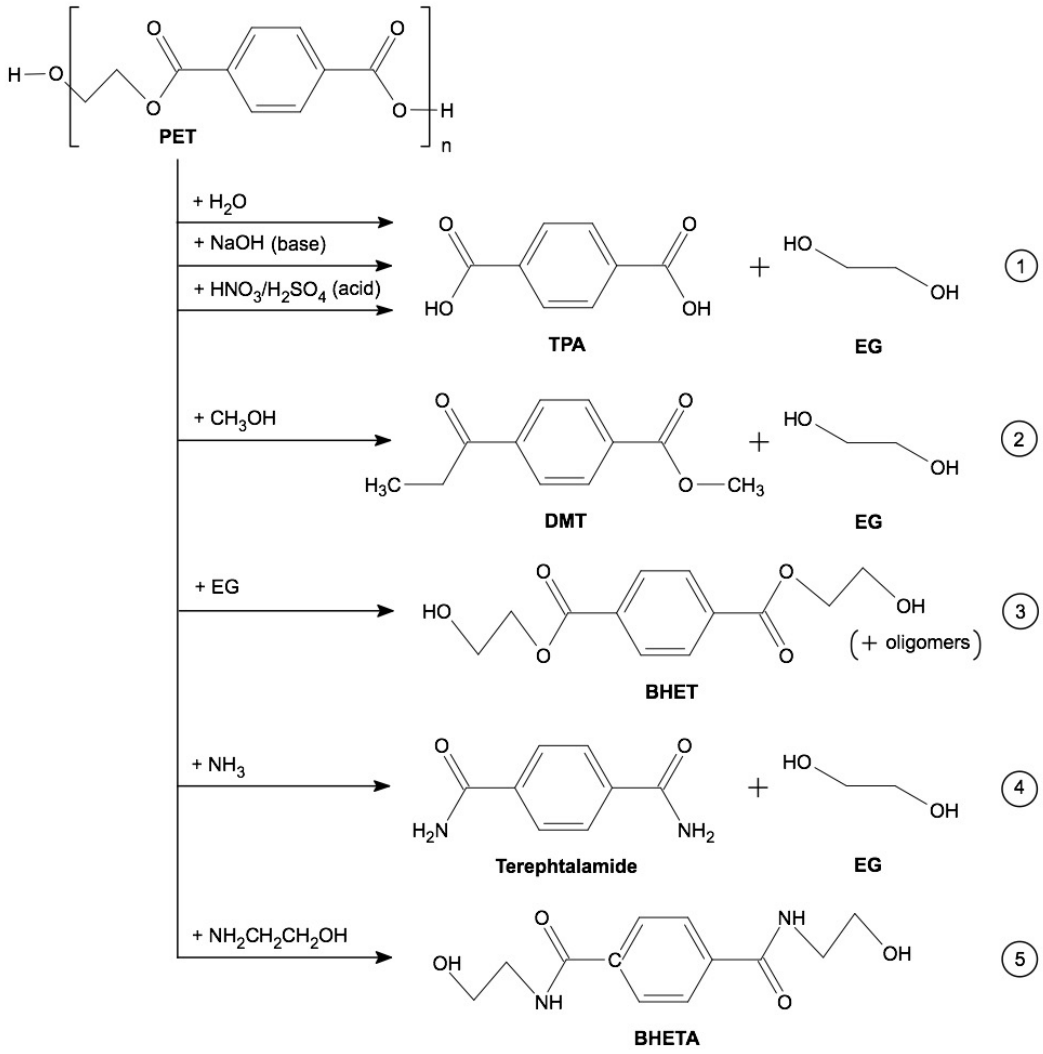

Figure 1.8: Solvolysis methods for PET depolymerisation. 1: hydrolysis (neutral, basic, acidic), 2: methanolysis, 3: glycolysis, 4: ammonolysis and 5: aminolysis.

As represented on Figure 1.8, five different methods exist and depend on the solvent used : hydrolysis (in neutral, acidic or alkaline environments), methanolysis, glycolysis, aminolysis and ammonolysis [24]. The agent, the reaction conditions (temperature, pressure) and the recovered products of all the different methods are described in Table 1.3. The three first methods are the most common since aminolysis and ammonolysis are not yet used at a commercial scale [28].

Table 1.3: Parameters of the different chemical recycling methods [24, 32].

	Depolymerising agent	**T** [℃]	**p [MPa]**	**Products**
1. Hydrolysis				
∘*Neutral*	Water or steam	200-300	1-4	TPA, EG
∘*Alkaline*	NaOH	180-250	1-2	
∘*Acidic*	HNO_3, H_2SO_4	85-150		
2. Methanolysis	Methanol	180-280	2-4	DMT, EG
3. Glycolysis	EG	180-250		BHET, oligomers
4. Aminolysis	Methylamine, ethylamine, ethanolamine	20-100		Diamides of TPA (BHETA)
5. Ammonolysis	Ammonia (NH_3)	120-180	2	Terephtalamide, EG

Glycolysis Depolymerisation by glycolysis with ethylene glycol as depolymerising agent and in the presence of zinc acetate is the most used solvolysis technique. Alternatives are diethylene glycol (DEG), triethylene glycol (TEG), dipropylene glycol, propylene glycol (PG), butanediol, polyethylene glycol, trimethanol propane, neopentyl glycol, 2-methyl-1,3-propanediol (MPD) [24, 32]. PET/glycol ratios and reaction conditions depend on the glycol compound and the applications. Different possibilities are found in the literature. Öztürk and Güçlü managed depolymerisation waste PET with EG (PET/EG molar ratio 1/6), PG, DEG, TEG, and PG-TEG mixture (PET/glycol molar ratio 1/2.5) in the presence of zinc acetate catalyst at 190-220℃ [44]. Kim et al. depolymerised PET with EG, DEG and MP-Diol in weight ratios PET/glycol of 250/142, 250/153 and 250/200 for polymer concrete, pultrusion and no-dipping pipe lining respectively. The reaction was carried out at 210℃ for 5h in the presence of 0.3% of zinc acetate (based on weight PET)[30]. Duque-Ingunza et al. used sodium carbonate as catalyst to reduce the environmentally damaging impact of zinc acetate [43].

Four different types of glycolysis exist : solvent-assisted, supercritical, microwave assisted or catalysed glycolysis [26, 28]. Glycolysed PET have numerous applications, such as for the synthesis of other materials (unsaturated polyester resins, polyurethanes foams, copolymers, concrete materials or epoxy resins) [**czub**, 24].

1.3.1.4 Quaternary recycling

Energy is recovered from waste plastic by incineration. Plastic is characterised by a low heating value (LHV) of 30-35 MJ/kg, and a low moisture and ash content. For PET in particular, the heat combustion varies between 23 and 24.2 $MJkg^{-1}$. Energy recovery happens with co-combustion in dedicated plants and existing industrial plants, and with combustion in dedicated fluidised bed incinerators [39].

1.3.2 Unsaturated polyester from recycled PET

One effective way to recycle PET is to synthesise unsaturated polyester (UP) from waste PET. The term "unsaturated" refers to the carbon-carbon double bond(s) in the chemical structure of the polyester. It allows curing into a harder material via radical polymerisation.

1.3.2.1 Synthesis

Unsaturated polyester is formed by polycondensation, via the reaction of the hydroxyl groups of an unsaturated or saturated diol, with the carboxyl groups of an unsaturated or saturated dibasic acid or anhydride [30]. After chemical recycling of PET, the recovered PET oligomers or monomers are repolymerised using a crosslinker, such as maleic anhydride (MA) [43, 45]. Glycolysis products and MA are often reacted in OH/COOH molar ratio 1-1.1/1 at 190-220℃ under nitrogen atmosphere [44, 46]. Other reactants can be phtalic anhydride and dicyclopentadiene [30]. However, Lu et al. observed that reaction with MA was faster. Duque-Ingunza et al. observed an increase in molecular weight with reaction time and temperature [43]. Many examples of unsaturated polyester synthesised from recyled oligomers of PET were found in the literature, but none of them were found using citraconic anhydride as crosslinker.

1.3.2.2 Curing into unsaturated polyester resins

Transforming unsaturated polyester into a structural material consists of adding an unsaturated monomer (UM) to produce thermosetting resins, also called unsaturated polyester resins (UPR). The addition of the unsaturated monomer helps decreasing the viscosity of the resin and processing, but mainly creates a network by reaction with the unsaturated carbon double bonds of the polyester [45]. UPRs are widely used as coating and constructions materials, and in the automotive and marine industry [43].

Resins based on recycling PET waste have the advantage of lowering the cost compared to traditional unsaturated polyester resins. Up to 20-25% of raw material

cost can be reduced. If the chemical and physical properties of the resins are lower, they can still be used in low cost production fields [30].

The most used UM is styrene due to its low cost, availability and because it provides good mechanical properties to the resin. However, styrene has high volatility and is released in the atmosphere during curing. Alternatives can be dimethacrylates, alkyl methacrylates vinyl esters and divinylbenzene [45]. 30 to 40 wt% of monomer are added to the UP mixture [30, 44]

1.3.2.3 Curing process

The reaction is a radical polymerisation and thus necessitates an initiator, the most employed being organic peroxides. For example, Kim et al. synthetised a resin with 1 % of BPO (w/w of the resin) [30]. In their study, Östürk and Güçlü used methyl-ethylketone peroxide with the same mass fraction [44]. As explained in section 1.1.1.1, accelerators such as vanadium, cobalt salts and tertiary amines can also be useful to reduce the activation energy for the initiator decomposition, and thus the temperature required for crosslinking [45].

Typical curing cycles are made of curing and post-curing steps, and eventually a final curing at high temperature [43]. Kim et al. established a cure system of three steps: 55℃ for 8 hours, 80℃ for 1 hour and 110℃ for two hours [30]. When the mixture is exposed to heat, light or radiation, crosslinking starts by initiator activation and production of free radicals. Long chain molecules are formed by connecting to vinyl monomers via intermolecular and intramolecular reactions. Gelation is quick (about 3 to 5% of conversion), resulting in most of the reaction being diffusion-controlled. Different reactions occur: UM-UP copolymerisation, UM homopolymerisation and UP homopolymerisation [45].

Given Lu at al., "assuming that the curing process only has a thermal effect and the heat produced by decomposition of initiator is negligible, the reaction advance will be directly proportional to the amount of heat generated and the maximum degree of curing reached when all double bonds that may have react have done so" [46]. The fraction of double bonds reacted during the curing reaction, or the relative degree of cure, at time can be given by equation (1.40).

$$a = \frac{Q_T}{Q_{total}} \tag{1.40}$$

1.3.2.4 Properties

UPRs are know to have good properties, easy synthesis, and high versatility and low cost. The physical and chemical properties of the resins depend on their molecular composition and also on the depolymerisation and cure reactions. UP with too low molecular weight will lead to resins with very poor mechanical properties. UP with too high molecular weight will produce viscous and hard to process resins [43]. Östürk and Güçlü synthesised UP resins from different glycolysed PET and maleic anhydride at a OH/COOH ratio of 1.1/1. Properties and characteristics of the resins were analysed and compared with properties of reference resins prepared from maleic anhydride, phtalic anhydride and the same glycol compounds and ratios. The mechanical properties and curing behaviour were showed to be comparable. DEG- and TEG-based resins showed more flexibility but PG-based resins higher tensile strength and hardness [44]. UPs prepared with only EG or DEG are known to be less soluble in styrene [45].

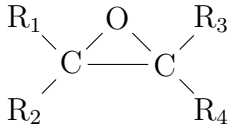

(a)

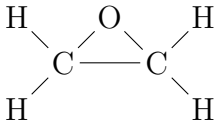

(b)

(c) $y = 5/x$

Figure 1.9: (a) Epoxide and (bà oxirane groups

1.4 Epoxy resins

Epoxy resins or epoxides are crosslinkable polyethers that possess at least one epoxy group, also called epoxide or oxirane. These three-membered ring of two carbons and one oxygen are represented in Figures 1.9a and 1.9b [15, 47, 48].

Epoxide and oxirane are different from other ethers since they have an equilateral triangle shape which implies high tension on the three atoms. This high strain also increases their reactivity compared to other cyclic ethers [48].

Epoxy resins are first synthesized as oligomers with epoxide end groups that can then further polymerise to form more complex networks of polymers. The term "epoxy resin" refers to both the prepolymer and the cured form of the resin (even if in the latter all of the functional groups have reacted with no epoxide group still present) [49].

1.4.1 Properties and applications

Epoxy resins are versatile due to their numerous chemical and mechanical properties: resistance to humidity and chemicals, good adhesion to many substrates, high toughness, high electrical resistivity and low shrinkage [49]. They are used as construction materials, adhesive and coating agents. They are also one of the most used thermosetting matrix resin in advanced composites for many different fields (especially for adhesives and structural materials in the aerospace and electronics industries) [48].

1.4.2 Synthesis

Many reactions exist to synthesise epoxides and oxiranes. The two most important routes are (1) the reaction of a halohydrin with hydroxyl compounds, such as epychlorydrin with phenol or an aliphatic alcool and (2) the oxidation of an olefin with a peracid [48, 50]. Commercially important epoxy resins are glycidyl resins, such as bisphenol A diglycidyl ether derived from the reaction of bisphenol A with epichlorhydrin in the presence of sodium hydroxide, and ene-oxide resins (eg.

epoxidized oils, rubbers), generated by the peroxidation of an unsaturated bond [51].

1.4.3 Curing

The crosslinking (epoxide or oxirane) group of epoxy resins is highly reactive due to its geometry and the ring strain. It is reactive to both nucleophilic and electrophilic species. It can be used with many reagents or curing agents, to produce the cured thermoset epoxy resin, converting the initially low molecular weight resin into its thermoset form. The cured resin has three-dimensional chemical structure that is needed for industrial applications [49, 50].

1.4.3.1 Curing agents

The curing agents can be of two types : catalysts or hardeners. Catalysts can be tertiary amines or Lewis acids. They initiate ionic polymerisation of the epoxy compound to produce polyether structures. Hardeners can be aliphatic or aromatic amines, or carboxylic anhydrides. They react directly with the epoxy and other groups of the resins, modifying its structure [49]. Curing agents can also be distinguish following their chemical composition. They can be nitrogen-containing (such as tertiary amines), oxygen-containing, sulphur-containing or miscellaneous curing agents [50]. The type of curing agent significantly affects the properties of the cured epoxy resin.

1.4.3.2 Mechanism of curing

Curing changes the epoxy resin properties, transforming the fluid resin-curing agent mixture into an elastic solid. It "can occur by homopolymerisation initiated by a catalytic curing agent or a polyaddition/copolymerisation reaction with a multifunctional curing agent" [50]. Because of the strain in the three-membered ring, i.e. the epoxide or oxirane group, epoxides are polymerised mainly through ring-opening polymerisation. The main reactions are divided into two classes: (1) reactions with nucleophilic reagent in neutral solution and (2) acid/base catalysed reactions [48].

a) Reactions with nucleophilic reagent Epoxides will polymerise in mild conditions through ring-opening processes when attacked by nucleophilic center. The mechanism corresponds to an addition reaction without elimination, as represented

in equation (1.41) [48].

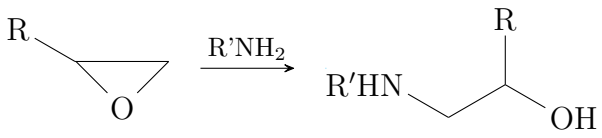

(1.41)

Nucleophilic reagents concerned by this reaction can be [48]:

- Ammonia and amines (primary, secondary and tertiary)
- Water, alcohol and phenol
- Sulphur-containing compounds
- Carbanion species

b) Acid- and base-catalysed reactions Acidic and basic reactions correspond respectively to cationic and anionic polymerisation, mentioned in section 1.1.1.4. In acidic conditions, ring-opening polymerisation is initiated by protonic and Lewis acid systems and involves proton attack on the ring oxygen atom. (equation (1.42)). In basic conditions, initiation is catalysed by sodium or potassium hydroxides, alkoxides, metal oxides or organometallic derivatives and propagation. An ion is formed and the reaction propagates by the nucleophilic displacement of this ion (equation (1.43)). Both types of reaction follow a S_N2 mechanism [15, 48, 50].

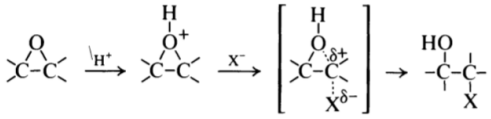

(1.42)

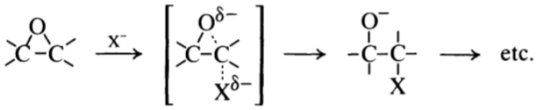

(1.43)

c) Homopolymerisation Epoxy resins are homopolymerised by catalytic curing with the aid of either Lewis acids or Lewis bases. Suitable Lewis bases are tertiary amines, such as 2,4,6-tris-(N,N-dimethylaminomethyl)phenol and N,N-dimethylben- zylamines. The effectiveness of the homopolymerisation will vary with the temperature, but also with the concentration and structure of the tertiary amine. The most common and mostly employed Lewis acid for homopolymerisation is boron trifluoride (BF_3). It crosslinks and forms a network in minutes. Lewis acids are also used with tertiary amines [47, 48].

1.4.4 Physical phenomenon during curing

The curing of epoxy resin involves different stages: **gelation**, **vitrification** and **degradation** [47, 48]. TTT diagrams are used to predict the times to gelation and to vitrification during isothermal cure versus temperature [49].

Gelation During initiation the epoxy monomer and the curing agent react to form oligomers. As cure continues, oligomers increase in size but the average molecular size stays low. When molecular size increases significantly, highly branched molecules are formed and react together to form even more highly branched structures. Gelation happens when these branched structures extend throughout the whole sample. Viscosity increases significantly and limits chain mobility. The molecular mass becomes infinite and the viscous liquid transforms into a viscoelastic gel. During gelation two fractions coexist: a soluble fraction called "gel", and an insoluble fraction called "sol". The sol fraction decreases as cure continues until a structural material is formed, i.e. when most of the sample is connected into the three-dimensional network. When polymerisation is complete the sol fraction will have disappeared. Gelation is irreversible. [47, 50].

Vitrification Vitrification corresponds to the change in state from a viscous liquid (or gel) and a glassy state. It occurs when the cure temperature T_c is below the glass transition temperature T_g. The more crosslinked the system, the higher will be T_g. Vitrification modifies diffusion and inhibits polymerisation, but is not irreversible. Devitrification is possible by simply heating the system above T_g [47, 50].

Degradation Post-cures at elevated temperatures can be necessary to have complete reaction of all epoxy groups [50]. However, at high temperature, polymerisation can be inhibited by thermal degradation of the resin, due to devitrification and revitrification. Devritification will form a rubber gel and decrease T_g below T_c due to the crosslinking density and the formation of plasticizers. Revitrification increases T_g due to densification or volatilisation of low molecular mass plasticizers [47].

1.5 Glycidyl methacrylate (GMA)

Glycidyl methacrylate (GMA), $C_7H_{10}O_3$, is a type of epoxy acrylate. It is an important bifunctional glycidated monomer used as a chemical intermediate for polymers and a monomer and diluent in epoxy resins [52]. It has many different applications such as coatings, adhesives, dental resins, paints and hydrogen lenses [53, 6]

GMA chemical structure is given in Figure 1.10. It contains an unsaturated group (C=C) capable of free-radical grafting on hydrocarbon polymers and a highly electrophilic epoxide that can react with different nucleophilic functions (carboxylic, hydroxide and amine groups) [54, 7, 55]. It can thus form homogeneous and heteregeneous networks [6].

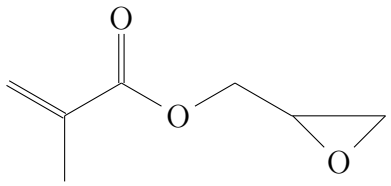

Figure 1.10: Chemical structure of glycidyl methacrylate

1.5.1 Synthesis

The conventional method to produce glycidyl methacrylate is the esterification of an alkali metal salt of methacrylic acid with epichlorohydrin in a molar ratio 1/3 to 1/10. They react in the presence of 0.2 to 2.0 mol% of a quaternary ammonium salt as catalyst and 0.01 to 0.2 wt% of hydroquinone monomethyl ether as polymerisation inhibitor. The reaction happens between 80 and 120℃ for 1 to 5 hours [56]. The by-products salts (NaCl) are removed by filtration, dissolved in added water and washed out from the reaction system. The crude GMA is purified by distillation [53].

The purified glycidyl methacrylate produced by the conventional method still contains 0.1 to 1.0 wt% residual chlorine compounds such as epichlorohydrin. The free chlorine accelerates metal corrosion which can be problematic for applications with electronic equipments (eg. paints, resins). Several methods exist to decrease the free chlorine content from epichlorohydrin such as distillation, stripping or acid treatment. Hosokawa et al. discovered a method in which epichlorydrin content is reduced by adjusting the water content in the reaction system to 500 to 2000ppm, and by distilling GMA with steam [56].

1.5.2 Properties

Glycidyl methacrylate is described as "a colourless liquid with a fruity colour" [52]. Its main properties are given in Table 1.4 below.

Table 1.4: Main properties of GMA [52].

Molecular weight (of r.u.)	142.15 ($gmol^{-1}$)
Density (at 25℃)	1.07 (gcm^{-3})
Boiling point	189℃
Melting temperature	-41.5 - -52℃
Flash point	84℃

GMA is soluble in benzene, ethyl ether and ethyl alcohol. It is sensible to ambient temperature. It must be kept at low temperature to avoid formation of peroxides (or other oxidation products) and evaporation [52].

1.5.3 Reactivity of GMA

Due to its bifunctionality, glycidyl methacrylate can be grafted with polyolefins through its vinyl (C=C) group and can react with polar groups such as amine, hydroxyl and carboxyl groups via its epoxy function. Two reaction mechanisms can be distinguished: its homopolymerisation into poly(glycidyl methacrylate) (pGMA) and its copolymerisation. The enthalpy of complete polymerisation of GMA is of 398.68 Jg^{-1} [57].

1.5.3.1 Homopolymerisation

Glycidyl methacrylate monomer is highly reactive. It polymerises to produce (poly-)glycidyl methacrylate (pGMA), as represented in Figure 1.11. Different polymerisation methods can be used. GMA can be polymerised via atom transfer radical polymerisation (ATRP), using a catalyst and an initiator [58] It is traditionally used to control the polymerisation behaviour [6]. GMA can also be polymerised via free-radical polymerisation using azoisobutyriitrile as initiator (AIBN) [54].

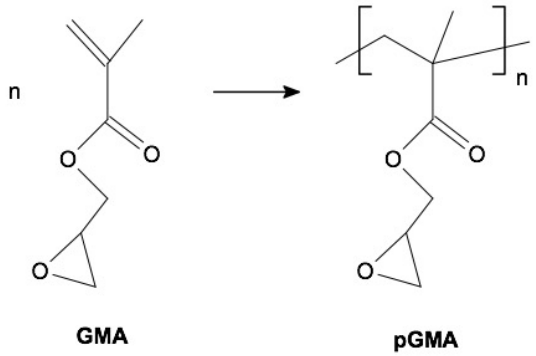

Figure 1.11: Homopolymerisation of GMA into pGMA

1.5.3.2 Copolymerisation

As previously said, copolymerisation of GMA can occur via reaction on the C=C function, resulting in a graft material with the remaining epoxy function. It can also occur on the epoxy function, by opening the epoxy bridge and anchoring desired species. The combination of both mechanisms in two curing stages is referred as dual polymerisation. The first stage forms a network and the second stage increases the network density and improve the mechanical and thermal properties of the material.

a) Grafting of GMA onto unsaturated carbon bonds

Grafting with unsaturated carbon bonds has been studied onto different types of polymers and following different methods. Le gars et al. grafted GMA onto cellulose nanocrystals (functionalised with bromide) at the brominated initiator sites. The reaction was conducted at low temperature, in anhydrous conditions and without any reagents able to react with epoxy functions, to avoid opening of epoxy groups and keep the possibility of further polymerisation [58]. Al-Malaika et al. melt grafted GMA on ethylene-propylene copolymer via free-radical polymerisation, with a peroxide initiator (T101) and the trifunctional coagent trimethylol propane triacrylate (Tris) [54]. Kunita et al. grafted GMA onto PP films using supercritical-CO_2 as a solvent and swelling agent, and benzoyl peroxide as initiator [59].

Effective grafting of GMA can be showed with FTIR technique, by analysing the peak at 1730 cm^{-1} assigned to the carbonyl group in GMA, and the peaks at 845 and 910 cm^{-1} assigned to the epoxy ring. Figure 1.12 is an example of FTIR spectra analysed to determine grafting efficiency. Peaks around 1731 cm^{-1} are present in spectra b, c, d and e, corresponding to PP-g-GMA spectra. Kunita and coworkers also determined the efficiency of the grafting process by immersing the grafted samples in a polymerising polyaniline solution. As epoxy is reactive so

amines, the high reactivity of the surface to polyaniline anchoring was a sign of effective grafting of GMA and of possible anchoring with other species.

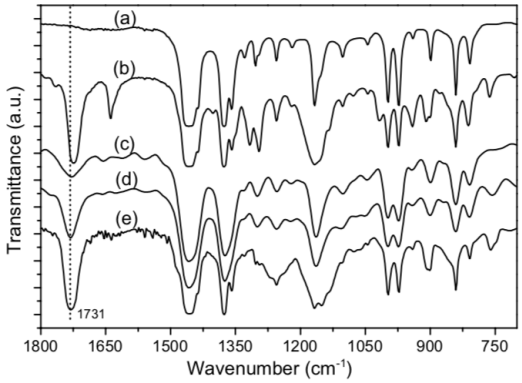

Figure 1.12: FTIR spectra of (a) virgin PP, (b) GMA-soaked PP (step 1, sample A), (c) PP-g-GMA (step 2, sample A, 1 h thermal treatment), (d) PP-g-GMA (step 2, sample A, 4 h thermal treatment), and (e) PP-g-GMA (sample B, 4 h thermal treatment) from GMA grafting on PP studied by Kunita et al. [59]

If grafting of GMA onto hydrocarbon polymers is effective, the efficiency is generally not very high. It can be explained by low reactivity towards macroradicals, difference in polarity, high tendency toward homopolymer formation and side reactions [54, 55]. It can be improved by cografting more reactive bi- or polyfunctional comonomers or coagents. For example, Al-Malaika and Kong, used trimethylol propane triacrylate with MA and antioxidants to increase grafting of GMA on ethylene-propylene copolymer [54]. Jazani and coworkers used styrene to increase grafting of GMA on PP [55].

b) Opening of epoxy bonds

The epoxy function in glycidyl methacrylate is highly reactive with amines, carboxylic and hydroxylic groups. Grafting involving the epoxide while the methacrylate function stays unreacted is however not very common. It is possible with specific initiating system and usually occurs at higher temperatures and with long reaction times [60, 61]. The opening of the epoxy function is usually encountered in a dual-polymerised system. Polymerisation with carboxylic an hydroxylic groups follows a ring opening mechanism. It occurs with different pathways and can result in different products. Reis et coworkers studied the dual polymerisation of GMA with poly(vinyl) alcool (PVA) and poly(acrylic acid) (PAAc). They observed different results depending on the pH of the polymerisation solution [62].

Zhang et al. grafted GMA onto a PE surface using photopolymerisation. Because of their reactivity with amines and after reaction in a dioxane solution, the epoxy groups created covalent bonds with the PE substrate and improved adhesion. FTIR analysis showed easy reaction of the epoxy groups with butylamine and effective hydrolysation with HCl [7]. Tahir et al. grafted GMA onto vinyl modified sepiolite with gamma radiation. The epoxy group of the GMA molecules grafted into sepilite were opened through a ring-opening process using sodium solfite as sulfonation agent [63]. Nystrom et al. grafted GMA onto modified cellulose surface to fabricate superhydrophobic and self-cleaning surfaces. Grafting was done using using 2-bromoisobutyryl bromide and via ATRP. The epoxy group of GMA were hydrolysed in acidic conditions and reacted with pentadecafluorooctanoyl chloride, transforming the surface into an hydrophobic one [64].

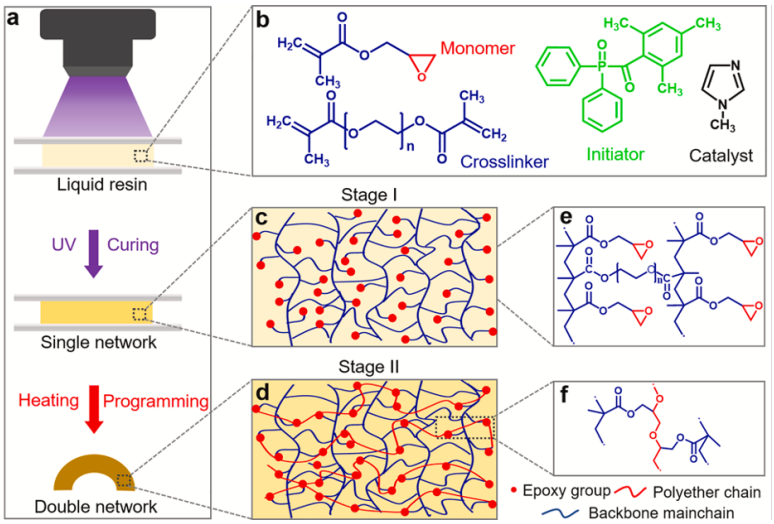

Figure 1.13: Synthesis methodology of dual-curing polymer network systems implemented by Zhang and coworkers [65]

Zhang et al. also synthesised GMA via dual polymerisation for 3D printing and imprint lithography applications. For this reason, GMA was polymerised with photo-activated radical polymerisation using polyethylene glycol dimethacrylate (PEGDMA) as crosslinker and diphneyl(2,4,6-triethylbenzoly) phosphine oxide (TPO) as the photoinitiator. The opening of the double carbon bonds formed a 2D crosslinked. The second stage was thermally activated estherification which increased the network density by opening the epoxy groups [65]. The process is represented in Figure 1.13.

Jazani et al. used GMA grafting to improve PET and PP blending. GMA was grafted onto PP via free-radical polymerisation using dicumyl peroxide as initiator and styrene as coagent. The formed PP-g-GMA was added to PET to

produce PET/PP-g-GMA via the reaction of PET carboxyl end-groups and epoxy. Grafting of GMA up to 6successfully increased impact strength [55]. The schematic representation of the reaction is shown in Figure 1.14.

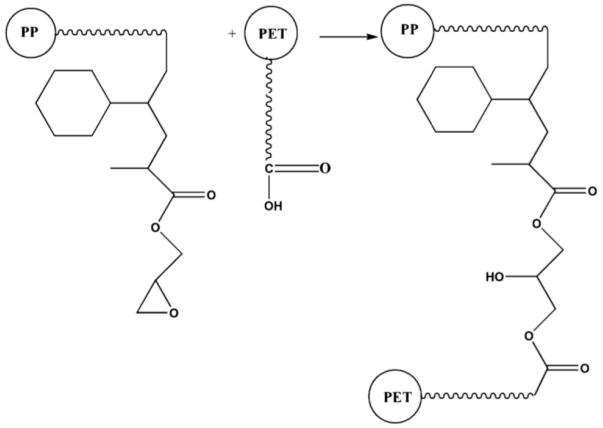

Figure 1.14: Schematic representation of reaction between PET end-groups and GMA grafted onto PP backbone, as studied by Jazani and coworkers [55]

1.5.3.3 Curing properties

a) Processing conditions Given Zhang et al., the mechanical performance of a polymer (especially cured from a dual-stage process) varies with several parameters: concentration of catalyst, stability of epoxy group, processing temperatures, curing time [65]. The catalyst concentration and processing temperature are the most important.

- Catalyst concentration: In dual stage polymerisation, Zhang et al. varied catalyst concentration from 0.5 to 2 wt%. They concluded that 0.5 wt% was too low to complete the reaction and that the mechanical properties increased with increasing catalyst concentration [65]. Jazani et al. also observed an increase in grafting with increased DCP content, but this lead also to increase in chains scission [55]. Wang et al. varied GMA concentration in GA photopolymerisation and determined that 2 wt% was the best concentration since it had the highest enthalpy. They explained this maximum enthalpy by reaction of chain radicals with the primary radicals, screening and self-termination effects of the primary radicals [66]. Al-Malaika et al. observed an increase in grafting yield with higher peroxide concentration due to higher macroradicals sites generation and crosslinking of polymer. However, they also observed an increase in polymer viscosity and polymer degradation due to higher peroxide yield [54].

- Processing temperature: Zhang et al. observed increasing mechanical properties with temperature increasing from 90 to 180℃ and stabilisation with temperatures higher than 180℃ [65].

b) Curing behaviour

Side-reactions Jazani et al. noticed a decrease in degree of grafting with increase of GMA concentration, suggesting partial homopolymerisation of GMA via free-radical mechanism [55]. During grafting of GMA onto EP, Al-Malaika et al. also noticed side-reactions such as homopolymerisation of GMA, crosslinking and chain scission of EP [54].

Kinetics Free-radical polymerisation of methacrylates shows a frequent behaviour called the "Trommsdorf effect". When conversion of the methacrylate monomer surpasses a certain critical value (about 20%), the viscosity increases. It creates a "gel effect" that prevents the diffusion of radicals and growing chains, and combination of chain ends. This leads to a decrease in rate of termination. The exothermic reaction will self-accelerate and the temperature inside the resin will increase. Because thermal conductivity of the medium is poor, a peak temperature point is reached [67, 19]. If the temperature is locally exceeded, it will lead to monomer boiling and creation of voids in the matrix. Such porosities can greatly influence mechanical properties of the resin. Figure 1.15 represents the conversion of benzoyl-initoated methacrylate polymerisation of MMA in benzene. Figure 1.16 represent the dependence of the graft density of GMA onto PE sheet on polymerisation time [54]. Both figures show typical curves of methacrylate polymerisation with Trommsdorf effect, depicting a clear acceleration and saturation.

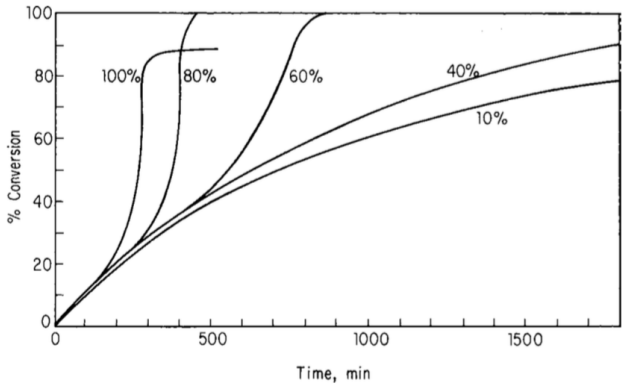

Figure 1.15: Autoacceleration in benzoyl peroxide–initiated polymerisation of methyl methacrylate in benzene at 50℃. [14]

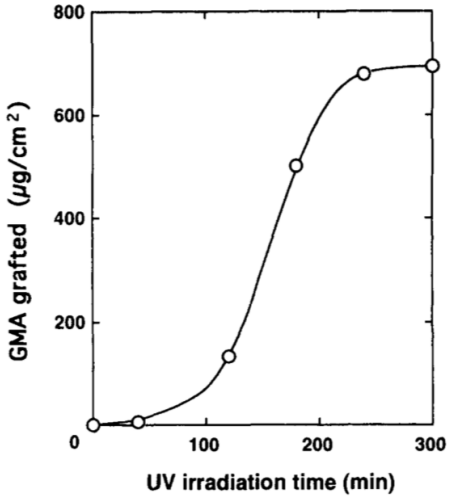

Figure 1.16: Grafting of GMA onto PET sheet with UV radiation time [54].

Given researches conducted by Gayot et al., control of the polymerisation is essential to avoid creation of cavitation. For example, using an external source is a common technique to reduce the polymerisation time and control the maximum temperature in the matrix. They implemented thermo-mechanical models to predict the occurrence of monomer boiling with temperature [68].

Chapter 2

Materials and methods

The objective of this study is to produce a modified GMA resin with increased thermal and mechanical properties. The material produced has to be biosourced to limit the impact on the environment. For these reason, POST-C PET was used to synthesise unsatured polyester (UP). Polymerisation was conducted using the ethylenic functions of UP and GMA, the end groups of UP and the epoxy ring of GMA.

This section focuses on the experimental part of this work. It reviews the different materials used and explains the steps employed to produce unsaturated polyester and to cure the resins. It also reviews the characterisation methods applied for analysing the different steps and components of the system. These methods are of different kinds: thermal (DSC, TGA), spectroscopic (FTIR, Raman), mechanical (DMA) and related to the analysis of polymer surfaces (SEM).

2.1 Materials

Polyethylene terephtalate granules were purchased from Equipolymer under the trade name LIGHTER^{TM}C88 with T_m of 247℃, T_g of 78℃, bulk density (ρ) of 0.88 gcm^{-3} and crystallinity superior to 50%. This type of very crystalline PET was designed to minimise the formation of acetaldehyde and is suitable for the processing of still and carbonated mineral water bottles [69]. 1,3-propanediol (PD, 99%), citraconic anhydride (>98%) and Antimony(III) oxide (>99.6%) were purchased from Alfa Ceasar. Zinc acetate dehydrate, 2-methyl-1,3-propanediol (MD, 99%), glycidyl methacrylate (>97%), benzoyl peroxide (75%) and *N,N*-Dimethylaniline (99%) were purchased from Sigma-Aldrich. Dichloromethane (99.8%) and methanol (98.5%) were also purchased from Sigma-Aldrich and used for solubilisation and precipitation of UP. All the chemicals were used as received.

2.2 Methods

This section presents the different steps used to synthetise unsaturated polyester from polyethylene terephtalate and to cure the resins. PET is first prepared to have the same grade as POST-C PET. PET flakes are then depolymerised with diols and repolymerised with citraconic anhydride and diols to form unsaturated polyester. UP is then used to polymerise with GMA. Curing of the UP/GMA mixture will form a resin. A summary of the transformation from PET to a cured resin is represented at the end of this subchapter in Figure 3.6.

2.2.1 Preparation of PET

The preparation of PET consists in physically modifying the synthetic PET to decrease its crystallinity and increase its contact surface. Modification is done by extrusion, pelletrisation and grinding. The modified PET will have a similar grade as the one of used (POST-C) PET. Samples of synthetic PET, extruded and pelletised PET, and grinded PET are represented in Figure 2.1a, 2.1b and 2.1c.

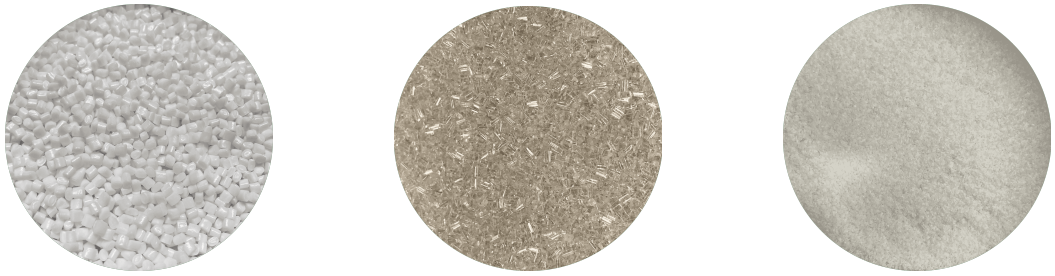

(a) **(b)** **(c)**

Figure 2.1: Samples of (a) synthetic PET (b) extruded and pelletised PET (c) grinded PET

2.2.1.1 Extrusion

Extrusion is a thermo-mechanical process used to create objects with a fixed cross-sectional profile. The material in the form of pellets or flakes is melted and pushed or forced through a die of the required cross-section. The extruded material, called the extrudate, leaves the die with the shape of the die opening and is quenched, i.e. cooled rapidly, to avoid crystallisation [70, 71].

A single screw extruder consists in three different sections, represented in Figure 2.2 [71].

- **Feed zone**. The polymer flakes or pellets are fed into the hopper and enter the heated barrel through the throat. It is sent to the melting zone with the rotary motion of the screw.
- **Melting zone**. The polymer melts by both the shear heating and the barrel heat.
- **Melt pumping zone**. The melted polymer is pushed through the filter screen into the die and out, where it takes the shape of the die.

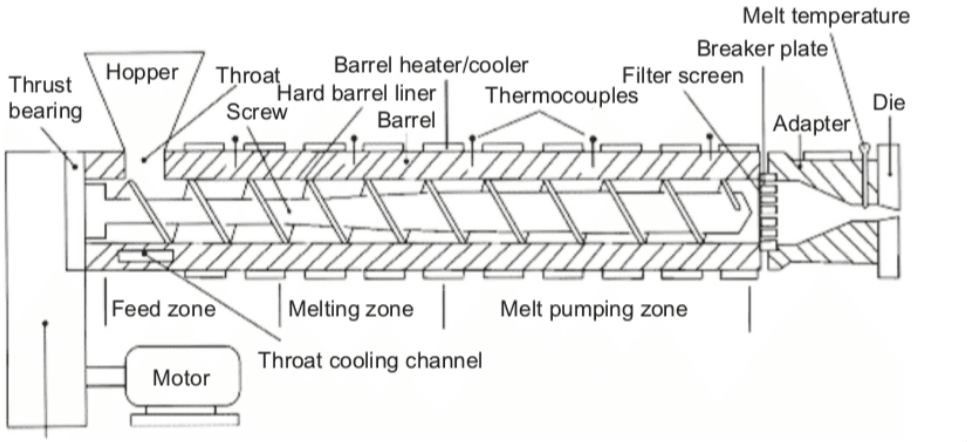

Figure 2.2: Cross section of a single screw extruder [71]

The extrusion process mainly involves solid conveying, homogeneous melting and plasticating, and melt pumping. The performance of the extruder is determined by the screw and varies with the ratio of its length to diameter. This ratio influences the mixing and uniformity of the output. Screws extruders are differenciated into single screw and multiscrew extruders (mainly twin-screw extruders). Single screw extruders are preferred for their low cost, simple designs, ruggedness and reliability. Twin-screw extruders provide better homogeneous mixing of the different ingredients [71].

The extrusion of synthetic PET was performed with the *Process 11 Parallel Twin-screw Extruder* provided by Thermo Scientific^{TM}, represented in Figure 2.3. This extruder is represented in Figure 2.3 and was used with the parameters given in Table 2.1.

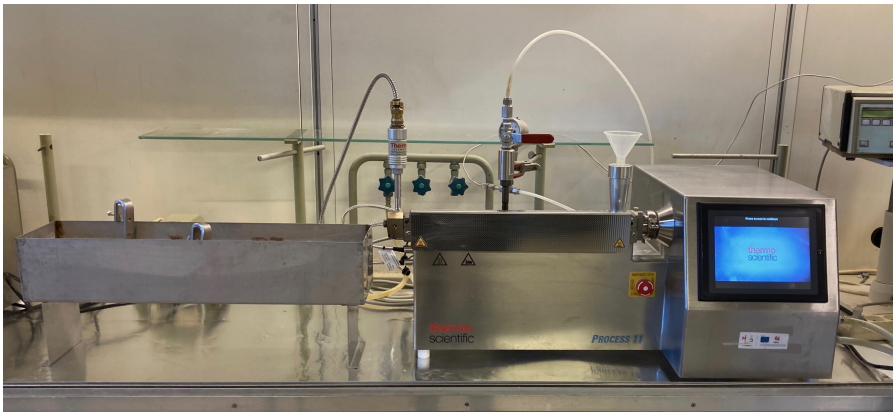

Figure 2.3: Thermo Scientific^{TM} Process 11 Parallel Twin-screw Extruder.

Table 2.1: Parameters of the Process 11 Parallel Twin-screw Extruder used for the extrusion of synthetic PET pellets

Temperature [°C]						**Rotation speed** [rpm]	**Torque** [%]
$\mathbf{T_2}$	$\mathbf{T_3}$	$\mathbf{T_4}$	$\mathbf{T_5}$ & $\mathbf{T_6}$	$\mathbf{T_7}$ & $\mathbf{T_8}$	$\mathbf{T_{die}}$		
205	245	250	255	260	260	100	50-60

The filament extruded is quenched and cut into uniformed pellets using the *VariCut Pelletizer* supplied by Thermo Fisher Scientific^{TM}. The pellets after extrusion have a grade similar to the one of used PET pellets. They are represented in Figure 2.1b.

Figure 2.4: Thermo Scientific^{TM} VariCut Pelletizer

2.2.1.2 Grinding

Grinding is used to increase the surface area of the material to maximise the yield of further reaction. It transforms pellets into a powder using impact with a rotor rotating at high speed and by shearing. The extruded pellets of PET are powdered using the *Variable Speed Rotor Mill Pulverisette 14* from Fritsch. This grinder is represented in Figure 2.5.

Figure 2.5: Variable Speed Rotor Mill Pulverisette 14

The extremely high speed of the rotor increases the temperature inside the grinder. The PET pellets are thus required to be first cooled into liquid nitrogen to avoid melting in the grinder. They are then fed through a funnel into the grinding chamber. The material accelerates outwards radially due to the high speed of the rotor and is caught by the impact rotor. It is grounded, and then discharged through the sieve ring into the collecting vessel. The speed of the rotor can be adjusted. 10 rpm was selected for the PET pellets. The mechanism of grinding is represented in Figures 2.6a and 2.6b [72].

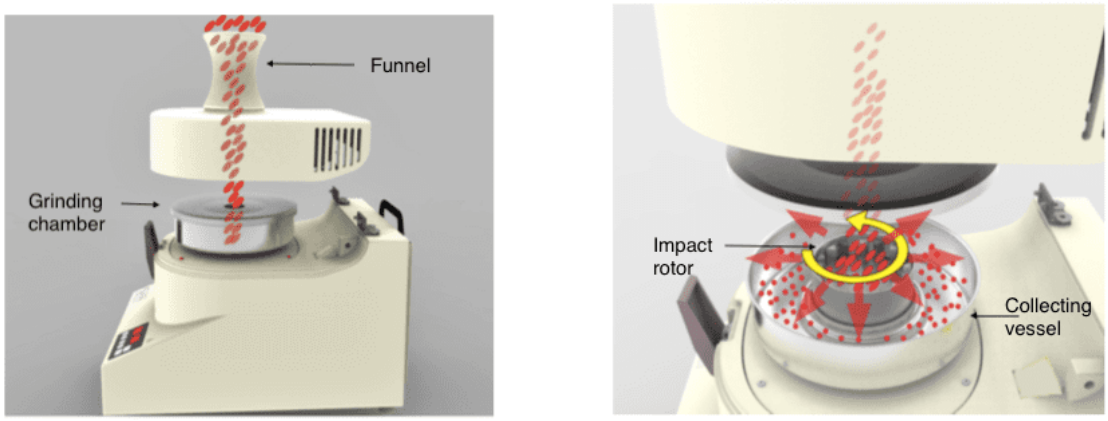

(a) **(b)**

Figure 2.6: Operating principles of the grinding process (a) feeding (b) powdering (adapted from [72]).

2.2.2 Depolymerisation by glycolysis

PET is depolymerised by a glycolysis reaction. It consists in the transesterification of PET and the destruction of the polymer chain to decrease the molecular weight. A diol is used as glycolysis agent in PET/diol mass ratio of 1/6 with about 0.1% (w/w PET) of zinc acetate dehydrate as catalyst. Two diols different diols were used: 1,3-propanediol (PD) and 2-methyl-1,3-propanediol (MPD). The masses of the components used for each sample of depolymerisation are given in Table 2.2.

Table 2.2: Parameters for the chemicals used in the glycolysis reaction

Material	**Quantity [mg]**
PET	50000
Diol (PD or MPD)	8160
Zinc acetate dehydrate	54.73

All the components are stirred with methanol at 35℃ in a 250-mL flat-bottom flask equipped with a reflux condenser and magnetic stirrer. Stirring is done to homogenise the dispersion of diol and optimise mixing. When the methanol is evaporated (usually after 12 hours), the components are heated at 175℃ for 30 minutes. This helps the diffusion of diols into the mix. The components are then heated at 200℃ for 2 hours for the glycolysis, and more specifically the transesterification to happen. An electric probe is used to control the temperature inside the flask and a distillation column is used to condense water and avoid evaporation of low molecular mass reactants. After the reaction, the glycolysed

PET contains oligomers (GPET) and monomers (BHET) of PET. The glycolysed product is cooled to room temperature, grinded and mixed with distilled water at 100℃. The oligomers are separated from the mixture by solubilisation of BHET in water, decantation of GPET and filtration. BHET is not used for further polymerisation because of its low molecular weight. Oligomers are preferred to increase the efficiency of the process, decreasing its cost. The reaction using 1,3-propanediol is given in Figure 2.7. The mechanism is similar when using 2-methyl-propanediol. The different steps of the depolymerisation process are illustrated in Appendix A.1.

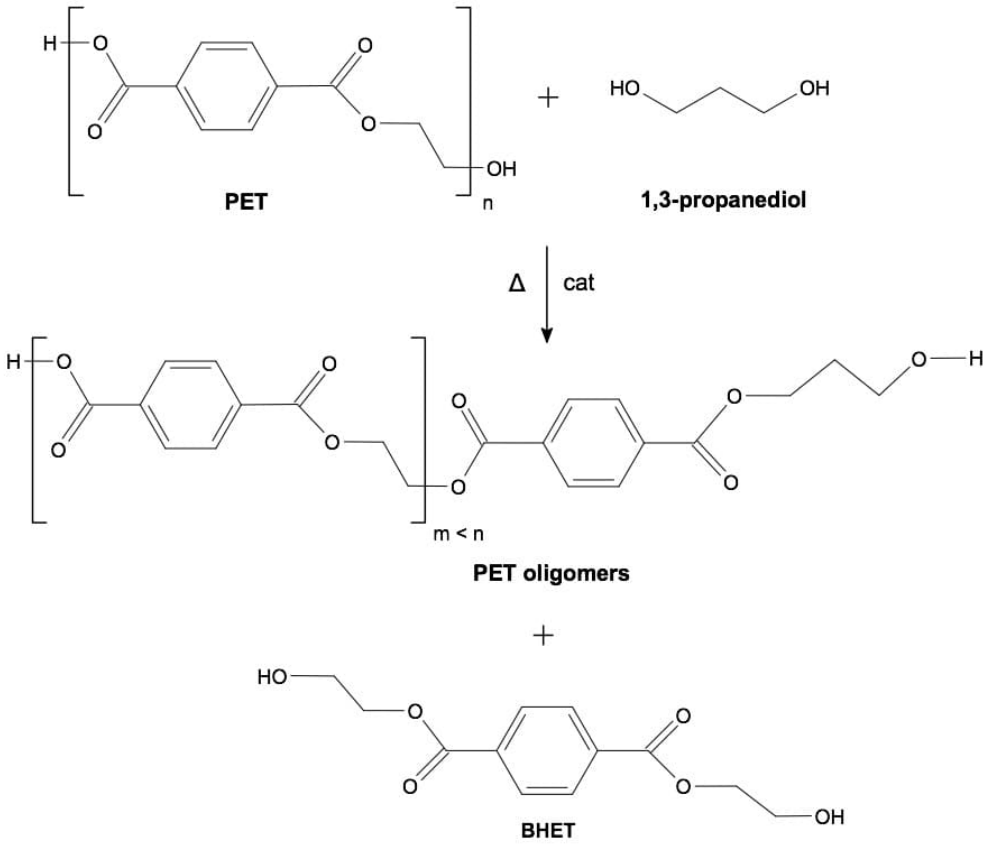

Figure 2.7: Reaction of glycolysis: transesterification with 1,3-propanediol

2.2.3 Repolymerisation

The reaction of repolymerisation consists in producing unsaturated polyester (UP). The glycolysed PET reacts with citraconic anhydride, diol (PD or MPD) and antimony oxide (Sb_2O_3) as catalyst, under nitrogen atmosphere. Citraconic anhydride acts as crosslinker and provides the ethylene group that makes the product unsaturated. It can also help increase thermal resistance of synthetised UP. The diol homogenises the mixture and facilitates the mixture with CA. The quantities of the chemicals used are provided in Table 2.3.

Table 2.3: Masses of the chemicals used in the repolymerisation reaction

Component	**Proportion [mg]**
GPET	40000
Citraconic anhydride	3161
Diol (PD or MPD)	1560
Sb_2O_3	29.5

Citraconic anhydride is first stirred and heated with diol (PD or MPD) and the catalyst in a three-necked glass reactor equipped with a magnetic stirrer, a nitrogen inlet tube and a distillation column. They react at 150℃ for 2 hours to form the crosslinker. The glycolysed PET is then added and reacts with the other components at 200℃ for 15 hours. An electric probe is also used to control the temperature of the reaction inside the glass. The unsaturated polyester is obtained by precipitation of the product (using dichloromethane as solvent) into methanol and filtration. The reaction is represented in Figure 2.8. UP is dried before use in a vacuum chamber at 50℃. The different experimental steps are illustrated in Appendix A.2.

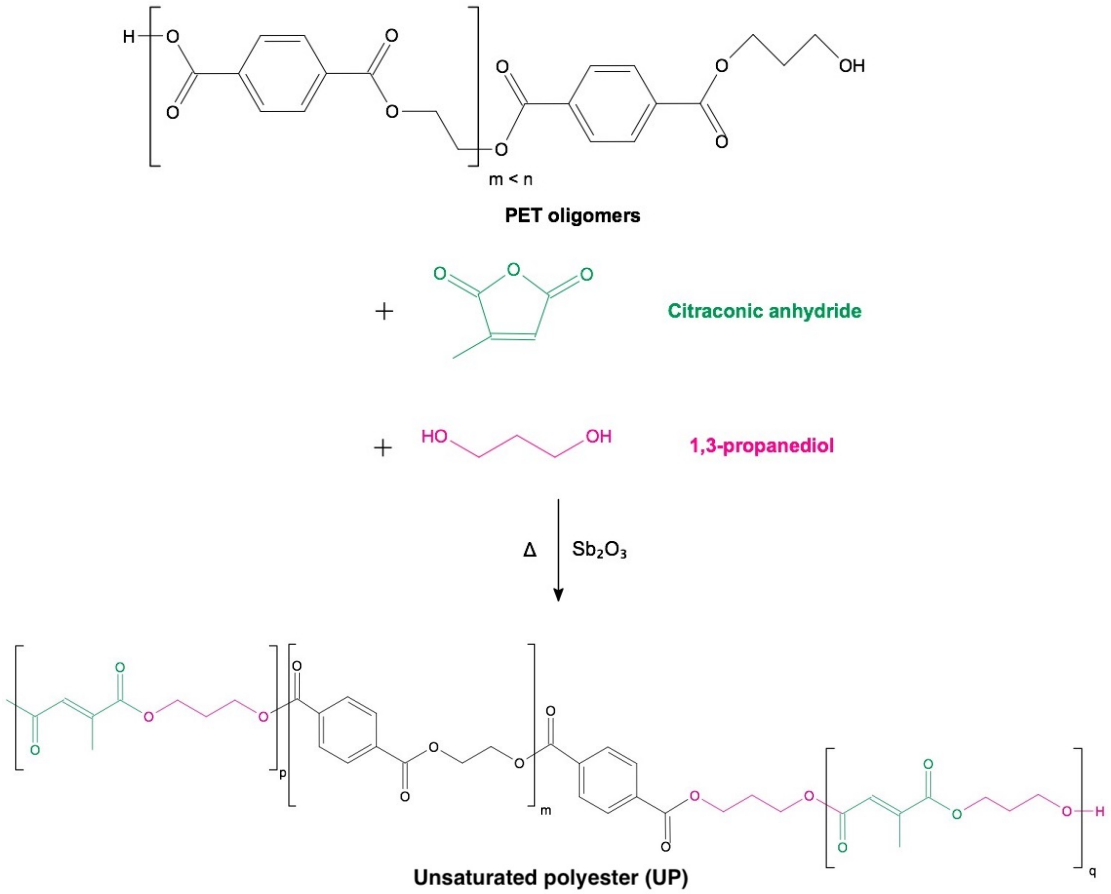

Figure 2.8: Reaction of repolymerisation from PET oligomers with citraconic anhydride as crosslinker and 1,3-propanediol.

2.2.4 Curing of resins

Resins are made of unsaturated polyester, glycidyl methacrylate and benzoyl peroxide through a multi-step polymerisation process. The first step of the curing reaction is the radical polymerisation of the ethylenic function of UP with the ethylenic function of GMA. Then, the epoxy ring reacts with the UP end of chains through a ring-opening mechanism.

The resin is prepared by mixing the GMA and UP at 80°C for 1.5 hours. The solution is cooled down to add BPO and mixed at room temperature for 5 minutes. The mixture is degassed and poured into a mold (cylindrical or rectangular) conditionned with *LOCTITE ® FREKOTE 770NC* and *Chemlease ® 41-90 EZ*. The resin is cured using a vacuum chamber as represented in Figure 2.9 and following a specific cycle that will be determined in the next chapter. The curing process is represented in Figure 2.10.

Figure 2.9: Vaccuum pump chamber

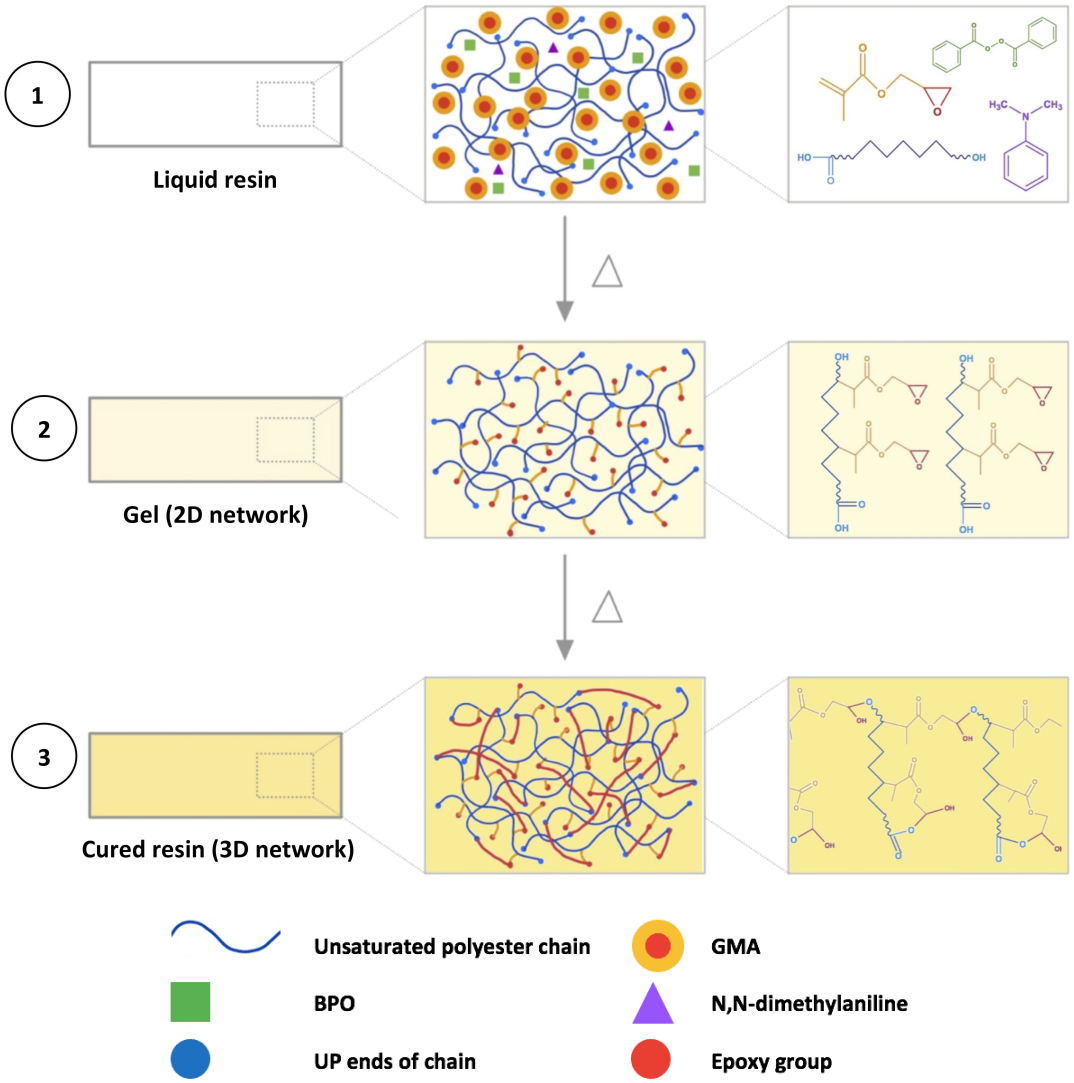

Figure 2.10: Polymerisation of GMA resin with UP using benzoyl peroxide as initiator

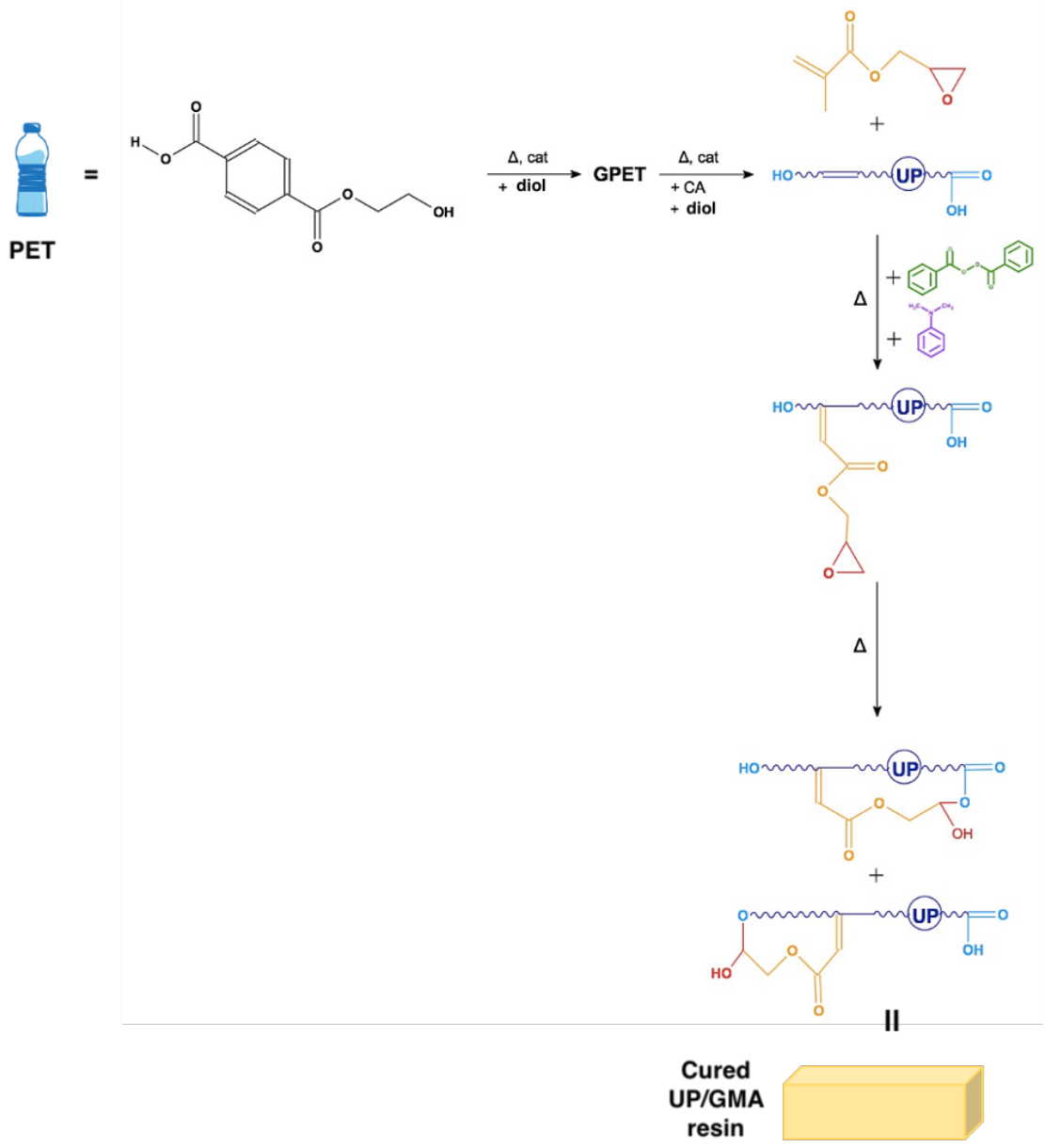

Figure 2.11: Summary of the recycling process of a bottle of PET into a UP/GMA resin.

2.3 Characterisation methods

2.3.1 Thermal analysis

2.3.1.1 Differential Scanning Calorimetry

Differential Scanning Calorimetry (DSC) is a thermoanalytical technique used to measure the heat flow of a sample while it is cooled, heated or held isothermally in a defined atmosphere. It can determine thermal transitions such as the glass transition temperature, the melting temperature, the crystallisation temperature (T_c), but also the specific heat capacity (c_p) and the enthalphy (ΔH) [73]. Different heating rates ranging from 1 μKmin^{-1} to 10 Kmin^{-1} can be used [74].

A DSC device is made of a thermal scanning chamber (also called measuring cell) and a computer. As represented in Figure 2.12 below, the system uses two pans for heating and cooling in the thermal scanning chamber: one is empty and is used as reference, and the second one holds the sample to be analysed [74]. Samples have sizes varying from 0.5 to 10 mg and are kept in very small aluminium cups. Both polymer sample and reference are heated (usually in inert atmosphere) and thermal transitions in the sample are measured [15] .

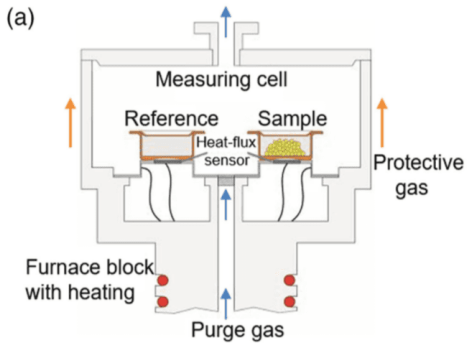

Figure 2.12: Schematic representation of a DSC device. Adaptated from [75].

A conventional DSC curve of a semi-crystalline polymer is represented in Figure 2.13. The measurement signal is the energy absorbed by or released by the sample (in mW) and is represented as a function of time or temperature [73]. The transition in 3 is the glass transition, where the polymer chains relax and switch from a glassy to a rubbery state. At temperatures higher than T_g, polymers become soft and can be moulded and processed. The glass transition is reversible and characteristic to amorphous and semicrystalline materials. The exothermic peak in 4 is the cold crystallisation, a reorganisation of the chains and a formation of small

crystallites at relatively low temperatures. It appears while heating samples that have been cooled very quickly and did not get time to crystallise. The transition in 5 is the melting, when the sample changes from a solid to a liquid state due to a complete relaxation of the chains. The peaks are endothermic and occur at different temperatures depending on the substance. They can be more or less concentrated, depending on the polydispersity of the polymers and the relaxation of the chains.

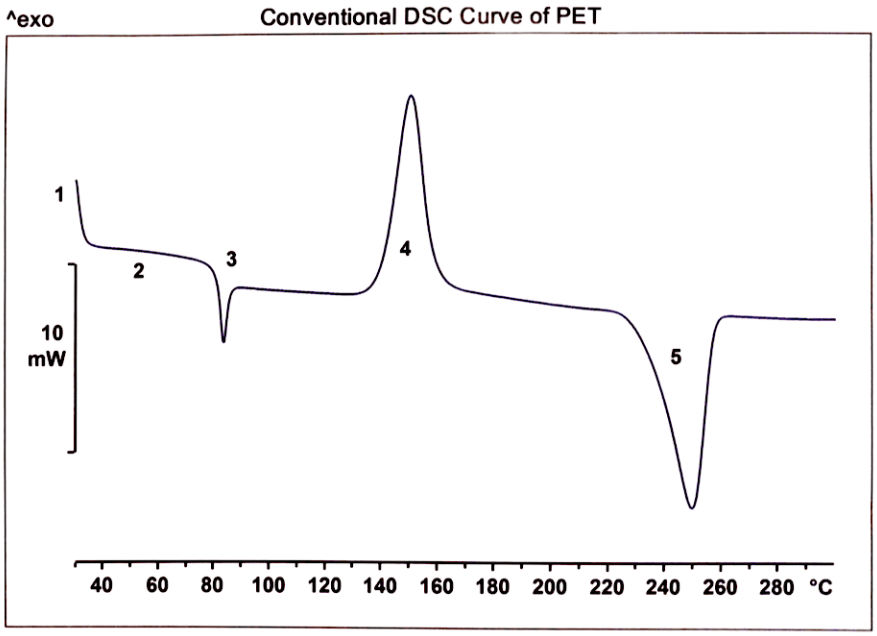

Figure 2.13: Conventional DSC curve of semicrystalline polymer showing the typical steps: (1) Initial deflection proportional to the heat capacity of the sample, (2) change of c_p with no other thermal effect, (3) glass transition of amorphous fraction, (4) cold crystallisation and (5) melting of the crystalline fraction [76].

Different techniques of DSC analysis have been performed and will be presented in this work:

- **Heating-cooling-heating experiments** have been used to characterise the different forms of PET during chemical modification (PET extruded, GPET and UP). They are used to eliminate thermal history of materials and determine their thermal behaviour. During the first heating and cooling, the sample is preheated and crystallises. A second heating gives information such as the glass transition (T_g), crystallisation (T_c) and melting temperatures (T_m), but also the corresponding enthalpies of crystallisation (ΔH_c) and melting (ΔH_m). The degree of crystallinity, i.e. the percentage crystalline

content, χ_c of the material can also be determined by equation (2.1). ΔH_f is the measured melting enthalpy during melting from room to final temperature and ΔH_f^0 is the melting enthalpy of a purely crystalline sample. For PET, it is about 140 [Jg^{-1}]. [73, 77, 78].

$$\chi_c = \frac{\Delta H_f}{\Delta H_f^0} = \frac{\Delta H_c + \Delta H_m}{\Delta H_f^0} \tag{2.1}$$

- **Single heating experiments** were performed on "crude mixtures", i.e. not reacted, to determine the enthalpy of reaction (ΔH_r) of a sample. This enthalpy is found by calculating the total area under the curves of the exothermic peaks. Parameters such as the influence of a reactant or the heating rate can be analysed.
- **Single heating experiments** were performed on cured mixtures to determine the residual enthalpy of reaction and the glass transition temperature of the polymer formed.

The DSC measurements presented in the following chapters were performed using the *DSC1* equipped with an *FRS5 sensor* and the *HP- DSC827*^{e}. All devices are from Mettler Toledo. The results were evaluated with the STARe Software.

2.3.1.2 Thermogravimetric Analysis

Thermogravimetric analysis (TGA) is a thermal analysis technique that measures the weight (hence the mass) of a sample as it is heated (cooled) or held at constant temperature in a defined atmosphere. TGA can provide information on the thermal stability and the composition of a sample. It can determine mass changes (gain or loss) of the sample and characteristic temperatures related to these changes. The DTG curve, i.e the first derivative of the TGA curve with time, can be represented to show the rate mass change, hence the rate of decomposition of the sample [73, 75].

As represented on Figure 2.14, the sample in a specific aluminium container (or "sample pan"). The pan is positionned on a sample holder in the furnace and connected to the thermobalance. The temperature is measured using a thermocouple which is in contact with the container. The weight of the sample is continuously measured with the thermobalance as the system is heated using an electric furnace and the temperature is increased [79].

The measurements are represented in terms of loss in mass (in % of the initial sample mass) as a function of time or temperature. As represented on the conventional TGA curve of a polymer on Figure 2.15, the loss in mass can be

related to the loss of volatile components (moisture, solvents, monomers), polymer decomposition or combustion of carbon (carbon black or carbon fibers) and final residues (ash, filler, glass fibers) [80].

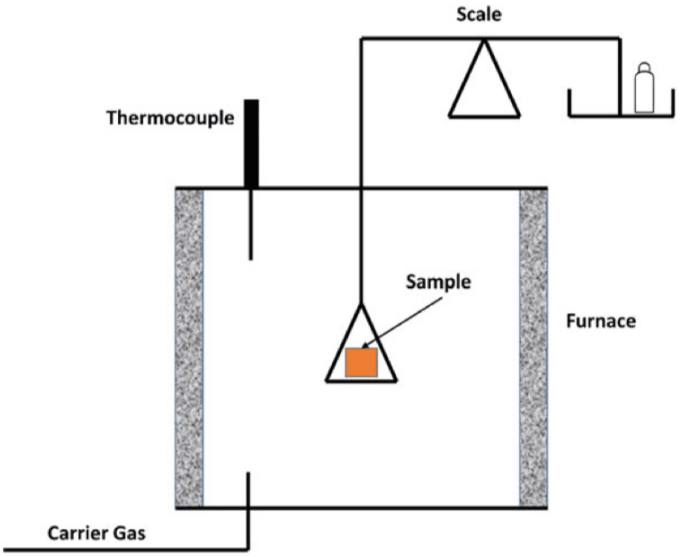

Figure 2.14: Schematic representation of a TGA device [79].

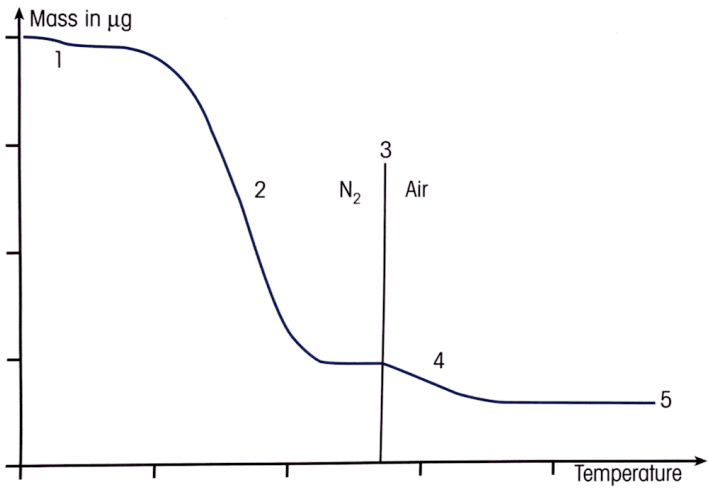

Figure 2.15: Conventional TGA curve of a polymer showing the typical mass loss steps: (1) volatile compounds, (2) polymer decomposition, (3) change of atmosphere, (4) burning step of carbon and (5) residues [80].

The TGA measurements presented in the following chapters were performed

using the *TGA/SDTA851^e* from Mettler Toledo. The results were evaluated with the STARe Software.

2.3.2 Spectroscopic methods of analysis

2.3.2.1 Fourier Transform Infrared spectroscopy

Fourier Transform Infrared Spectroscopy (FTIR) is an experimental method that uses the principles of spectroscopy. It is used to analyse qualitatively and quantitatively organic, inorganic and polymeric materials. It provides information on the substance chemical composition, such as molecular structure, chemical bonding and molecular environment and is thus useful to identify unknow materials, detecting contaminants or additions and identifying decomposition and oxidation. [15, 81, 82]. IR is most useful to indicate the presence or absence of specific functional groups.

Figure 2.16 schematically represents the mechanism of a FTIR device. It includes a source, a sample cell, a detector, an amplifier, an A/D convertor and a computer. The sample is exposed to infrared light repeating the exposure of various frequencies ranges (about 100-10,000 cm^1). During exposure to the broad spectrum energy, some wavelengths are absorbed in the material and cause the molecules to vibrate. The conversion of infrared light (by the interferometer) into molecular motion absorbs some of the applied energy while some goes through or pass the sample. The energy that makes it through is recorded by the detector, the signal is amplified by the amplifier and converted to a digital signal by the A/D convertor. It is then transferred to the computer where the Fourier transform is carried out [82].

FTIR results are represented graphically by a spectrum of the material, where the light absorbed (or transmitted) is given in terms of wavenumber, ranging from 400 cm to 4000 cm^1. It represents the amount of energy that has been absorbed at each wavelength. The shape, position and intensity of the peaks are related to the chemical compounds and functions present in the sample. The spectrum is sometimes referred to as the sample's molecular footprint" [82]. The peaks in the high frequencies (> 1500 cm^{-1}) are related to specific functional groups while the peaks in low frequencies (< 1500 cm^{-1}) are characteristic of the molecule behaviour. Below 1500 cm^{-1} the absence of a bond is more meaningful than its presence [83]. Typical analysis of FTIR spectra will start with the high frequencies to identify the functional groups present. Table 2.4 is used to identify those peaks.

The FTIR measurements presented in the following chapters were recorded using the *Nicolet iN10* from Thermo Scientific^{TM}, in transmission mode collecting

64 scans in the wavelengths range of 600 to 4000 cm^{-1}. The peaks were normalised with the harmonised peak in 1953 cm^{-1}. The peaks in 1508 and 1610 cm^{-1} corresponding to the benzene ring of glycidyl polyethers could also have been used as a reference [84].

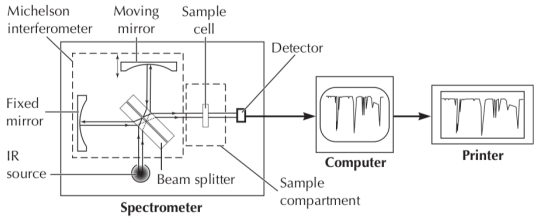

Figure 2.16: Schematic representation of a FTIR device [85]

Table 2.4: Wavelengths associated to chemical functions in polymers [43, 47, 55, 59, 63, 86, 87, 88]

Chemical function	**Wavelength [cm^{-1}]**
Stretching vibration of double bond of the methacrylate group	813
Stretching vibration of oxirane group C-O-C	830-845
Stretching vibration of oxirane group C-O	905-915
Stretching vibrations of ether groups -R-C-O-O-R'	1015
Stretching vibration of ether groups -R-O-R'	1035
Symmetric oxirane ring deformation of the epoxy group	1247
Stretching vibration of para-sub of hydroxyl end-groups	1507
Stretching vibration of aromatic cycles C-C	1510
Stretching vibration of aromatic cycles C=C	1608
Stretching vibration of ethylenic double bond -C=C- of GMA	1640
Stretching vibration of ethylenic double bond -C=C- of UP	1650
Stretching vibration of carbonyl end-groups -C=O of GMA	1710-1730
Symmetrical stretching of methylene	2870
Assymmetrical stretching of methylene	2960
Stretching vibration of acid end groups -COOH	3270
Stretching vibration of hydroxyl end-groups -OH	3431-3550

2.3.2.2 Raman Spectroscopy

Raman spectroscopy is a spectroscopic technique that uses Raman scattering of monochromatic laser light. The mechanism is based on the *Raman effect*, which responds to the symmetrical vibrational modes [15].

A laser beam is used to illuminate the sample. The electromagnetic radiation from the laser is collected with a lens and passes through a collimator. When the light hits the molecules, they will become excited, switch from an excited state from a ground state and will relaxed into a vibrational excited state. It creates the Stokes Raman scattering: the light is scattered and its frequency will vary depending on the scattering molecules. [15, 82].

Raman spectroscopy is used to identify polarisable groups. It is effective to detect symmetrical stretching in C-C bonds and has been applied by comparing polymer chains with long-chain "model" alkanes [15]. In particular, it is used in this work to identify the conversion of C=C bonds in GMA. It can be calculated with equation 2.2,

$$\text{Conversion } [\%] = 1 - \frac{A_i(1640)/A_i(1610)}{A_0(1640)/A_0(1610)} \tag{2.2}$$

where A_i is the absorbance at temperature i, A_0 is the absorbance of the uncured mixture, A(1610) is the aromatic peak at 1610 cm^{-1} and A(1640) is the reactionary methacrylate at 1640 cm^{-1} [89]. The wavelengths of the functional groups are of the same order as for FTIR.

The Raman measurements presented in the following chapters were recorded using the *DXR Raman Microscope* from Thermo Scientific™ with the TH4-200 laser from Olympus.

2.3.3 Characterisation and analysis of polymer surface

Characterisation of polymer surface requires extremely smooth surfaces. Before SEM and ATR analysis, the samples are polished using the manual polisher *FORCIPOL102* with Si-C paper of 80, 320, 600, 800 and 1200µm, and the *Allied High Tech Techprep Polisher* with the magnetic plate #5-2005M and MD-Piano disks of 1200 and 4000µm, and the MD-Dur disks with AP-D 0,3ppm as agent.

2.3.3.1 Scanning Electron Microscopy

Scanning Electron Miscroscopy (SEM) is a characterisation technique used to visualise and characterise materials surfaces.

The schematic representation of SEM principle is represented in Figure 2.17. SEM scans the sample surface with a very fine electron incident beam, created from thermionic sources or from field emission gun (FEG) sources. The beam passes through several electromagnetic lenses before hitting the surface. The

electrons interact with the sample surface and penetrate the sample. They emit backscattered (or primary) electrons and secondary electrons. Secondary electrons are weak energy electrons, meaning only the ones close to the surface of the sample can be ejected out of it. These secondary electrons are collected by specific detectors to produce a signal. Electronic devices amplify the detected signals to display them as high-resolution images (about 100Å (10nm)). These images correspond to a distribution map of the signal intensity emitted from the scanned area of the specimen. The high sensitivity of the secondary electrons towards surface variations gives information on the topography of the sample [15, 70, 82].

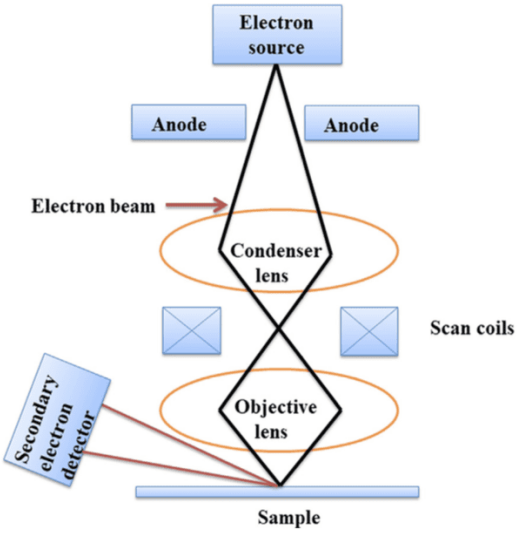

Figure 2.17: Schematic representation of a SEM device [82]

The SEM images provided later in this work have been recorded with the *Scanning Electron Microscopy 7600F* supplied by JEOL. A vacuum pump system was also used to limit the noise and to avoid the broadening of the beam [70]. The samples were prepared by coating with a thin conducting material layer of about 8 mm (Pt). The coating guarantees a good interaction between the electron beam and the sample.

2.3.4 Mechanical properties

2.3.4.1 Dynamic mechanical analysis

Dynamic mechanical analysis (DMA) is a thermalmechanical technique used to measure mechanical properties of a viscoelastic material. The material is subjected to a sinusoidal mechanical stress and the measured properties are given as a function

of time, temperature and frequency. It also measures thermal effects based on changes in the modulus or damping behaviour of the sample [73].

A typical measurement consists in applying an oscillating force at different frequencies. This techniques measures the storage (E' or G') and loss modulus (E" or G") respectively. The storage modulus E' determines the elastic behaviour of the sample while the loss modulus E" determines its viscous behaviour. These results can then determine other effects such as the mechanical loss factor, also called the damping factor and represented as tan δ. It is calculated as the ratio between the storage and the loss modulus : $\tan\delta = \frac{E''}{E'}$. DMA is more sensitive than other methods and can thus measure transitions and effects difficult to detect with DSC, TMA or TGA such as the β relaxation, i.e. the local movement of polymer groups or the glass transition of filled materials or thin layers [73, 90].

In this work modulus E is calculated with the equation of the complex modulus in equation (2.3) [91].

$$|\mathrm{E}^*| = \sqrt{(E')^2 + (E'')^2} \tag{2.3}$$

The complex modulus (also called dynamic modulus) E^* is actually the data measured during the DMA analysis and used to determine E' and E" [92]. It is defined as the instantaneous ratio of the stress/strain under vibratory conditions [93].

The DMA measurements presented in the following chapters were performed using the *DMA/SDTA861^e* from Mettler Toledo. The configuration chosen for the experiments is tension. Samples were prepared with dimensions of L x W x H = 9 x 2 x 0.5mm. The method used consists of heating the sample from about 0℃ to 150℃ at a rate of 3Kmin^{-1} and setting the oscillation frequency at 1 Hz. The amplitude selected for the force and the strain is 0.5 N and 1 1μm respectively. The results were evaluated with the STARe Software.

Chapter 3

Results and discussion

As explained in the previous sections, glycidyl methacrylate is a bifunctional epoxy resin. However, it has a tendency to homopolymerise through its C=C function and less with the epoxy function. Its synthesis with unsaturated polyester from PET waste bottles aims at valorising both functions to produce a denser network. Valorising PET waste has an important ecological and economic purpose.

Before curing, industrial grade of PET is physically modified to have a similar grade as bottle-grade PET. This PET is then chemically modified by recycling through glycolysis and repolymerisation into unsaturated polyester. Chemical modification decreases the glass transition temperature for better processing, and introduces an unsaturated bond that will be used to polymerise the C=C bond of GMA. The curing cycle is studied and the cured resin analysed along the way.

This section presents and discusses the results obtained from thermal, spectroscopic, microscopic and mechanical analysis on the samples during the different steps of the process.

3.1 Chemical modification of PET

PET is chemically modified before polymerisation with glycidyl methacrylate to form a resin. As explained in section 2.2.1, PET is first extruded and grinded, then depolymerised and repolymerised to form unsaturated polyester. This section analyses the different steps of the process of chemical modification of PET via thermal and spectroscopic methods.

3.1.1 Extrusion and grinding

Extruding mimics the processing of PET, especially into PET bottles, by decreasing the crystallinity through melting and quenching. Pelletrisation and grinding are no chemical modifications as they only increase the surface area to favour further reaction. However, PET slightly crystallises due to local heating. Thermal characterisation of extruded PET consists in analysing how similar its thermal behaviour is to POST-C PET, and determine if this modified PET can be considered as recycled PET.

Thermal characterisation

In Figure 3.3, normalised DSC curves of the second heating of synthetic PET, modified PET and POST-C PET, from room temperature to 280℃ are analysed. POST-C PET data is taken using two different waste bottles of PET (Figures 3.1 and 3.2). A piece is cut from each bottle, washed with ethanol and distilled water, and dried in a vacuum chamber.

Figure 3.1: First POST-C bottle analysed.

Figure 3.2: Second POST-C bottle analysed.

The samples are heated from room temperature to 280℃, cooled to room temperature and heated again to 280℃ at 10K/min. As explained in section 2.3.1.1, heating-cooling-heating experiments are used to eliminate thermal history of materials. During the first heating and cooling, the sample is preheated and crystallises. Heating a second time gives information on the thermal behaviour of the material. Results are given in Table 3.1 in terms of glass transition, crystallisation and melting temperatures and crystallisation and melting enthalpies.

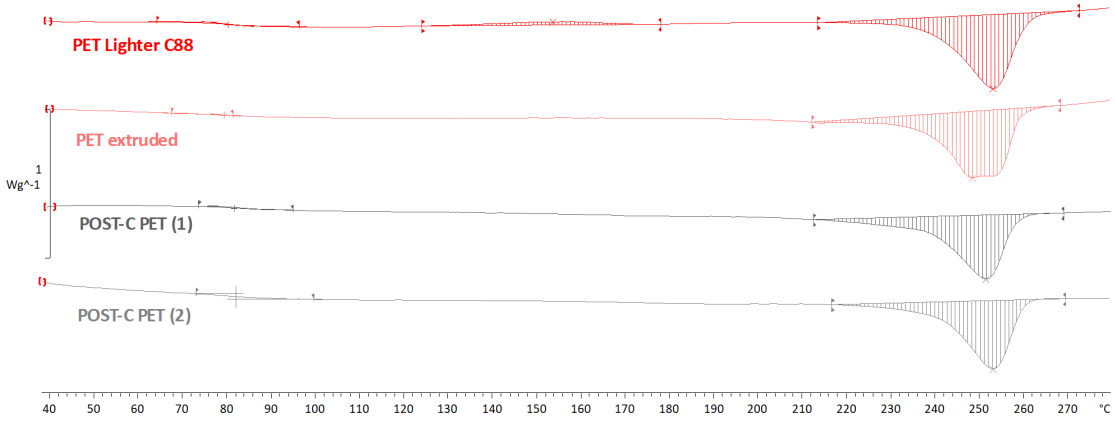

Figure 3.3: Normalised DSC second heating curves of PET after its modification through extrusion and grinding. PET lighter C88 is the industrial and synthetic PET. PET ext-grind is the PET after extrusion and grinding. POST-C PET (1) and (2) are waste PET from used bottle.

Table 3.1: Results from the DSC curve in Figure 3.3. The values are averaged over three analysis.

	Temperatures [°C]			Enthalpies [Jg^{-1}]		χ_c[%]
	T_g	T_c	T_m	ΔH_c	ΔH_m	
PET synthetic	79.67	158.59	253.47	5.24	41.56	32.28
PET extruded	78.79	/	248.86 253.51	/	42.17	29.08
POST-C PET 1	82.65	/	251.52	/	42.23	30.16
POST-C PET 2	81.48	/	252.34	/	38.78	26.74

Synthetic PET shows a small and broad cold crystallisation peak. It means that PET crystallises slowly and is fully crystallised under the conditions of cooling rate. Extruded and grinded PET does not have a cold crystallisation peak. However, extruded PET still has a high degree of crystallinity. It is explained by the preheating and quite slow cooling of the sample that favoured crystallisation. Extruded PET also shows a double endothermic peak at the melting point. It could be attributed to melting-recrystallisation effects or to separate crystal morphologies. This suggests the possibility of having different groups of lamella tickness, with thin lamellaes lying in between thick ones. By all of these results, it can be concluded that extruded PET has a similar thermal behaviour as post-consumer PET, meaning it can be considered as waste PET in this work.

3.1.2 Depolymerisation by glycolysis and repolymerisation into unsaturated polyester (UP)

Depolymerisation and repolymerisation of PET has the purpose of recycling PET to produce unsaturated polyester (UP). It decreases the polymer T_g and χ_c and inserts an ethylenic function in the polymer chain. This will facilitate dual-polymerisation from functional groups of UP (-OH, -COOH and ethylenic functions) and GMA (ethylenic and epoxy function) and the formation of a 3D-network. The waste (extruded and grinded) PET is recycled via glycolysis using diols to produce oligomers of PET, denoted as GPET. Two different diols are used: 1,3-propanediol (PD) and 2-methyl-1,3-propanediol (MPD). The GPET are repolymerised by esterification with citraconic anhydride (CA) and the same diols (PD and MPD) to form unsaturated polyester. The unsaturated polyesters produced with PD and MPD will be referred as UPs and UPam in this work. Their chemical formula are given in Figures 3.4a and Figures 3.4b.

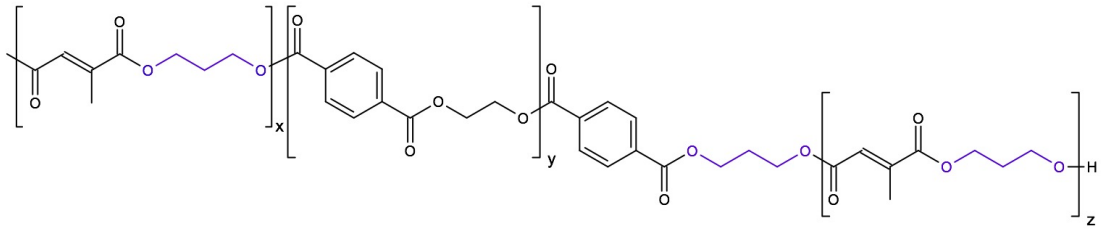

(a)

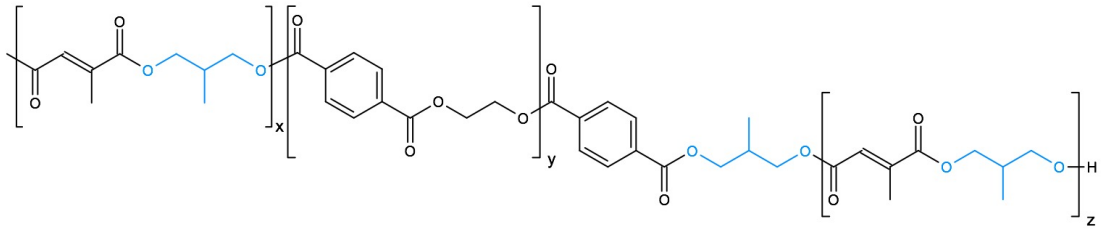

(b)

Figure 3.4: Chemical formula of (a) semi-crystalline UP synthesised with citraconic anhydride and 1,3-propanediol (b) amorphous UP synthesised with citraconic anhydride and 2-methylpropane-1,3-diol.

Both UPs are represented in Figure 3.5. Amorphous UP (3.5b) has the same aspect as semi-crystalline UP (3.5a) but has a more yellowish colour. This is due to its amorphous form, since crystalline species tend to get whiter.

(a) UPsc **(b)** UPam

Figure 3.5: Samples of (a) semi-crystalline (b) amorphous unsaturated polyester.

UPs are characterised by thermal and spectroscopic analysis to determine their thermal behaviour and to show the evolution of well-defined chemical functions such as ethylene ones.

3.1.2.1 Thermal analysis

In Figure 3.6, normalised DSC curves of the second heating from room temperature to 280℃ of extruded PET and UPs are analysed. The samples (except UP) were heated with the cycle described in section 2.3.1.1 and used to characterise extruded and grinded PET (section 3.1.1). UPs were first heated to 200℃, cooled down to room temperature and then heated again to 250℃. Heating at higher temperatures leads to degradation of the samples and prevents observation of crystallinity.

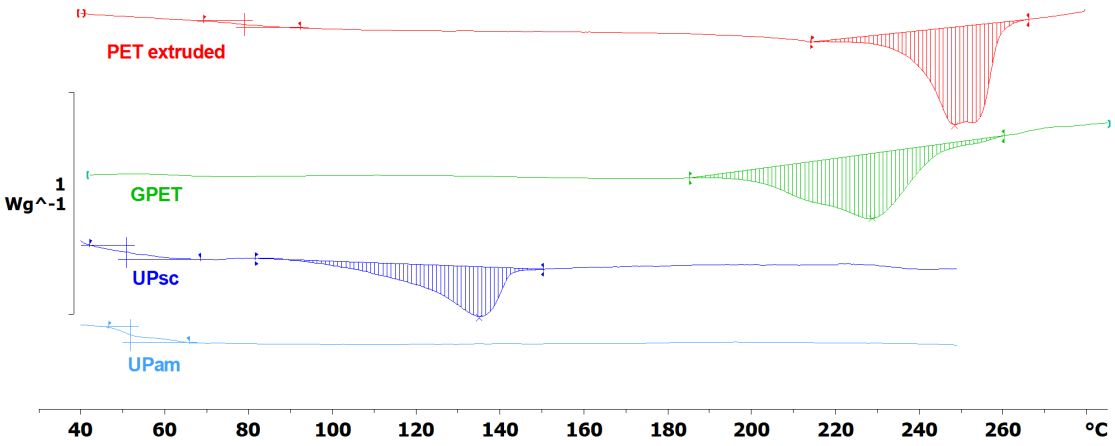

Figure 3.6: Normalised DSC curves of PET during the different stages leading to unsaturated polyester. PET extruded is the PET after extrusion and grinding. GPET is the PET depolymerised through glycolysis. UPam and UPsc are the repolymerised PET through esterification with citraconic anhydride and 1,3-propanediol (PD) or 2-methyl-1,3-propanediol (MPD) respectively.

Results are given in Table 3.1 in terms of glass transition, crystallisation and melting temperatures and crystallisation and melting enthalpies. Crystallisation is calculated with equation (2.1) and the data provided by the DSC analysis.

Table 3.2: Results from the DSC curves in Figure 3.6. The values are averaged over three analysis.

	Temperatures [°C]			**Enthalpies [Jg^{-1}]**		χ_c[%]
	T_g	T_c	T_m	ΔH_c	ΔH_m	
PET extruded	78.79	/	248.86	/	42.17	29.08
GPET	65.63	/	231.79	/	41.52	28.63
UPsc	52.24	/	135.163	/	25.89	17.86
UPam	51.63	/	/	/	/	0.00

Glycolysed PET shows a broader, slightly smaller and shifted melting peak. The melting temperature is smaller and is due to the decrease in molecular weight by glycolysis. The crystallinity is also slightly reduced due to the diol structure inserted inside GPET. Semi-crystalline unsaturated polyester (UPsc) has a considerably smaller crystallinity. It is due to the modification in the material structure by reaction with citraconic anhydride and 1,3-propanediol. UPam is obtained by reaction with MPD. As expected, it doesn't show any crystallisation or melting peak which proves its amorphous properties. This shows that the chemical structure of the diol used in the repolymerisation modifies the kinetic of UP crystallisation. Both UPs have a smaller glass transition temperature, which will allow further polymerisation with glycidyl methacrylate without the use of any solvent to homogenise the UP/GMA mixture. Amorphous UP shows a slightly lower T_g than semi-crystalline UP. Theoretically, sterically hindered polymers should have a higher T_g because more thermal energy is needed to transition from a glass to a rubbery state, i.e. to "set the chain in motion" [12]. This incoherence could be due to a lack of precision in the measurements.

3.1.2.2 Spectroscopic analysis

Samples of PET, GPET and UP were analysed with FTIR to identify the impact of chemical modification on some functional chemical groups during depolymerisation and repolymerisation of PET. The spectra were normalised using the harmonic band at 1953 cm^{-1}. They are represented in Figure 3.7.

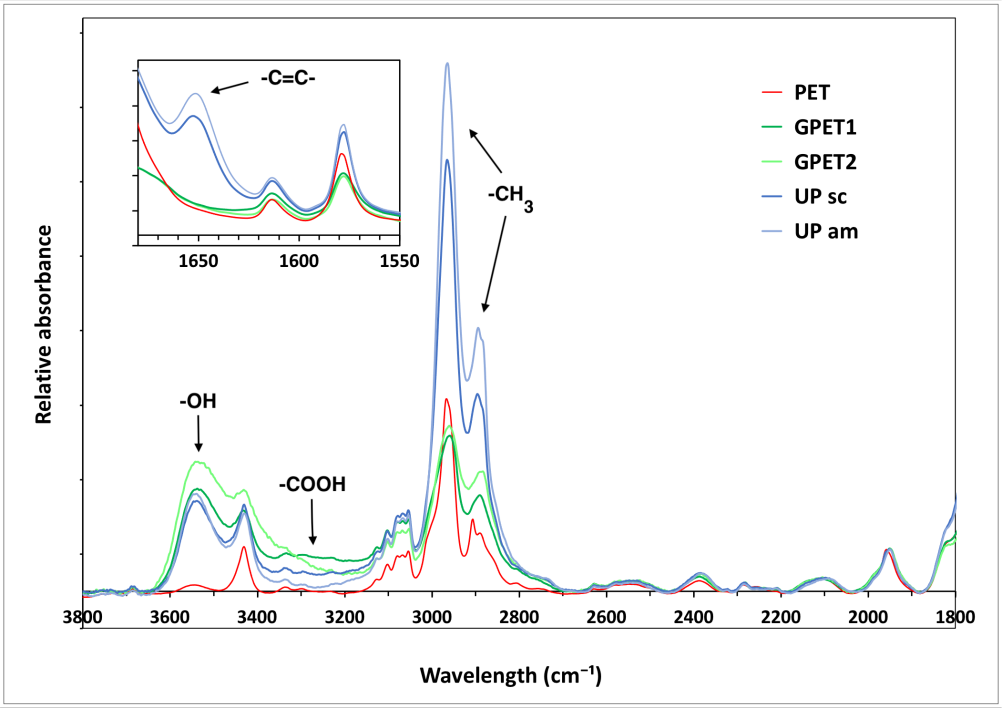

Figure 3.7: FTIR spectra of PET, PET depolymerized with PD (GPET1), PET depolymerised with MPD (GPET2), semi-crystalline UP (UP sc) and amorphous UP (UP am), normalised at 1951 cm^{-1}.

In Figure 3.7, peaks around 3550 cm^{-1} and 3270 cm^{-1} correspond to hydroxyl and carboxyl groups and are increased after depolymerisation. This can be explained by the rupture of the ester bonds of PET during glycolysis and their replacement with hydroxyl terminals, which contributes to the reduction of PET molecular weight [27, 28, 42, 94]. Hydroxyl and carboxyl end-groups after repolymerisation of GPET could be due to the increase in molecular weight. This observation has been seen in other systems in the literature [95]. Peaks around 2870 and 2980 cm^{-1} correspond to methylene and methyl groups. They increase in the second step of chemical modification (repolymerisation) of PET, especially for UPam. This is explained by its structure that contains more methyl groups (see Figure 3.4b). As expected, the repolymerisation of PET into unsaturated polyester introduces a double carbon bond (C=C) in the polymer chain. It is showed by the apparition of the corresponding peak around 1650 cm^{-1}. High peaks of hydroxyl and carbonyl groups are interesting for polymerisation with GMA as these functions are the ones intended to open the epoxy groups.

3.2 Polymerisation and thermal degradation mechanism of glycidyl methacrylate

Glycidyl methacrylate is a bifunctional monomer that can react via 1) a radical polymerisation on its carbon double bond and 2) through ring-opening polymerisation of its epoxy function with hydroxyl, carboxyl and amine groups. Homopolymerisation is referred to as the first reaction. Studies have showed that the reactivity of the double carbon bond is higher than the epoxy group, and that homopolymerisation is favoured to ring-opening mechanism, which usually happens after a longer time or at higher temperature [61]. Thermal and spectroscopic analysis of crude GMA and polymerised GMA were conducted to characterise the system and confirm the theoretical polymerisation process.

3.2.1 Spectroscopic characterisation

Raman analysis is used to identify polarisable groups for spectroscopic analysis and was used to understand the polymerisation mechanism of glycidyl methacrylate with benzoyl peroxide. Samples of crude GMA (mixed with 1wt% BPO) and cured GMA were analysed. Both spectra are represented in Figure 3.8. The strong peak at 1726 cm^{-1} can be associated to the GMA ester group. As it is not involved in the homopolymerisation of GMA, it was used to normalise the two spectra.

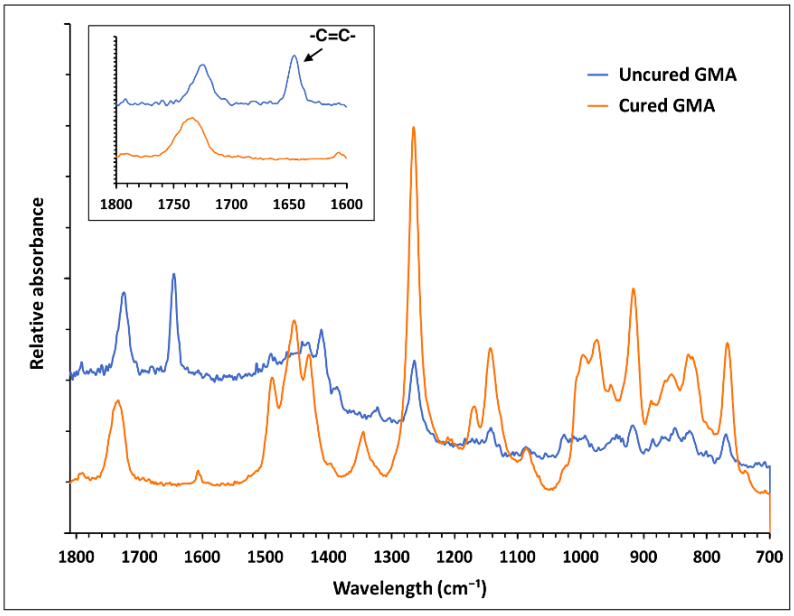

Figure 3.8: Raman spectra of crude and cured glycidyl methacrylate containing 1 wt% of benzoyl peroxide, normalised with the peak in 1726 cm^{-1}.

Peaks at 1640 cm^{-1}, corresponding to the ethylene function of GMA, were analysed. It is very clear that this function is present before curing and disappears after curing. It represents the homopolymerisation of GMA through radical polymerisation on the ethylenic function. Analysis of the epoxy was not conclusive via Raman technique. FTIR is a more suitable spectroscopic technique to analyse organic material, but could unfortunately not be conducted.

3.2.2 Thermal characterisation

GMA samples with 1 wt% of benzoyl peroxide were analysed with DSC and TGA techniques. The influence of BPO on the polymerisation process will be analysed and discussed in the next section.

3.2.2.1 DSC analysis

The sample was heated from room temperature to 250°C at 10K/min. Figure 3.9 shows the normalised DSC curve of GMA/BPO.

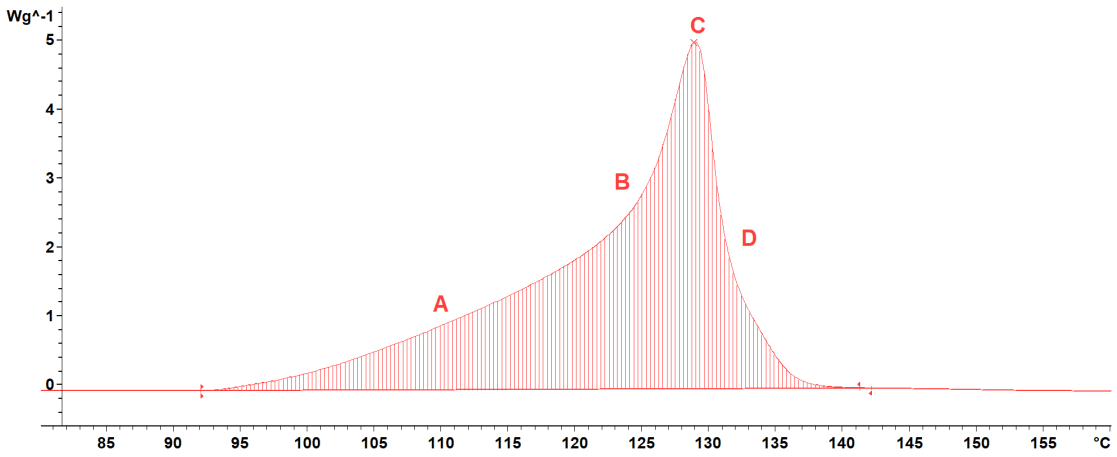

Figure 3.9: Normalised DSC curve of GMA initiated by benzoyl peroxide. A)s start of the reaction B) acceleration of the reaction C) Peak temperature D) Effet Trommsdorf.

The figure above shows that the averaged polymerisation enthalpy was 366.41 Jg^{-1} and corresponds to approximately 92% of conversion. This slight difference is due to vitrification during cure and prevents complete polymerisation of the sample [57]. The shape of the curve is representative of the Trommsdorf effect explained in section 1.5.3. The reaction starts around 95°C. As the conversion of GMA increases (A), the viscosity also increases, leading to the acceleration of the reaction around 120-125°C (B). The temperature inside the resin keeps increasing

and reaches a peak temperature of 129.57℃ (C). Above it, the rate of the reaction declines abruptly and the curve drops (D).

3.2.2.2 Thermogravimetric analysis

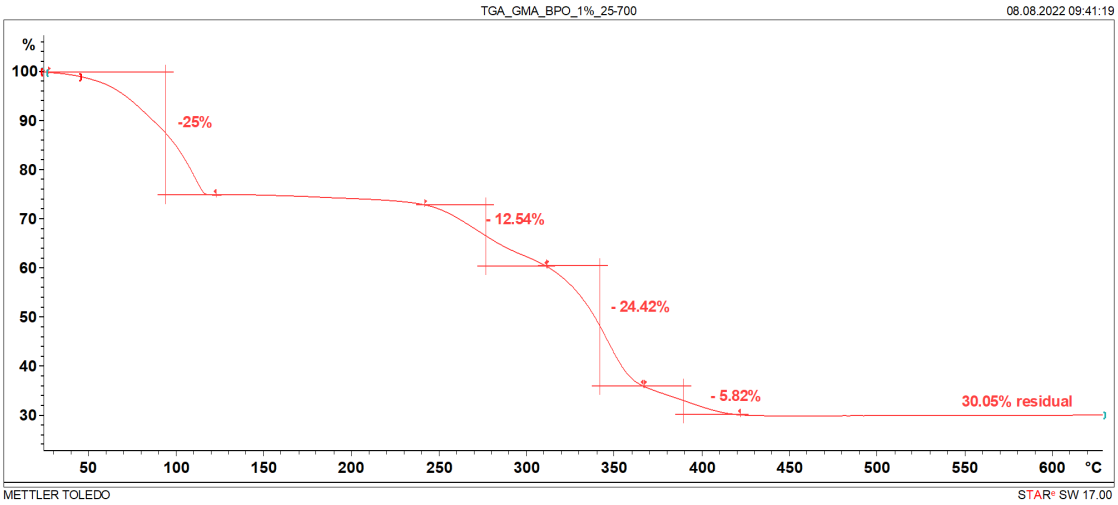

Figure 3.10: TGA curve curve of GMA initiated by benzoyl peroxide.

Figure 3.10 shows the TGA curve of glycidyl methacrylate. The sample was heated from room temperature to 700℃. Four mechanisms of degradation can be distinguished and assumed from the curve. The degradation starts from room temperature. The first drop is a loss of mass of about 25 wt% between room temperature and 120℃. It can be associated to GMA evaporation, as the monomer is very sensible to temperature. The second and third drop appear between 240 and 365℃ and represents about 12.5 wt% and 24.5 wt% of respective mass loss. It corresponds to GMA degradation. In the literature, thermal degradation of pGMA around 300℃ is associated to GMA decomposition and CO_2 formation [96]. The final mass loss of about 6 wt% could be associated to the burning step of carbon [79]. After the heating treatment, 30.05 wt% are left as residues.

3.3 Polymerisation mechanism of UP/GMA resin

As indicated in the literature, glycidyl methacrylate can react with unsaturated polyester by radical polymerisation on the double C=C liaison. The reaction needs to be initiated by a radical initiator, such as benzoyl peroxide. This reaction should increase the end chains -OH in the system. As the oxirane is sensible to hydroxyl function, it will be opened through ring-opening polarisation by the end chains of UP. This will increase the crosslinking of the system. As this process is only theoretical, thermal and spectroscopic methods are used to characterise the synthesised resin and describe the effective reaction mechanism. To understand the mechanism, experiments were done on a theoretical system with weight fractions of BPO and heating rates determined in the next sections. The weight ratio between UP and GMA was 50:50 (w/w). Semi-crystalline UP was used for the first analysis.

3.3.1 Influence of benzoyl peroxide content on polymerisation kinetic

For the following tests, two resins of UP, GMA and BPO were prepared with proportions given in Table 3.3. The amount of BPO varies between 0.2 and 1 wt% to understand the impact of the concentration of radical initiators in the curing system.

Table 3.3: Mass concentrations of the two systems used for the experiments. *Proportions of BPO are given in % of the weight of the UP/GMA mixture

	Proportion wt%	
	System 1	**System 2**
UP	50	50
GMA	50	50
BPO*	0.2	1

3.3.1.1 Thermal characterisation

The influence of BPO on the polymerisation process of the two UP/GMA systems was analysed with DSC technique. Both samples were heated from room temperature to 280℃ at 10Kmin^{-1}.

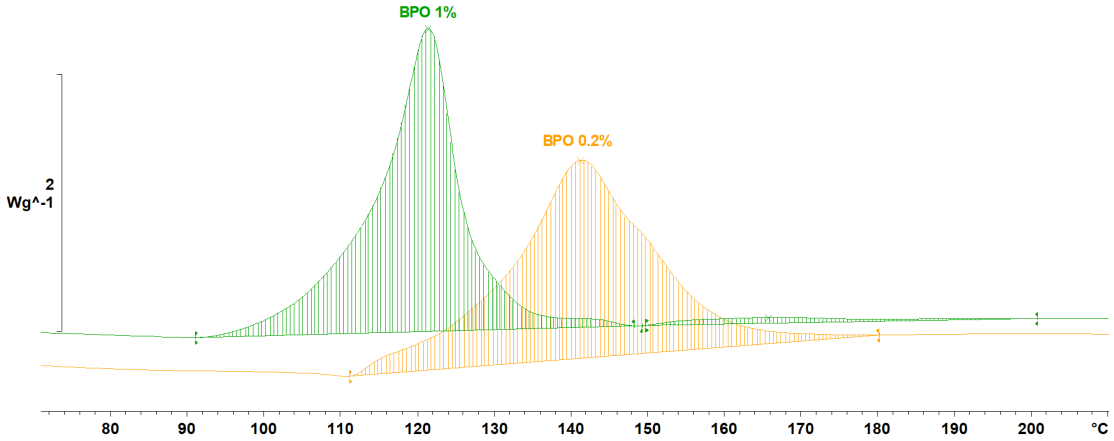

Figure 3.11: Normalised DSC curves for UP/GMA resins with 0.2 and 1 wt% of benzoyl peroxide heated from room temperature to 280°C at 10Kmin^{-1}.

Table 3.4: Results from the DSC curves in Figure 3.11.

	ΔH_r [Jg^{-1}]	T_{start} [°C]	T_{end} [°C]	T_{peak} [°C]
System 1	204.09	110.42	190.42	141.72
System 2	188.91	92.80	185.23	121.47

Figure 3.11 represents the normalised DSC curves of GMA/BPO for system 1 and 2. Values of reaction enthalpy, start, end and peak temperatures are summarised in 3.4. For system 1 and 2, the reaction starts around 110°C and 95°C respectively. The reaction appears earlier for system 2 because the amount of BPO in the system is higher. On the contrary, the reaction peak is obtained at higher temperature for system 1 and the reaction is slower. Radicals produce a lot of internal energy in the system and contribute to the evolution of the polymerisation reaction [54]. System 1 (0.2 wt%) has a reaction enthalpy slightly higher than system 2 (1 wt%). System 2 presents two peaks: the first one is large and the other one is smaller. These could be related to the presence of two reaction mechanisms. The first one is activated by BPO after the production of free radicals. The second one follows the epoxy ring-opening and is promoted at high temperature. As reaction of system 2 is faster and necessitates lower reaction temperatures, it would have a positive economic and energetic impact.

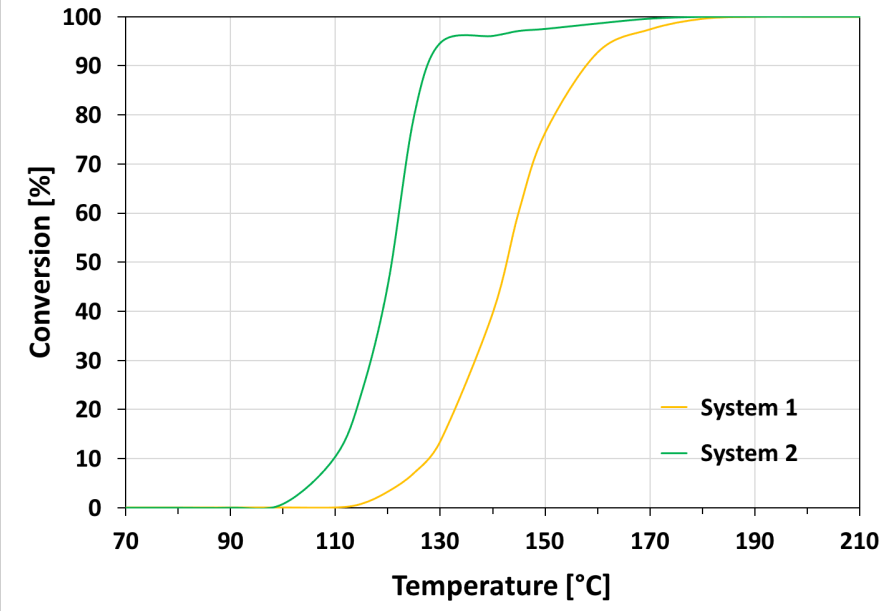

Figure 3.12: Kinetic of polymerisation for resin containing 0.2 and 1 wt% of benzoyl peroxide.

As represented on 3.12, the conversion vs temperature curve of both systems show the typical aspect of a Trommsdorf effect. The second peak is much lower than the first one but suggests a second reaction in the system. Its meaning will be analysed later. Curve of system 1 does not show a similar double peak, but as reaction proceeds at higher temperature, the second peak could still be "hidden" in the first one.

System 2 with 1 wt% BPO was chosen for the rest of this study. A higher concentration was not studied. As explained in section 3.3, higher peroxide concentrations increase viscosity [54]. It could also increase the Trommsdorf effect and lead to undesirable behaviour of the resin during curing and decrease in the mechanical properties.

3.3.2 Influence of heating rate on the kinetic of polymerisation

The heating rate can influence the kinetics of polymerisation. The analysis of the impact of the heating rate on the thermal behaviour of the sample allowed to choose the most suitable heating rate for the polymerisation. In this part, the UP/GMA resins are heated at the rates of 2.5, 5, 10 and 20K/min^{-1} respectively.

3.3.2.1 Thermal characterisation

Figure 3.13 shows normalised DSC curves of the mixture UP/GMA with mass fractions of system 2 (cf. Table 3.3). The samples were heated from room temperature to 250℃ at different heating rates. Results in terms of enthalpy of reaction and temperature peak are given in Table 3.5. The values at 10Kmin^{-1} is slightly different than the ones in Table 3.4 since the experiments were conducted on two different DSC machines.

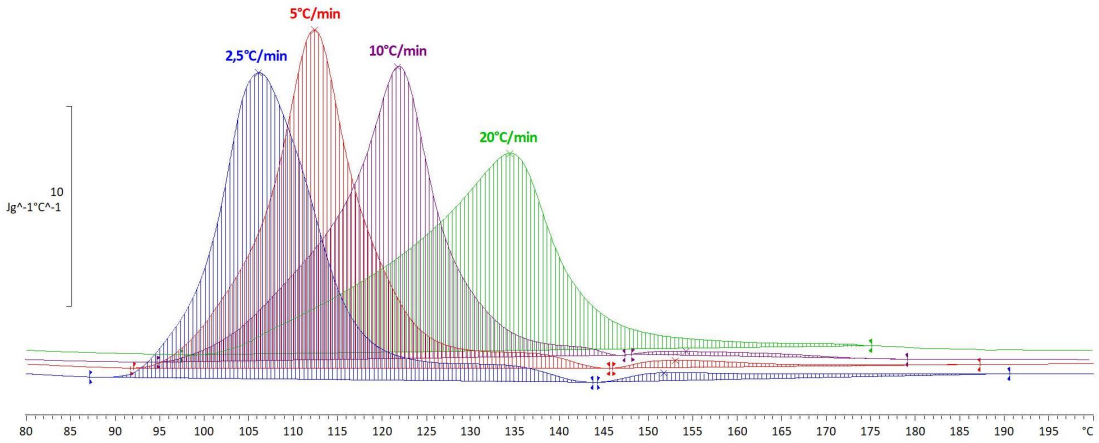

Figure 3.13: Normalised DSC curves for UP/GMA resins heated at different rates: 2.5, 5, 10 and 20K/min^{-1}

Table 3.5: Results from the DSC curves in Figure 3.13

Heating rate [K/min^{-1}]	**H$_r$ [Jsg^{-1}K^{-1}]**	**H$_r$ [Jsg^{-1}]**	**H$_r$ [Jg^{-1}]**	**T$_{peak}$ [℃]**
2.5	5102.99	12757	212.62	103.25
5	2686.17	13430	223.85	112.42
10	1279.54	12795.4	213.26	121.83
20	597.96	11959.2	199.32	134.40

The rate of heating does not impact the enthalpy of reaction as all rates have enthalpies about 12000 Jsg^{-1}. The kinetic of reaction, illustrating the reaction mechanism, is also similar, as represented in Figure 3.14. However, reactions at lower rates will start reacting at lower temperatures and have lower peak temperatures. These reactions will continue until higher temperatures. The rate of 10K/min was chosen for the next experiments in this work to optimise the range of temperatures of the reaction and the duration of the reaction. 20K/min was not chosen since it is harder to implement at an industrial scale.

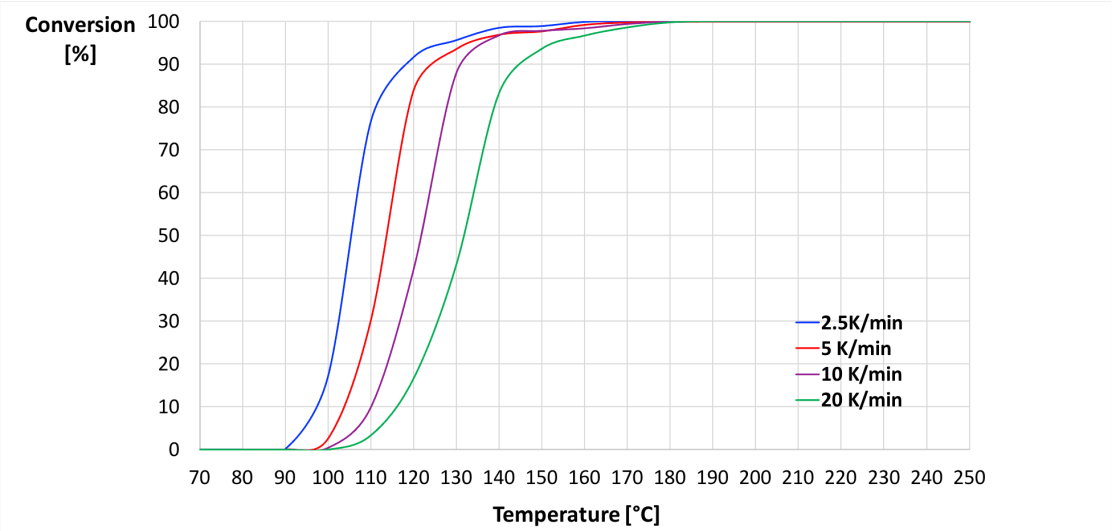

Figure 3.14: Conversion of reaction for different heating rates: 2.5, 5, 10 and 20Kmin^{-1}

3.3.3 Evaluation of polymerisation mechanism

This section aims at understanding how the UP/GMA system reacts and polymerises with temperature. Experiments were done on a model sample: 50 wt% UP + 50 wt% GMA + 1% (w/w resin) BPO. Samples were heated from room temperature to temperatures varying from 80℃ to 250℃. After heating, they were cooled in liquid nitrogen to avoid further polymerisation and analysed by spectroscopic methods.

3.3.3.1 Spectroscopic characterisation

Spectroscopic analysis is used to determine the chemical functions present in a sample. In particular, Raman and FTIR are complementary techniques used to understand the modification of chemical bonds during the chemical reactions. As explained in section 2.3.2.1, methacrylates are analysed by observing the C=C peak around 1640 cm^{-1} [89]. Unsaturated polyester is characterised by the double carbon bond around 1650 cm^{-1}. Copolymerisation of UP and GMA on both of their ethylenic function would induce a decrease in these peaks. Epoxy functions are analysed with the bands at 755, 1253 and between 845 and 910 cm^{-1} [65]. Opening of the epoxy ring with the -OH and -COOH end chains of UP should reduce the peaks corresponding to epoxide and oxirane. Other peaks should appear corresponding to functions created by the ring-opening mechanism. As represented in equation 3.15, an increase in peaks corresponding to ether (-C-O-H) and/or ester (-C-O-O-C-) functions would be expected. An increase in hydroxyl (-OH) and a decrease in carboxyl (-COOH) end groups would also appear.

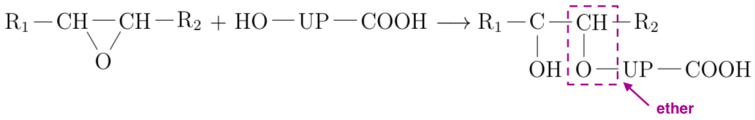

(a)

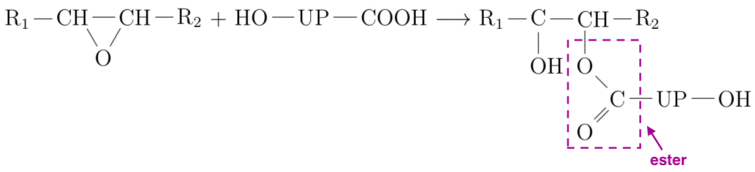

(b)

Figure 3.15: Reaction mechanism of epoxy opening with -OH end chains of UP, producing (a) ether and (b) ester groups.

Raman spectroscopy was used to determine the evolution of the ethylenic function in GMA. FTIR spectroscopy was used to determine the evolution of the hydroxyl, carboxyl, epoxy, ester and ether functions.

Modification of ethylenic bond (Raman spectroscopy)

The spectra obtained from Raman spectroscopy on the samples are represented in Figure 3.16. They were normalised with the aromatic peak of GMA in 1610 cm^{-1}.

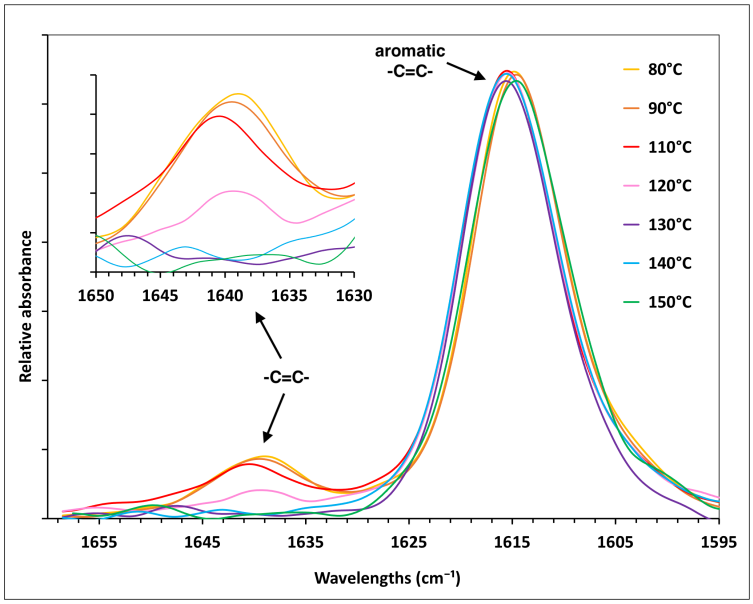

Figure 3.16: Raman spectra of UP/GMA resins heated to temperatures ranging from 80 to 150℃, normalised with the aromatic peak in 1610 cm^{-1}.

Figure 3.16 shows that the ethylenic function of GMA effectively disappears with the increase in temperature. After 130℃, the peak are stable, meaning the conversion of the double carbon bond is over. A more representative way to analyse these results is to plot the degree of GMA conversion with temperature. This was done using equation 2.2 described in section 2.3.2.2.

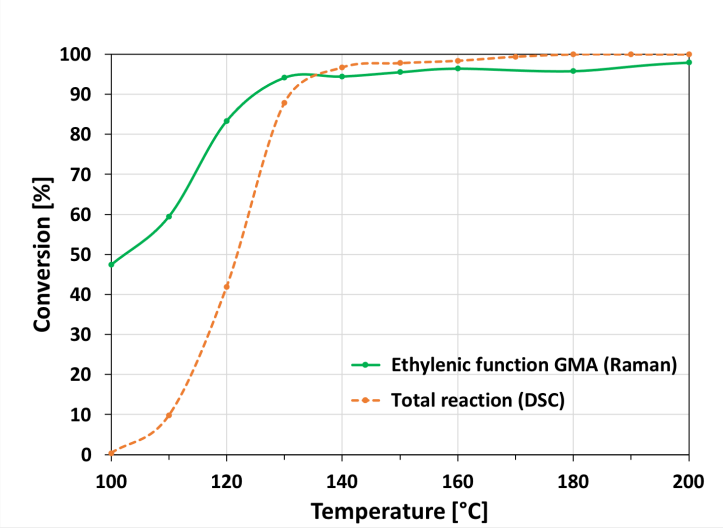

Figure 3.17: Conversion of the ethylenic function of glycidyl methacrylate (at 1640 cm^{-1}) with temperature.

Figure 3.17 shows the conversion of GMA with temperature. The results from Figures 3.16 and 3.17 have to be analysed carefully. In both Figures, it appears that the conversion of the double carbon bond begins earlier with the Raman analysis than the quantification energy produced in DSC analysis. According to Raman analysis, the reaction starts before 100℃ but in the DSC conversion curve in Figure 3.12 (and represented in orange in Figure 3.17) the reaction starts around 100℃. This difference can be explained by the local heating induced by the Raman laser. The samples can absorb some of the incident light and polymerise further during analysis [97]. The increase in temperature depends on the laser power and sampling time, but also on the thermal conductivity and colour of the sample [98]. The difference between the Raman and DSC results could also be due to a lack of precision during the preparation of the samples by heating. For example, the sample heated to 100℃ could have reached a higher temperature between the stop of the sample heating, the removal of the sample and its cooling in liquid nitrogen.

However, both curves show that the conversion of the ethylenic function of GMA follows a similar path as the total reaction, and stops around 130℃. As in

Figure 3.16, it is observed that the ethylenic function of GMA disappears with temperature, meaning GMA is effectively polymerised during the reaction. The curve is characteristic of an increase in viscosity during polymerisation: it reaches a peak and stops abruptly.

Even if the conversion of the double carbon bond of GMA has been observed and proves polymerisation of the monomer, the reaction mechanism is still unclear. The conversion of GMA could be a consequence of polymerisation with the ethylenic function of UP, but also of GMA homopolymerisation. Because the ethylenic function of UP is represented by a peak at 1650 cm^{-1}, at a wavelength very close to the ethylenic function of GMA, its disappearance cannot be easily determined.

Modification of polarised bond (FTIR)

Figure 3.18 shows the spectra obtained with FTIR spectroscopy on the UP/GMA samples heated from 80 to 250℃.

The spectra were analysed by observing the peaks related in Table 2.4 in Section 2.3.2.1. The main peaks appearing and disappearing are represented from Figure 3.18a to Figure 3.18c.

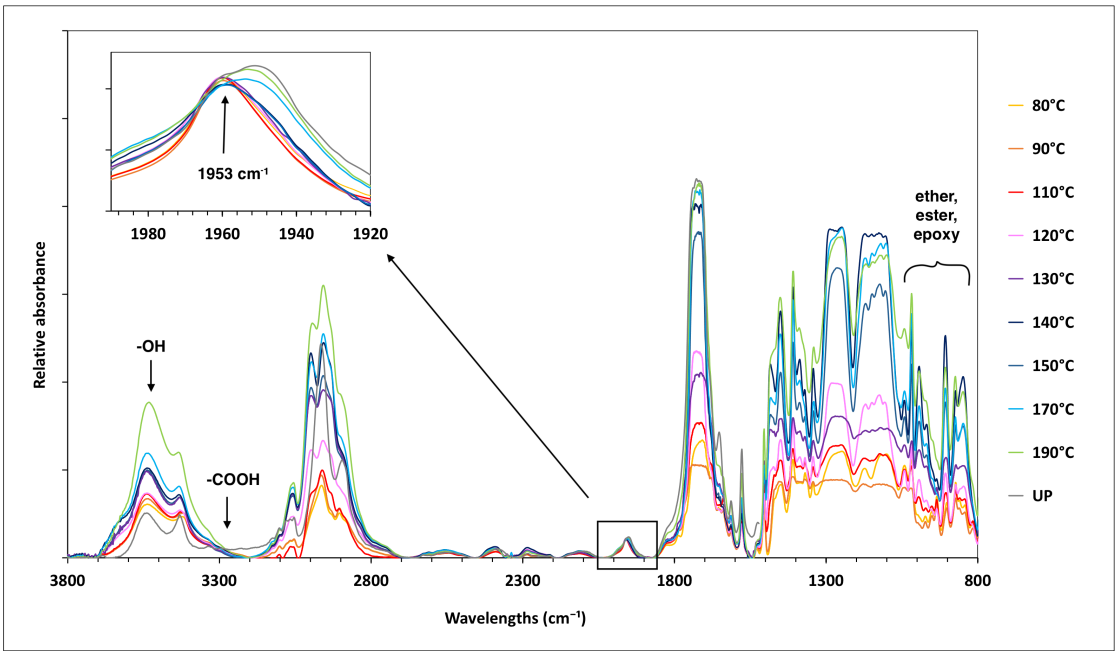

Figure 3.18: FTIR spectra of UP/GMA resins heated to temperatures ranging from 80 to 250℃ normalised with the peak in 1953 cm^{-1}

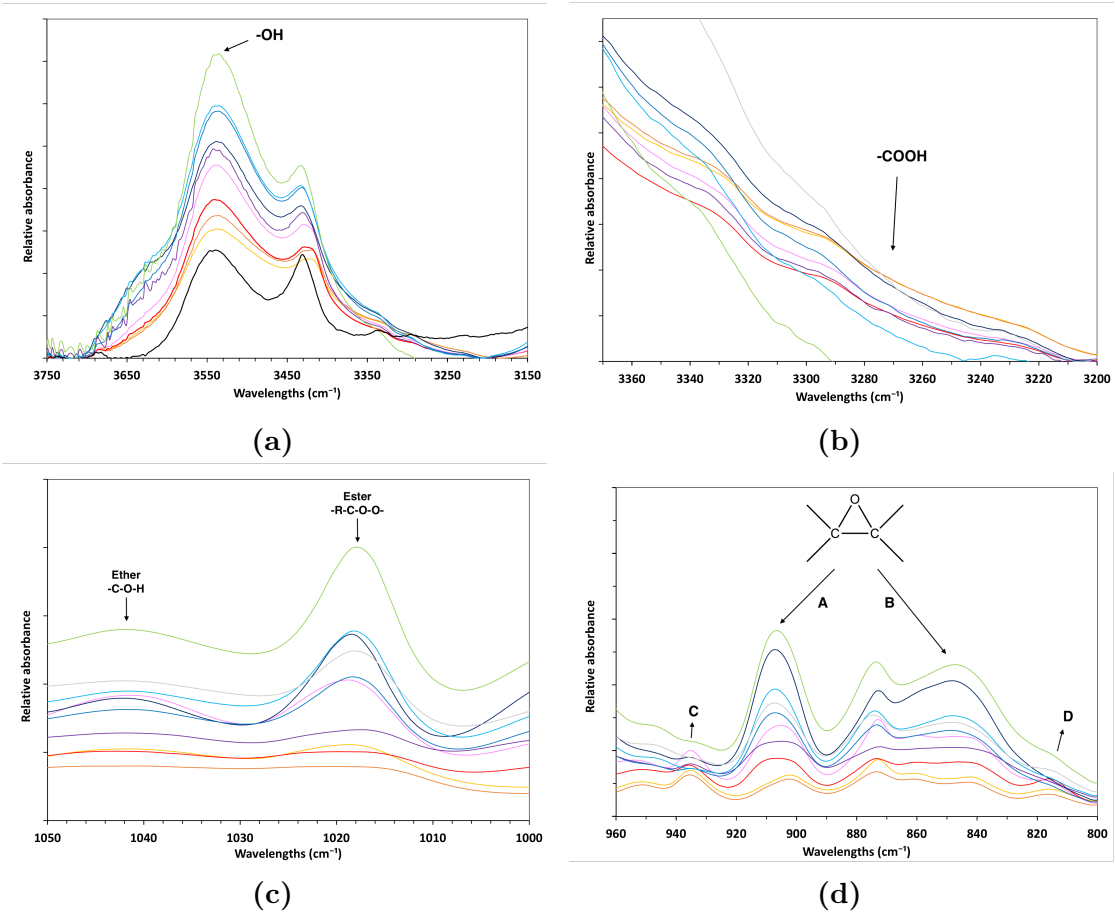

Figure 3.18: FTIR spectra of (a) the hydroxyl end groups -OH at 3550 cm^{-1} (b) the acid end groups -COOH at 3270 cm^{-1} (c) the ether -R-C-O-O-R' group around 1015 cm^{-1} and ester -C-O-H group at 1040 cm^{-1} (d) the epoxy functions between 845 and 910 cm^{-1}

In Figure 3.18a, an increase of the peaks around 3550 cm^{-1} is observed with the increase in temperature and is related to the increase of the hydroxyl groups -OH. This increase could be a consequence of the oxirane opening during polymerisation. The height of the peaks is calculated and their variation is plotted with temperature in Figure 3.19. The resulting curve of the conversion with temperature shows that the increase in -OH groups starts around 120 ℃ and stabilises around 200 ℃. It is difficult to observe the evolution of -COOH groups. This could be linked to their higher reactivity.

Figure 3.18c shows an increase of the ester function (-C-O-C-) from 120 to 170 ℃. This is a consequence of epoxy ring opening following the first mechanism described in Figure 3.15b.

The expected FTIR results from the opening of the epoxy ring would be a decrease in the intensity of the vibration band of the terminal epoxy groups [84, 99]. In Figure 3.18d, (A) corresponds to the stretching -CO of the oxirane group and (B) to the stretching C-O-C of the oxirane group. Both of the peaks show an increase until 170℃, contrary to what would be expected. A slight increase is observed at higher temperatures, around 190℃. However, Figure 3.18d also shows a decrease in the peak 935 cm^{-1} (C) and 810 cm^{-1} starting around 110℃ and until about 180℃ and 140℃ respectively. Peaks shifts in the lower wavelengths area is common [83]. The height of the peaks is plotted with temperature in Figure 3.19. It shows a clear correlation with the increase of the -OH end chains. The decrease in epoxy functions at temperatures higher than 170 ℃ could be linked to ring-opening mechanism [54, 58, 65].

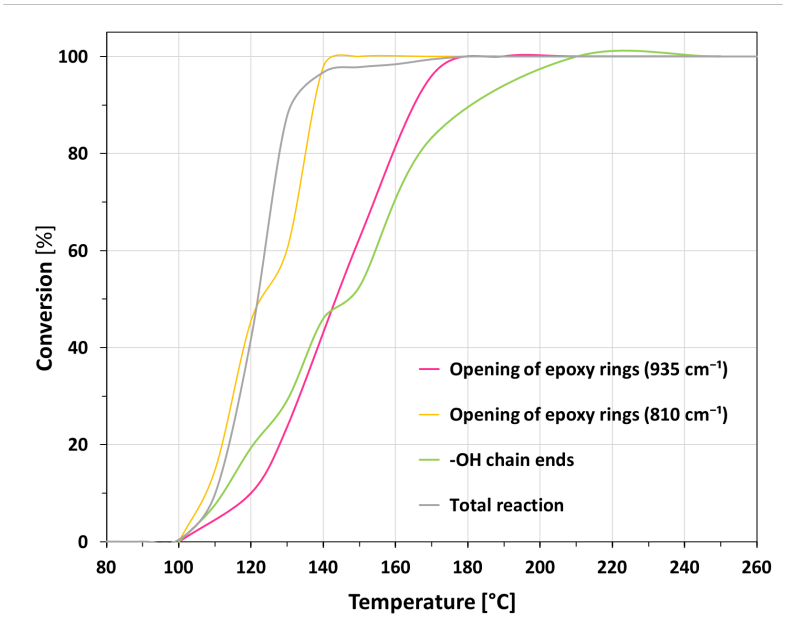

Figure 3.19: Evolution with temperature of hydroxyl (-OH) and carboxyl (-COOH) groups and epoxy rings

Table 3.6 summarises the different observations made with Raman spectroscopy and FTIR results. These can be linked to the behaviour of the DSC curve.

Temperature [°C]	FTIR observations
80(95)-150	Decrease in ethylenic function of GMA
120-170	Increase in ester function -C=O
120-180	Decrease in epoxy functions
170-190	
120-200	Increase of -OH functions

Table 3.6: Summary of the different mechanisms in the UP/GMA reaction with temperature.

From these results, the different steps of the reaction are presumed:

1. Radical polymerisation on the ethylenic function of GMA, with possible reaction of the ethylenic function of UP;

2. opening of epoxy ring with -OH end chains of UP and formation of ester functions.

3.4 Determination of curing cycle of the resin

After analysis and comprehension of the system, curing of the resin in the conditions presented in the last sections was established. First, UP and GMA were mixed in different proportions. The maximum mass fraction of UP possible in the mixture was determined to be 20 wt%. Over this limit, the system becomes too viscous, and is not possible to degas and pour into a mould. Experiments using dichloromethane as solvent to liquefy the mixture were ineffective (cf. Appendix A, Figure 4.10).

To analyse the curing behaviour, 10 wt% of UP were mixed with 90 wt% of GMA. 1% (w/w resin) of BPO was added and the mixture was degassed in a vacuum chamber. A first curing cycle was established from similar experiments found in the literature, and is represented in Figure 3.20 [65]. It consists of a cure at 80°C during 12 to 16 hours, and a post-cure at 180°C during 3 hours. 80°C is an acceptable temperature as BPO starts decomposing around 75°C [100, 101]. Theoretically, and following the obtained results, the first cure would correspond to polymerisation of the ethylenic function of GMA, and the post-cure would favour the opening of the epoxy groups.

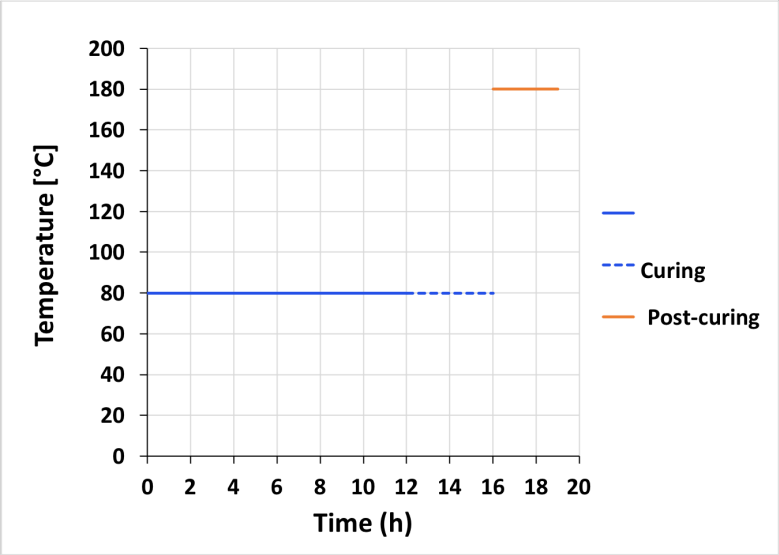

Figure 3.20: Curing cycle 1.

Some porosities start to appear after the first curing step at 80°C. After the post-cure, the sample had so many of them that it had the appearance of a sponge. The samples also showed some volume loss. As explained in section 1.5.3, these behaviours can be explained by many phenomena: incomplete degassing of the resin, entrapment of air during resin pouring into the mold, volatilisation of polymerisation by-products or matrix schrinkage during curing. A more probable explanation is the manifestation of the Trommsdorf effect [67, 68]. To "freeze" the system and avoid apparition of voids, a step of gelation was added.

3.4.1 Study of gelation conditions

Different gel temperature were studied experimentally. The gel time was set to 48 hours. After gelation, the resins were cured at 80°C for 3 hours and 180°C for 1 hour. The resulting cured samples are represented on Figure 3.21. Curing with gelation at temperatures from 50°C to 70°C showed apparition of voids (porosities, cavities). 45°C seems to be the adequate gel temperature as none appeared. Gelation was even possible in 24 hours. Gelation under 40°C was not effective. To confirm these results, thermal stability of the UP/GMA system was analysed with thermogravimetric analysis.

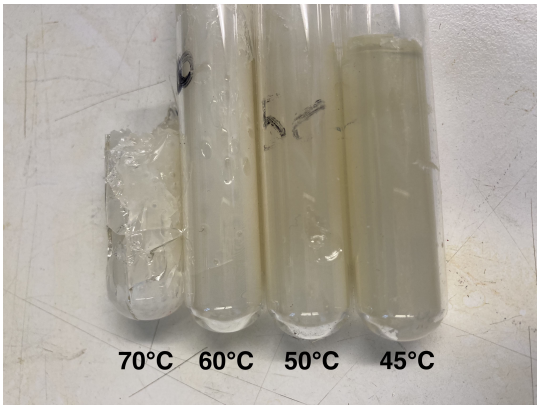

Figure 3.21: Resin cured with different gel temperatures.

3.4.2 Analysis of the thermal stability during curing

As just explained, thermal degradation of the system during curing was investigated using thermogravimetric analysis (TGA).

3.4.2.1 Thermal analysis

Two samples were used for the experiments, both with 1% (w/w resin) of BPO: 1) 100 wt% GMA and 2) 50 wt% UP + 50 wt% GMA. The samples were first heated from room temperature to 700°C. The loss of mass was measured for each sample. The results are represented in Figure 3.22.

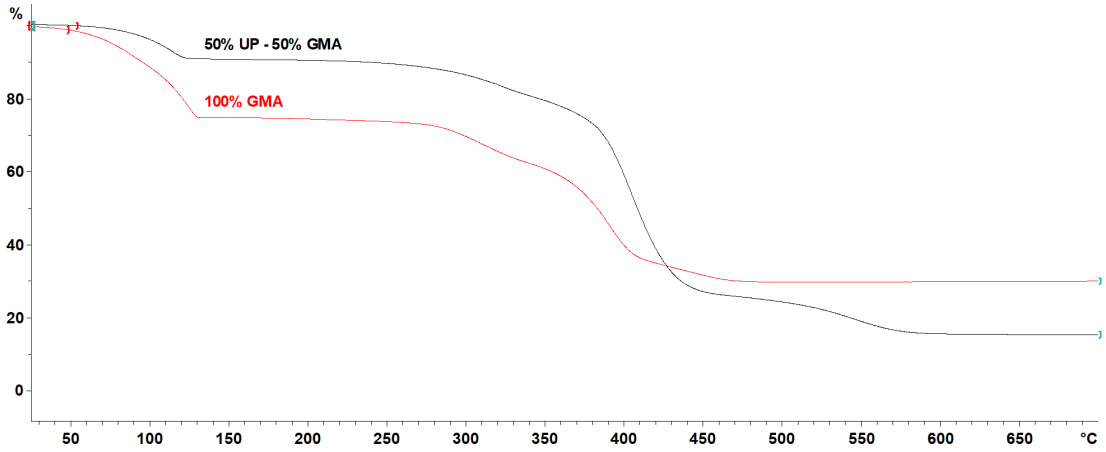

Figure 3.22: TGA curves of GMA and the mixture UP/GMA

Thermal degradation of both mixtures follows the same three steps explained in section 3.2 with the analysis of the thermal degradation of GMA: 1) GMA

evaporation, 2) GMA degradation and CO_2 formation and 3) burning step of carbon. The UP/GMA mixture however, has a residual mass of less than 20% after degradation. The last degradation mechanism could also be explained by the degradation of the polymer at high temperature.

A sample of 50 wt% of UP + 50 wt% of GMA initialised with 1% (w/w resin) of BPO was heated to temperatures from 25 to 70°C for 6 hours to identify gel temperature. The loss of mass was measured and represented in Figure 3.23 and Table 3.7.

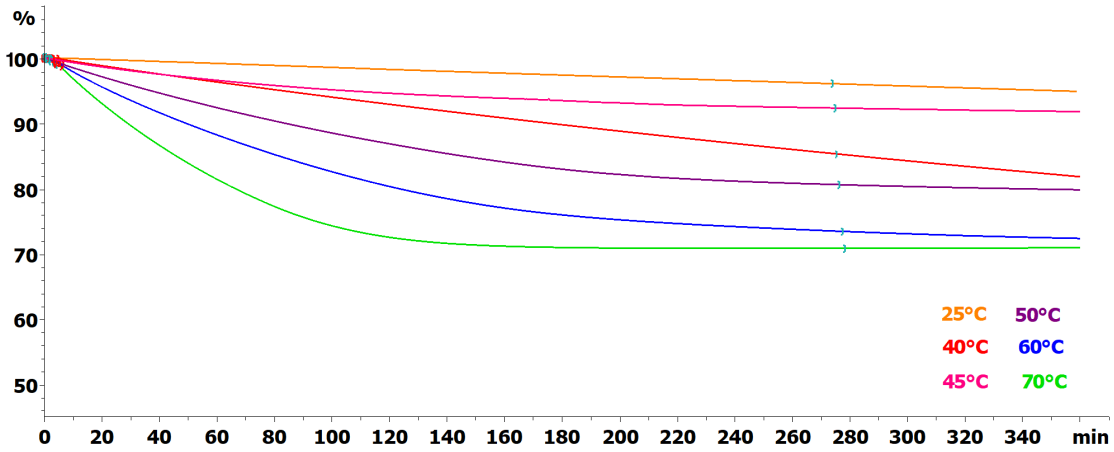

Figure 3.23: TGA curves of UP/GMA mixture showing different gel temperatures and the resulting mass loss.

Table 3.7: Loss of mass of UP/GMA sample for different gel temperatures

T [°C]	25	40	45	50	60	70
Δm [%]	5	18	8	20	28	19

As GMA evaporates at temperatures as low as 25°C, gel at 25 °C shows a mass loss of about 5%. As seen in Table 3.10. Mass loss increases with gel temperature. Gelation at 70°C shows the highest mass loss (28%) as the temperature is very close to the flash point of GMA and because higher temperature will favour its evaporation. An exception is found with the gel at 45°C that seems to show a smaller loss of mass. This concludes that 45°C was proven to be a suitable gel temperature for a system with 50 wt% UP and 50 wt% GMA.

3.4.3 Modifications of curing cycle

According to the thermal analysis, the curing cycle was modified. It is represented in Figure 3.24. A step of gelation at 45℃ was added, followed by curing at 80℃ for 2 hours and post-curing at 180℃ for 1 hour. The gelation time varied but averaged 24 hours.

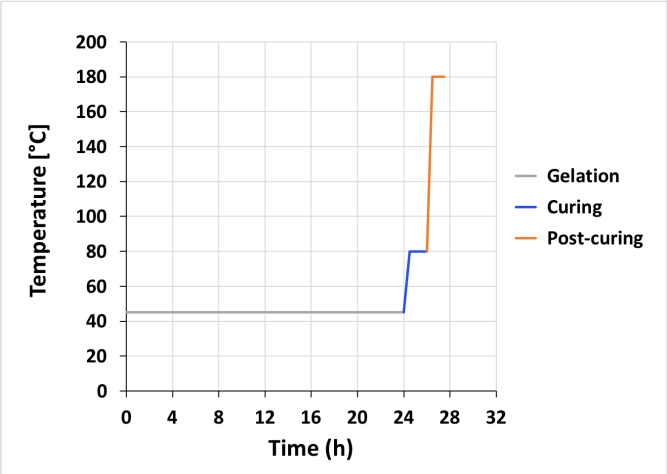

Figure 3.24: Curing cycle 2.

Resins with 5 and 10 wt% of UP were tested with this cycle. As represented in Figure 3.25, common observations were A) loss in volume, B) apparent colour change, C) apparition of voids/cavities. These results show that the gelation at 45℃ is not efficient enough to limit the Trommsdorf effect.

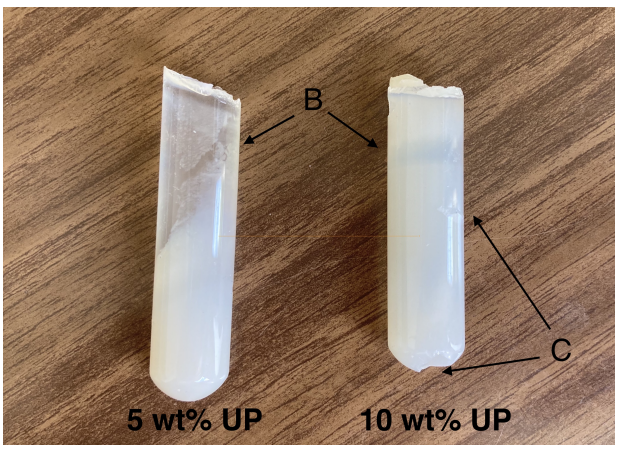

Figure 3.25: Resins curing with cycle 2 and with 5 wt% and 10 wt% of UP. B = phase change, C = cavities/bubbles.

Another curing cycle was established to avoid the gel effect. It is represented in Figure 3.26. The temperature of curing was increased to limit the time of reaction and avoid formation of voids. After gelation, the samples were inserted in the hot oven at 100℃. It stayed for 2 hours, after which the temperature was increased to 180℃.

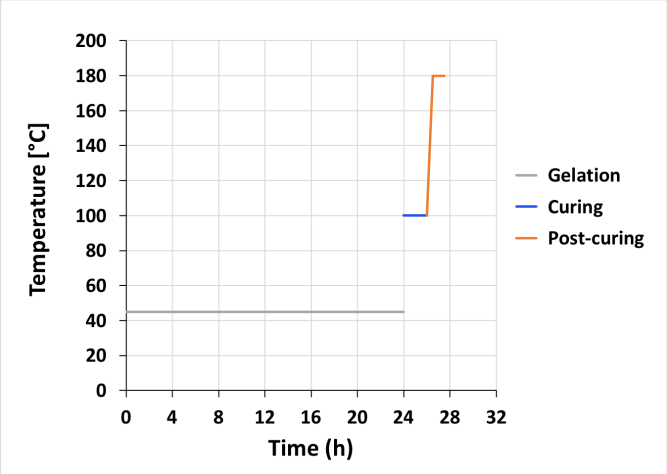

Figure 3.26: Curing cycle 3.

Resins with 0, 5 and 10 wt% of UP were cured in glass tubes with curing cycle 3. They are represented in Figure 3.27.

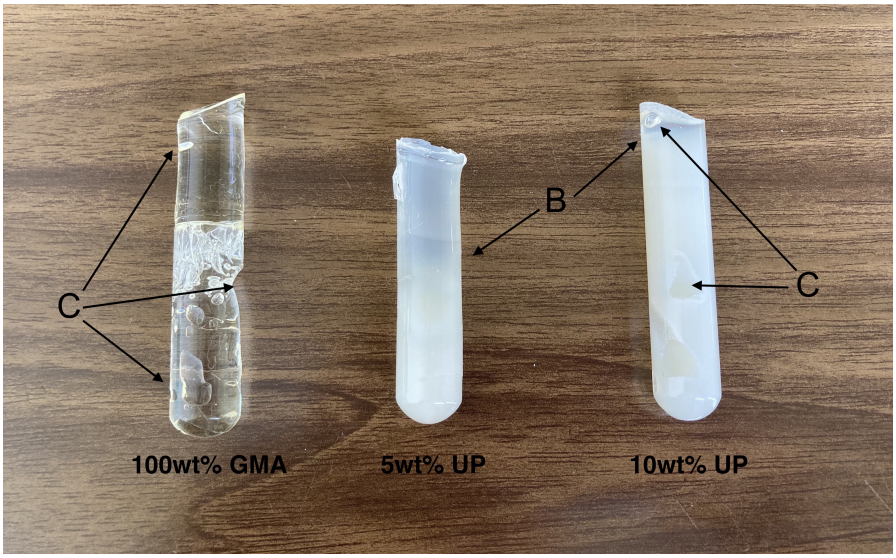

Figure 3.27: Resins curing with cycle 3 and with 0, 5 and 10 wt% of UP. B = phase change, C = cavities/voids.

All of the samples showed a change in colour and the apparition of voids (cavities, porosities or bubbles). The colour change could be a sign of a phase difference in the sample. It could be explained by the decantation of UP due to improper and/or insufficient mixing during samples preparation. The preparation and curing of the sample was further investigated to optimise the samples. The impact of the mixing during samples preparation was analysed by modifying the conditions (time and temperature). As the apparition of the voids does not have a single explanation and could also be explained by components volatilisation, curing in closed tubes was investigated.

3.5 Optimisation of the curing

3.5.1 Modification of the mixing during preparation of the samples to cure

To increase diffusivity of the UP in GMA, the mixing of the two components was done at temperature higher than the T_g of UP, i.e. 80℃, and for 90 minutes. With this process, resins with more than 10 wt% of UP were not possible to produce due to a too high viscosity during cooling. This means that the change in mixing conditions must have some influence on UP diffusion.

Figures 3.28 and 3.29 show the sample containing 1 wt% UP after mixing and degassing respectively. It can be observed that UP, or at least its crystalline part (given the "white appearing" flakes on Figure 3.28), still appears to be insoluble in GMA and decants with time.

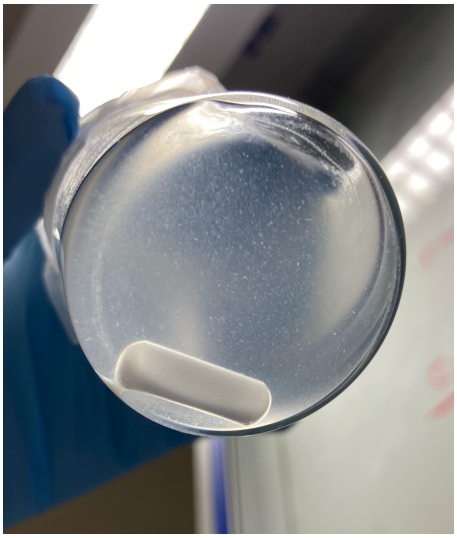

Figure 3.28: UP/GMA mixture containing 1wt% of UP and 1 wt% of BPO after mixing at 80℃ for 90 minutes.

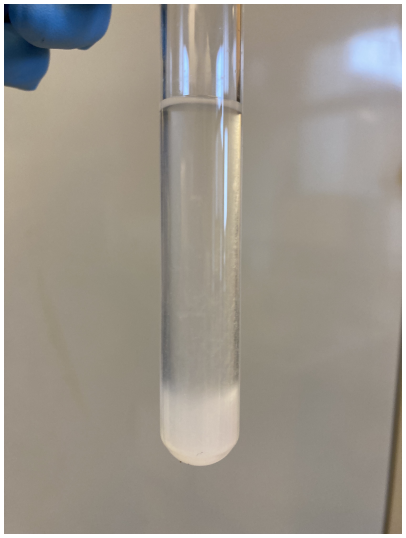

Figure 3.29: UP/GMA mixture containing 1wt% of UP and 1 wt% of BPO after degassing.

Curing of the samples was done in sealed tubes to avoid volatilisation of unreacted components. Figures 3.30a, 3.30b, 3.30c and 3.30d represent the different samples cured with this process.

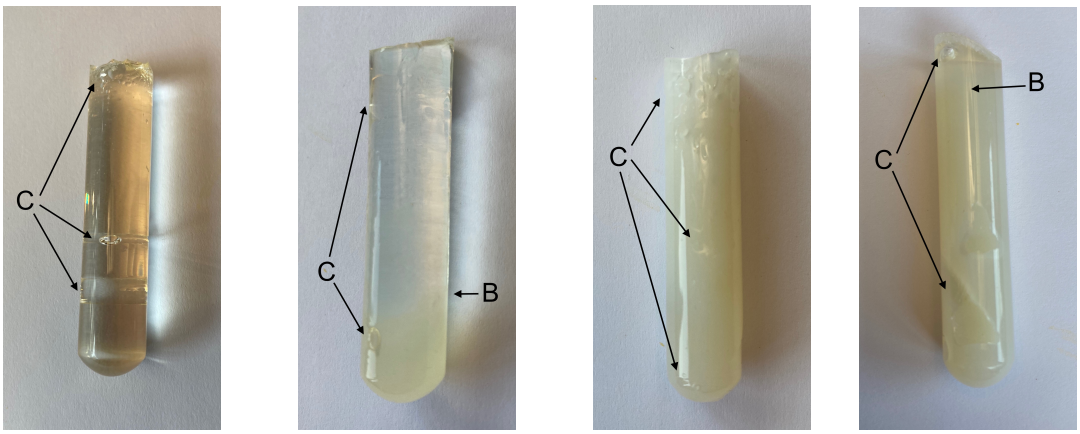

(a) **(b)** **(c)** **(d)**

Figure 3.30: UP/GMA resins containing (a) 100wt% GMA, (b) 1wt% UP, (c) 5wt% UP and (d) 10wt% UP. B = phase change, C= cavities/voids

Apparition of voids and colour change (and phase change?) are still observed. To determine if the UP in the samples reacts with the GMA matrix, Raman analysis were done on a section of a sample. All the spectra came back identical, so it was assumed that the sample were homogenised. Unfortunately, the Raman spectra could not be included in this thesis.

3.5.2 Use of an accelerator

Dimethylaniline is used as accelerator to activate peroxides by quick formation of radicals and to decrease gel time and curing temperature.

Resins with 1, 2 and 5 wt% of UP and 0.1% (w/w resin) of dimethylaniline were cured in the same previous thermal conditions (mixing at 80℃, gelation at 45℃, cure at 100℃ and post-cure at 180℃). Dimethylaniline was added after the mixing of BPO in the system. The gel time was drastically reduced with the accelerator. After 6 hours, the resin were turned into a gel and were ready for the cure and post-cure. This reduction of gel time could be limiting the precipitation of crystalline UP in gel condition. A yellowing of the resins is observed with the use of the accelerator. It could be explained by carbonyl formation during curing and ageing [102]. A new cycle, about 18 hours shorter than the previous one, was

then established and is represented in Figure 3.31. The reduction of curing time is a very important economical and ecological advantage as it can reduce costs and energy consumption.

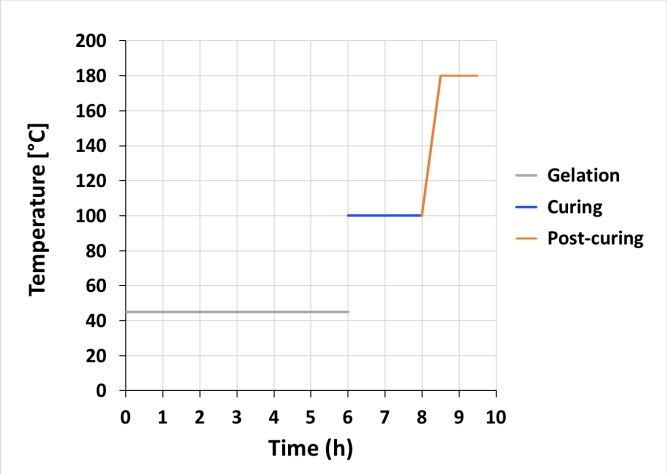

Figure 3.31: Curing cycle 4

The samples of resin cured are represented in Figure 3.32. There still seems to be a fraction of UP insoluble in GMA. One way to explain the lack of diffusion of UP into GMA is the crystallinity of such semi-crystalline UP. The amorphous part of UP could react with GMA but the crystalline part of UP would be entrapped in the network.

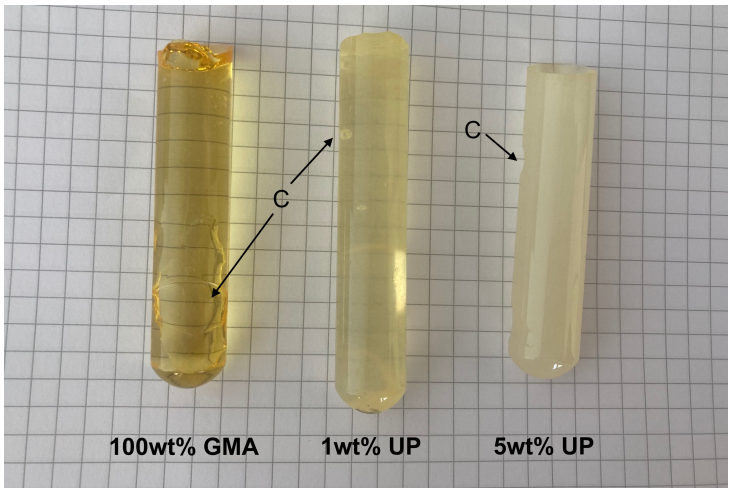

Figure 3.32: Resins 1-2-5% UP with 0,1% dimethlaniline

To determine the impact of the crystalline function on the polymerisation, the

same resin preparation was done with an amorphous unsaturated polyester (UP).

3.5.3 Utilisation of amorphous UP

The amorphous UP is the UP synthetised from recycled PET with 2-methyl-1,3-propanediol. Resins were cured with amorphous UP in the same conditions as the optimal curing cycle determined before. First, UP was mixed with GMA at 80℃ for 90 minutes. BPO was then added and mixed at room temperature for 5 minutes. Dimethylaniline was added and mixed for about a minute before degassing the mixture and pouring it into a mould. Resins with 5 and 10 wt% of UP were cured in these conditions. They are represented in Figures 3.33 and 3.34.

Figure 3.33: Resin with 5% UP amorphous - 0.1% dimethylaniline

Figure 3.34: Resin with 10% UP amorphous - 0.1% dimethylaniline

Compared to the resins cured in the previous experiments, these resins have a different colour. It can be explained by the amorphous characteristic of the UP that gives them more of a yellowish colour. The samples did not present any void and appearance of dephasing. Curing into perpendicular steel moulds changed the heat diffusion and showed to be more effective.

Thermal analysis

Samples of the different cured resins were analysed with DSC to determine the residual enthalpy and the glass transition temperature. Results are represented in Figure 3.35 and summarised in Table 3.8 and Figure 3.35.

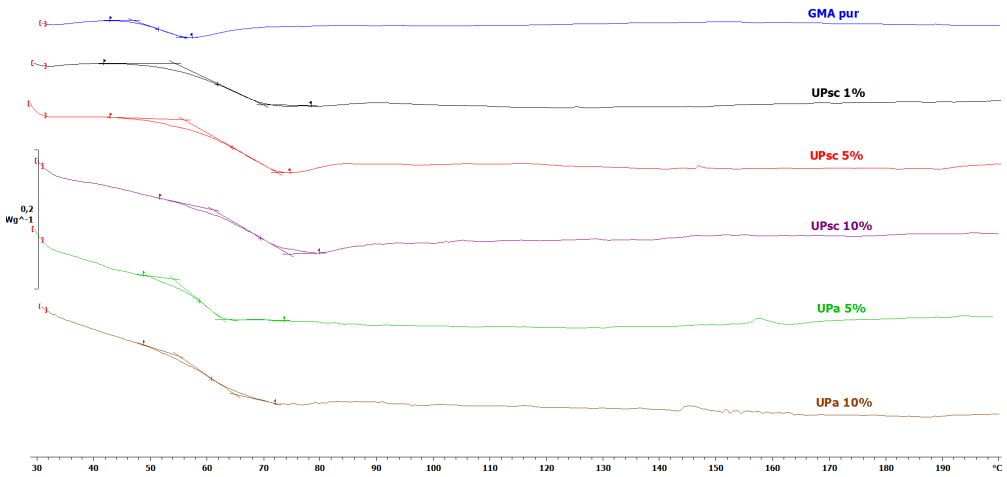

Figure 3.35: Normalised DSC curves of the second heating of different sample of UP/GMA resins.

Sample type	T_g[°C]
Pure GMA	51.37
UPsc 1 wt%	61.86
UPsc 5 wt%	64.46
UPsc 10 wt%	69.54
UPam 5 wt%	58.65
UPam 10 wt%	60.73

Table 3.8: Results from the DSC curve in Figure 3.35.

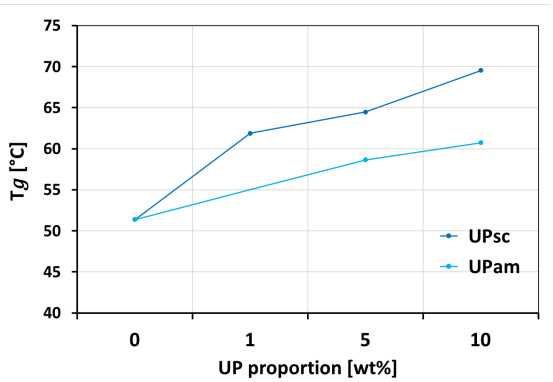

Figure 3.36: Evolution of the resins T_g with UP mass proportion

The curing reaction of all the different resins is complete as no enthalpic peak appears in Figure 3.35. The resins seem to be homogeneous and contain only one phase as only one T_g appears for all of the samples. Transition temperature increases with the mass proportion of UP and is lower for amorphous UP. Since T_g of GMA and T_g of the resins are close, a second T_g could also not appear. To certify the presence of only one phase, microscopic analysis were conducted. Samples containing UPsc and UPam were observed with a microscope and SEM. None of these analysis were conclusive as no unreacted UP could be observed in the matrix and no difference could be observed between resins containing semi-crystalline or amorphous UP (see Appendix Figures 4.11, 4.12 and 4.13).

3.6 Evaluation of mechanical properties of the resins

Dynamic mechanical analysis (DMA) was performed to evaluate the impact of UP content (in wt%) on the mechanical properties of UP/GMA resins. To evaluate this impact, DMA was performed on a resin with 100 wt% of GMA and used as reference. Resins with 5 and 10 wt% of semi-crystalline and amorphous UP were compared with the reference.

Storage and loss modulus

Figures 3.37a and 3.37b represent respectively the storage modulus E' and loss modulus E" as functions of the temperature and the samples composition.

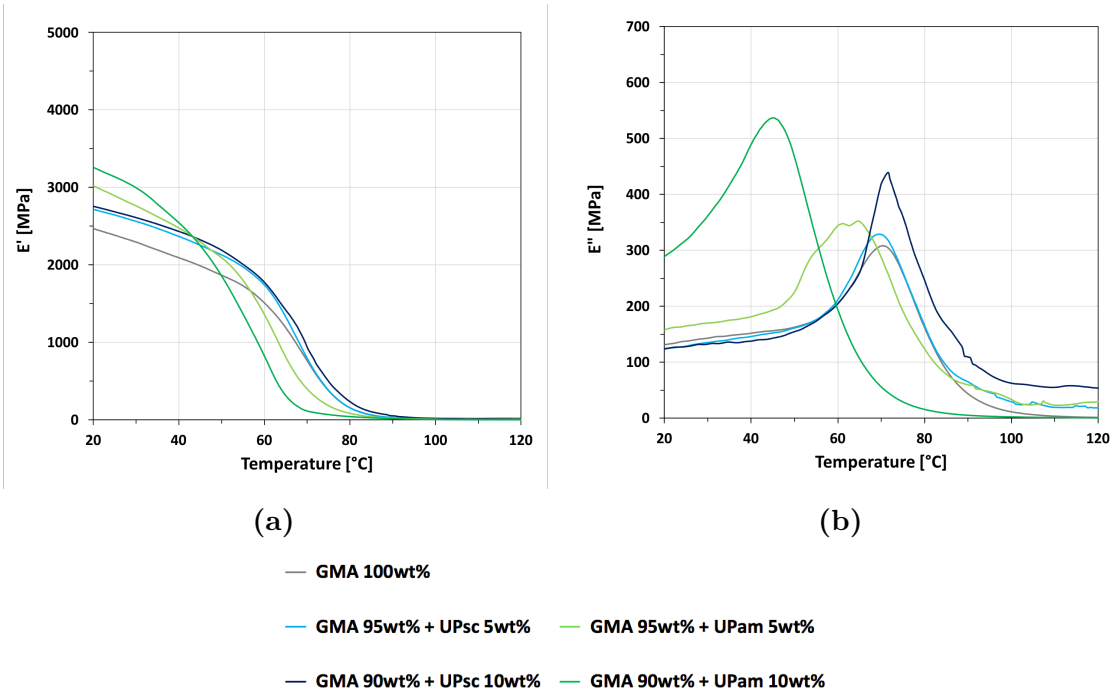

Figure 3.37: (a) Storage and (b) loss modulus for different resins of UP and GMA.

The complex modulus E*at 30°C for each sample was calculated with equation (2.3). The results are summarised in Table 3.9 and Figure 3.9.

Sample	E'(30°C) [MPa]
GMA 100wt%	2511.44
UPsc 5%	2665.58
UPsc 10%	2684.85
UPam 5%	2763.48
UPam 10%	2990.09

Table 3.9: Modulus at 30°C of each sample.

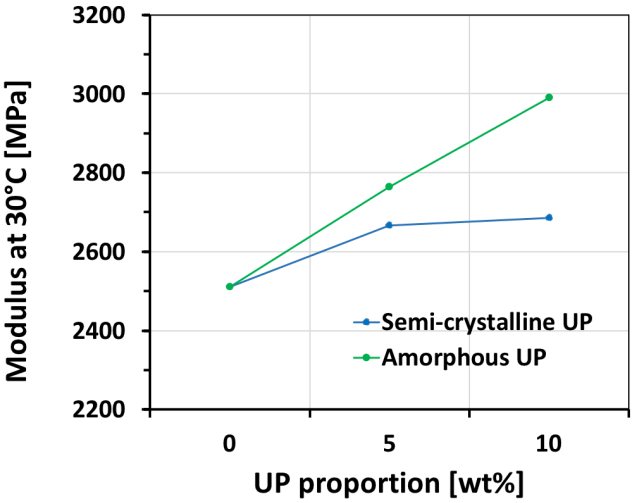

Figure 3.38: Complex modulus E* of the different resins at 30°C.

The complex modulus at 30°C shows an increase with the presence of UP in the system, for both semi-crystalline and amorphous UP. With the presence of 5 and 10 wt% of semi-crystalline UP, the E* of the resin increases with 6.13 and 6.9%. With the presence of 5 and 10 wt% of amorphous UP, the E* of the resin increases with 10.03 and 19.05%. Moreover, the behaviour of the blue curve in Figure 3.38 shows that increasing the weight content of semi-crystalline UP in the resin over 10% would not increase significantly E*. 10wt% of UP seem to be close to the maximum of the curve. The green curve has a different behaviour. E* for 10 wt% of amorphous UP is not the maximum of the curve. A much further increase of the complex modulus for higher content of amorphous UP can be expected.

Chapter 4

Conclusion and perspectives

In this work, a resin made of glycidyl methacrylate and unsaturated polyester synthesised from recycled PET was efficiently polymerised. Thermal, spectroscopic and mechanical analysis were performed in order to characterise the different components, understand the polymerisation mechanism, establish a suitable curing system and optimise the properties of the resin.

First, PET was chemically modified into unsaturated polyester. The first step was PET modification through extrusion and grinding to mimic the properties of POST-C PET. DSC analysis showed similar thermal behaviour between modified PET and POST-C, and concluded that modified PET could be considered and used as POST-C PET. The second step was the depolymerisation and repolymerisation of modified PET into unsaturated polyester (UP). Glycolysis depolymerised PET into oligomers (GPET) using 1,3-propanediol (PD) or 2-methyl-1,3-propanediol (MPD) as diols. GPET was repolymerised into UP using citraconic anhydride and diols. UP synthesised with PD and MPD were denoted as semi-crystalline (UPsc) and amorphous UP (UPam) respectively. UPsc showed a decrease of almost 40% in crystallinity, while UPam was proved to be completely amorphous. This difference proves the influence of the diol chemical structure in the kinetic of UP crystallisation. Both UPsc and UPam showed a decrease of about 30% in glass transition temperature compared to PET. This drop in T_g will favour further polymerisation. Spectroscopic analysis showed similar spectra for UPsc and UPam with characteristic peaks of C=C bonds and hydroxyl and carboxyl groups. These three functions are also important for further polymerisation as they are the ones intended to react with GMA.

Second, the polymerisation and thermal degradation mechanism of GMA were analysed with spectroscopic and thermal methods. It showed homopolymerisation of GMA folowwing Raman analysis showed the disappearance of the unsaturated

bond after polymerisation. This is a characteristic of GMA homopolymerisation. DSC analysis identified four steps in the polymerisation and a behavior characteristic of the Trommsdorf effect. TGA analysis identified different steps in the degradation mechanism and a residual mass loss of about 30 wt%.

The third step of the analysis was the identification and comprehension of the polymerisation mechanism of the UP/GMA resin. The influence of the benzoyl peroxide content and of the heating rate on the kinetic of polymerisation were first analysed. 1 wt% of BPO and 10Kmin^{-1} were determined to be the suitable concentration and heating rate to favour quicker reaction at lower temperature. Spectroscopic analysis were used to determine the mechanism of polymerisation. The reaction starts with the radical polymerisation on the ethylenic function of GMA between 95 and 150℃. Ring-opening polymerisation occurs between 120 and 190 ℃ via reaction with the hydroxyl end groups of UP and forms ester functions. The reaction of the ethylenic function of UP was difficult to identify as it is close to the peak corresponding to the ethylenic function of GMA. The reaction between both ethylenic function is possible.

The fourth part consisted in establishing a curing cycle via a trial-error approach. The final cycle consists in three steps. The resin is heated at 45℃ for 24 hours to form a gel and is cured at 100℃ to increase the degree of crosslinking and form a 3D network. The temperature is then increased to 180℃ for the post-cure. This cycle seemed to limit the apparition of cavities/voids and phase change encountered in the first cured resins.

The final part of this study was the optimisation of the resin properties and of its curing. To solve the lack of diffusivity of UP in GMA observed during curing, the mixing conditions were optimised. The diffusivity was increased by mixing at higher temperature (80℃) and for a longer time (90 minutes) the system before gelation. To reduce the long gel time of the resin, dimethylaniline was used as accelerator. It reduced gel time down to 6 hours. As some of the semi-crystalline UP still seemed to not diffuse and react with GMA, a resin with amorphous UP was produced in the same conditions. No voids and no phase change were encountered. Thermal and mechanical analysis were performed to determine the influence of the amorphous UP on the system. Modifying GMA with UP increases T_g: up to 35% with 10 wt% of UPsc and 17% with 10 wt% UPam). The complex modulus is also increased: up to 10% using UPsc and 19% using UPam.

These results show the potential of using unsaturated polyesters as modifier in a glycidyl methacrylate resin. The polymerisation mechanism is optimised

by facilitating the opening of the oxirane rings with the UP end of chains. The addition of UPs increases the complex modulus of the resins, improving the viscous properties of the resins. This effect is even favoured using amorphous polyester. The UP/GMA resins have an economical and ecological interest as they use potentially bio-sourced material and valorise PET waste.

To go further in the comprehension and optimisation of this subject, other aspects could be interesting to study:

- It could be interesting to analyse the surface of the resins with selective etching. By choosing a solvent suitable for UP and not GMA, etching could determine the presence of unreacted UP in the resin.
- The polymerisation mechanism was not analysed with the system containing dimethylaniline. As epoxy functions react with amines, the polymerisation mechanism could be modified. The same spectroscopic analysis could be done to observe possible changes.
- Compression tests could be done on the samples to further analyse the mechanical properties of the resin and the influence of UP content.
- The proportion of semi-crystalline UP in the system could not exceed 10 wt%. This was not observed with amorphous UP. Even the mechanical results showed that the complex modulus could be further increased with higher concentration of UPam. Increasing the proportion of UPam in the resin and study the thermal and mechanical properties could be interesting.

Bibliography

[1] IPCC. *Climate Change 2007: Synthesis Report. Contribution of Working Groups I, II and III to the Fourth Assessment Report of the Intergovernmental Panel on Climate Change*. Tech. rep. Geneva: IPCC, 2007. URL: https://www.ipcc.ch/site/assets/uploads/2018/02/ar4_syr.pdf.

[2] Silpa Kaza et al. *What a Waste 2.0 : A Global Snapshot of Solid Waste Management to 2050*. Tech. rep. 2018. URL: http://hdl.handle.net/10986/30317.

[3] PlascticsEurope. *Plastics-the Facts 2021 An analysis of European plastics production, demand and waste data*. Tech. rep. 2021.

[4] Anvita Sheel and Deepak Pant. "Chemical Depolymerization of PET Bottles via Glycolysis". In: *Recycling of Polyethylene Terephthalate Bottles*. Elsevier, 2019, pp. 61–84. DOI: 10.1016/b978-0-12-811361-5.00004-3.

[5] Alexander W. Bassett et al. "Dual-functional, aromatic, epoxy-methacrylate monomers from bio-based feedstocks and their respective epoxy-functional thermoplastics". In: *Journal of Polymer Science* 58.5 (Mar. 2020), pp. 673–682. ISSN: 2642-4150. DOI: 10.1002/pol.20190110.

[6] Pedro Francisco Cañamero et al. "Atom Transfer Radical Polymerization of Glycidyl Methacrylate: A Functional Monomer". In: *Macromolecular Chemistry and Physics* 205.16 (Nov. 2004), pp. 2221–2228. ISSN: 10221352. DOI: 10.1002/macp.200400186.

[7] Junfeng Zhang et al. "Surface Graft Polymerization of Glycidyl Methacrylate onto Polyethylene and the Adhesion with Epoxy Resin". In: *Journal of Polymer Science: Part A: Polymer Chemistry* 33 (1995), pp. 2329–2638.

[8] Greg T. Hermanson. "Functional Targets for Bioconjugation". In: *Bioconjugate Techniques*. Elsevier, 2013, pp. 127–228. DOI: 10.1016/B978-0-12-382239-0.00002-9.

[9] Robert Wojcieszak et al. "Recent developments in maleic acid synthesis from bio-based chemicals". In: *Sustainable Chemical Processes* 3.1 (Dec. 2015), p. 9. ISSN: 2043-7129. DOI: 10.1186/s40508-015-0034-5.

[10] Mengmeng Ruan et al. “Bio-polyols synthesized from bio-based 1,3-propanediol and applications on polyurethane reactive hot melt adhesives”. In: *Industrial Crops and Products* 128 (Feb. 2019), pp. 436–444. ISSN: 09266690. DOI: 10.1016/j.indcrop.2018.11.045.

[11] A. D. Jenkins et al. “Glossary of basic terms in polymer science (IUPAC Recommendations 1996)”. In: *Pure and Applied Chemistry* 68.12 (Jan. 1996), pp. 2287–2311. ISSN: 1365-3075. DOI: 10.1351/pac199668122287.

[12] Manas Chanda. *Introduction to Polymer Science and Chemistry*. CRC Press, Mar. 2006. ISBN: 9780429128721. DOI: 10.1201/9781420007329.

[13] Sophie Demoustier. *Polymer Science and Engineering*. Louvain-la-Neuve, 2019.

[14] George Odian. *PRINCIPLES OF POLYMERIZATION Fourth Edition*. Tech. rep. 2004.

[15] Malcolm P Stevens. *Polymer Chemistry An introduction*. Third edition. New York: Oxford University Press, 1999.

[16] Naresh D. Patel and Mark W. Brown. *Method and apparatus for preventing yellowing of benzoyl peroxide solutions en acrylc adhesives*. 1991.

[17] R. G. Weatherhead. “CATALYSTS, ACCELERATORS AND INHIBITORS FOR UNSATURATED POLYESTER RESINS”. In: *FRP Technology*. Dordrecht: Springer, 1980, pp. 204–239.

[18] Joginder Lal et al. *Effect of Amine Accelerators on the Polymerization of Methyl Methacrylate with Benzoyl Peroxide*. Tech. rep. 1955, pp. 403–409.

[19] Kemal Serbetci and Nesrin Hasirci. “Recent Developments in Bone Cements”. In: *Biomaterials in Orthopedics*. CRC Press, Oct. 2003, pp. 229–246. DOI: 10.1201/b14227-13.

[20] K.F. O’Driscoll and A.V. Tobolsky. “Kinetics of polymerization of methylmethacrylate initiated by the system benzoyl peroxide-dimethylaniline”. In: *Journal of Colloid Science* 11.3 (June 1956), pp. 244–249. ISSN: 00958522. DOI: 10.1016/0095-8522(56)90048-4.

[21] Derakane. *Fabrication guide - A guide to frabricating FRP composites*. Tech. rep. 2019.

[22] Dimitris S. Achilias and Irini Sideridou. “Study of the effect of two BPO/amine initiation systems on the free-radical polymerization of MMA used in dental resins and bone cements”. In: *Journal of Macromolecular Science - Pure and Applied Chemistry* 39.12 (Dec. 2002), pp. 1435–1450. ISSN: 10601325. DOI: 10.1081/MA-120016045.

[23] Qizhi Yang et al. “Synergetic effect of the epoxide functional groups in the photocatalyzed atom transfer radical copolymerization of glycidyl methacrylate”. In: *Polymer Chemistry* 7.39 (2016), pp. 6084–6093. ISSN: 1759-9954. DOI: 10.1039/C6PY01443G.

[24] Roberto Nisticò. *Polyethylene terephthalate (PET) in the packaging industry*. Oct. 2020. DOI: 10.1016/j.polymertesting.2020.106707.

[25] Granta Design Limited. *CES Granta EduPack Software*. Cambridge, UK, 2009.

[26] Leian Bartolome et al. “Recent Developments in the Chemical Recycling of PET”. In: *Material Recycling - Trends and Perspectives*. InTech, Mar. 2012. DOI: 10.5772/33800.

[27] Firas Awaja and Dumitru Pavel. *Recycling of PET*. July 2005. DOI: 10.1016/j.eurpolymj.2005.02.005.

[28] A. M. Al-Sabagh et al. *Greener routes for recycling of polyethylene terephthalate*. Mar. 2016. DOI: 10.1016/j.ejpe.2015.03.001.

[29] John M Krochta. “Food Packaging”. In: *Handbook of Food Engineering*. 2007.

[30] Jinkyung Kim et al. *Synthesis and applications of unsaturated polyester resins based on PET waste*. Tech. rep. 6. 2007, pp. 1076–1083.

[31] Ali Yaraş et al. *Crystallization Behavior of PET Materials*. Tech. rep. 1. 2011, pp. 26–35. URL: https://www.researchgate.net/publication/290429725.

[32] Vandana Jamdar, Mukesh Kathalewar, and Anagha Sabnis. “Glycolytic depolymerization of PET waste using MP-diol and utilization of recycled product for UV-curable wood coating”. In: *Journal of Coatings Technology and Research* 15.2 (Mar. 2018), pp. 259–270. ISSN: 15470091. DOI: 10.1007/s11998-017-9992-8.

[33] James Sherwood. “Closed-Loop Recycling of Polymers Using Solvents : Remaking plastics for a circular economy”. In: *Johnson Matthey Technology Review* 64.1 (Jan. 2020), pp. 4–15. ISSN: 2056-5135. DOI: 10.1595/205651319X15574756736831.

[34] Bruno A. Pulido et al. “Recycled Poly(ethylene terephthalate) for High Temperature Solvent Resistant Membranes”. In: *ACS Applied Polymer Materials* 1.9 (Sept. 2019), pp. 2379–2387. ISSN: 2637-6105. DOI: 10.1021/acsapm.9b00493.

[35] Palova Santos and Sérgio Henrique Pezzin. "Mechanical properties of polypropylene reinforced with recycled-pet fibres". In: *Journal of Materials Processing Technology* 143-144 (Dec. 2003), pp. 517–520. ISSN: 09240136. DOI: 10.1016/S0924-0136(03)00391-1.

[36] Vogt Bryan D. Vogt, Kumar Sanat K., and Stokes Kristoffer K. "Why is recycling of post consumer plastics so challenging?" In: *ACS Applied Polymer Materials* 3 (2021), pp. 4325–4346.

[37] Cancer Association of South Africa (CASA). *Plastic Identification Codes*. Tech. rep. 2012.

[38] ACT Government. *Plastic Identification Codes*. Tech. rep. 2019. URL: http://www3.weforum.org/docs/WEF_The_New_Plastics_Economy.pdf.

[39] Adrian Merrington. "Recycling of Plastics". In: *Applied Plastics Engineering Handbook: Processing, Materials, and Applications: Second Edition*. Elsevier Inc., 2017, pp. 167–189. ISBN: 9780323390408. DOI: 10.1016/B978-0-323-39040-8.00009-2.

[40] Kim Ragaert, Laurens Delva, and Kevin Van Geem. *Mechanical and chemical recycling of solid plastic waste*. Nov. 2017. DOI: 10.1016/j.wasman.2017.07.044.

[41] Emine Sert, Esra Yılmaz, and Ferhan Sami Atalay. "Chemical Recycling of Polyethlylene Terephthalate by Glycolysis Using Deep Eutectic Solvents". In: *Journal of Polymers and the Environment* 27.12 (Dec. 2019), pp. 2956–2962. ISSN: 15728919. DOI: 10.1007/s10924-019-01578-w.

[42] Nicholas A. Rorrer et al. "Combining Reclaimed PET with Bio-based Monomers Enables Plastics Upcycling". In: *Joule* 3.4 (Apr. 2019), pp. 1006–1027. ISSN: 25424351. DOI: 10.1016/j.joule.2019.01.018.

[43] I. Duque-Ingunza et al. "Synthesis of unsaturated polyester resin from glycolysed postconsumer PET wastes". In: *Journal of Material Cycles and Waste Management* 15.3 (Sept. 2013), pp. 256–263. ISSN: 1438-4957. DOI: 10.1007/s10163-013-0117-x.

[44] Yeliz Öztürk and Gamze Güçlü. "Unsaturated Polyester Resins Obtained from Glycolysis Products of Waste PET". In: *Polymer-Plastics Technology and Engineering* 43.5 (Jan. 2005), pp. 1539–1552. ISSN: 0360-2559. DOI: 10.1081/PPT-200030272.

[45] F.A.M.M. Gonçalves et al. "The potential of unsaturated polyesters in biomedicine and tissue engineering: Synthesis, structure-properties relationships and additive manufacturing". In: *Progress in Polymer Science* 68 (May 2017), pp. 1–34. ISSN: 00796700. DOI: 10.1016/j.progpolymsci.2016.12.008.

[46] Mangeng Lu and Sangwook Kim. "Unsaturated Polyester Resins Based on Recycled PET: Preparation and Curing Behavior". In: (2001). ISSN: 1052-1057.

[47] de Halleux. "Analyse des propriétés physico-chimiques de résines époxy biosourcées". PhD thesis. 2019. URL: http://hdl.handle.net/2078.1/thesis:19534.

[48] Michael Dornbusch, Ulrich Christ, and Rob Rasing. *Epoxy Resins Fundamentals and Applications*. Hanover, Germany, 2016. ISBN: 3866306407.

[49] Kenn Hood. "Epoxy resins". In: *Comprehensive Polymer Science and Supplements*. Vol. 5. Uxbridge, UK, 1989. Chap. 37, pp. 667–699.

[50] Bryan Ellis. *Chemistry and Technology of Epoxy Resins*. Springer Netherlands, 1993. DOI: 10.1007/978-94-011-2932-9.

[51] Johannes Karl Fink. "Epoxy Resins". In: *Reactive Polymers: Fundamentals and Applications*. Elsevier, 2018, pp. 139–223. DOI: 10.1016/B978-0-12-814509-8.00003-8. URL: https://linkinghub.elsevier.com/retrieve/pii/B9780128145098000038.

[52] National Center for Biotechnology Information. *PubChem Compound Summary for CID 7837, Glycidyl methacrylate*. Tech. rep. 2022. URL: https://pubchem.ncbi.nlm.nih.gov/compound/Glycidyl-methacrylate.

[53] Yakang LIU Yuzheng XIA, Guantai Jin, and Luo Yang Henguang. "THE PRODUCTION OF GLYCIDYL METHACRYLATE". In: *RadTech Asia'95*. Beijing, 1995.

[54] S Al-Malaika and W Kong. *Reactive Processing of Polymers: Melt Grafting of Glycidyl Methacrylate on Ethylene Propylene Copolymer in the Presence of a Coagent*. Tech. rep. 2000.

[55] Omid Moini Jazani et al. "An investigation on the role of GMA grafting degree on the efficiency of PET/PP-g-GMA reactive blending: morphology and mechanical properties". In: *Polymer Bulletin* 74.11 (Nov. 2017), pp. 4483–4497. ISSN: 0170-0839. DOI: 10.1007/s00289-017-1962-x.

[56] Hideo Hosokawa, Misao Shikatsu, and Takahiro Fujimoto. *Method for producing glycidyl methacrylate*. 1994.

[57] F. Mustata, N. Tudorachi, and I. Bicu. "Thermosetting resins obtained via sequential photo and thermal crosslinking of epoxy resins. Curing kinetics, thermal properties and morphology". In: *Composites Part B: Engineering* 55 (Dec. 2013), pp. 470–478. ISSN: 13598368. DOI: 10.1016/j.compositesb.2013.07.023.

[58] Manon Le Gars et al. “Polymerization of glycidyl methacrylate from the surface of cellulose nanocrystals for the elaboration of PLA-based nanocomposites”. In: *Carbohydrate Polymers* 234 (Apr. 2020), p. 115899. ISSN: 01448617. DOI: 10.1016/j.carbpol.2020.115899.

[59] M. H. Kunita et al. “Grafting of glycidyl methacrylate onto polypropylene using supercritical carbon dioxide”. In: *European Polymer Journal* 41.9 (Sept. 2005), pp. 2176–2182. ISSN: 00143057. DOI: 10.1016/j.eurpolymj.2005.04.004.

[60] Amélie Labbé et al. “Selective Ring-Opening Polymerization of Glycidyl Methacrylate: Toward the Synthesis of Cross-Linked (Co)polyethers with Thermoresponsive Properties”. In: *Macromolecules* 44.16 (Aug. 2011), pp. 6356–6364. ISSN: 0024-9297. DOI: 10.1021/ma201075n.

[61] M. Teresa Muñoz et al. “Aluminum Aryloxide Compounds as Very Active Catalysts for Glycidyl Methacrylate Selective Ring-Opening Polymerization”. In: *ChemCatChem* 10.5 (Mar. 2018), pp. 936–939. ISSN: 18673880. DOI: 10.1002/cctc.201701377.

[62] Adriano V. Reis et al. “Reaction of Glycidyl Methacrylate at the Hydroxyl and Carboxylic Groups of Poly(vinyl alcohol) and Poly(acrylic acid): Is This Reaction Mechanism Still Unclear?” In: *The Journal of Organic Chemistry* 74.10 (May 2009), pp. 3750–3757. ISSN: 0022-3263. DOI: 10.1021/jo900033c.

[63] Mehwish Tahir et al. “Radiation induced graft polymerization of glycidyl methacrylate onto sepiolite”. In: *Radiation Physics and Chemistry* 179 (Feb. 2021), p. 109259. ISSN: 0969806X. DOI: 10.1016/j.radphyschem.2020.109259.

[64] Daniel Nyström et al. “Superhydrophobic bio-fibre surfaces via tailored grafting architecture”. In: *Chem. Commun.* 34 (2006), pp. 3594–3596. ISSN: 1359-7345. DOI: 10.1039/B607411A.

[65] Biao Zhang et al. “Dual-stage thermosetting photopolymers for advanced manufacturing”. In: *Chemical Engineering Journal* 411 (May 2021), p. 128466. ISSN: 13858947. DOI: 10.1016/j.cej.2021.128466.

[66] Daike Wang, Luiz Carrera, and Marc J.M. Abadie. “Photopolymerization of glycidyl acrylate and glycidyl methacrylate investigated by differential photocalorimetry and FT-I.R.” In: *European Polymer Journal* 29.10 (Oct. 1993), pp. 1379–1386. ISSN: 00143057. DOI: 10.1016/0014-3057(93)90197-N.

[67] Sarah Gayot et al. *A computationally efficient thermomechanical model for the in-situ polymerization of a methyl methacrylate-based resin in a thick glass fiber laminate*. Tech. rep. URL: http://hdl.handle.net/2078.1/235896.

[68] Sarah F. Gayot et al. "Processing maps based on polymerization modelling of thick methacrylic laminates". In: *Materials & Design* 196 (Nov. 2020), p. 109170. ISSN: 02641275. DOI: 10.1016/j.matdes.2020.109170.

[69] MatWeb. *Dow LIGHTER™ C88 Polyethylene Terephthalate (PET) Resin*. 2022.

[70] Sophie Vanpee. "Study of biocomposites based on PLA and natural fibers: influence of fibers and fibers treatment". PhD thesis. Louvain-la-Neuve: Ecole Polytechnique de Louvain, 2020.

[71] Anshuman Shrivastava. "Plastics Processing". In: *Introduction to Plastics Engineering*. Elsevier, 2018, pp. 143–177. DOI: 10.1016/b978-0-323-39500-7.00005-8.

[72] FRITSCH GmbH. *Operating instructions (Variable Speed Rotor Pulverisette 14)*. Tech. rep. 2013. URL: www.fritsch.de.

[73] Mettler Toledo. *Thermal Analysis of Polymers: Selected Applications*. Tech. rep. 2016.

[74] Mukesh Kumar Singh and Annika Singh. "Thermal characterization of materials using differential scanning calorimeter". In: *Characterization of Polymers and Fibres*. Elsevier, 2022, pp. 201–222. DOI: 10.1016/B978-0-12-823986-5.00006-3.

[75] Qian-Kui Zhang et al. "Thermally Stable and Nonflammable Electrolytes for Lithium Metal Batteries: Progress and Perspectives". In: *Small Science* 1.10 (Oct. 2021), p. 2100058. ISSN: 2688-4046. DOI: 10.1002/smsc.202100058.

[76] Mettler Toledo. *Thermal Analysis Premium : Differential Scanning Calorimetry*. Schwerzenbach, May 2015.

[77] Mettler Toledo. *Determination of polymer crystallinity with DSC measurements*. Tech. rep. URL: https://www.mt.com/dam/Analytical/MatcharApps/uc134.pdf.

[78] Baptiste Lambert. *Environmentally friendly thermoplastic composite from natural banana fibers and recycled PET*. Tech. rep. Louvain-la-Neuve: UCLouvain, 2022. URL: http://hdl.handle.net/2078.1/thesis:35693.

[79] Cataldo De Blasio. "Thermogravimetric Analysis (TGA)". In: *Fundamentals of Biofuels Engineering and Technology. Green Energy and Technology*. 2019, pp. 91–102. DOI: 10.1007/978-3-030-11599-9{_}7.

[80] Mettler Toledo. *Thermal analysis : Thermogravimetry*. Schwerzenbach, Sept. 2006.

[81] Klaus Gerwert and Carsten Kötting. "Fourier Transform Infrared (<scp>FTIR</scp>) Spectroscopy". In: *eLS*. Wiley, Sept. 2010. DOI: 10.1002/9780470015902.a0003112.pub2. URL: https://onlinelibrary.wiley.com/doi/10.1002/9780470015902.a0003112.pub2.

[82] Deena Titus, E. James Jebaseelan Samuel, and Selvaraj Mohana Roopan. "Nanoparticle characterization techniques". In: *Green Synthesis, Characterization and Applications of Nanoparticles*. Elsevier, 2019, pp. 303–319. DOI: 10.1016/B978-0-08-102579-6.00012-5.

[83] Sergio Cortes. *Infrared Spectroscopy (IR) - Theory and Interpretation of IR spectra*. Dallas. URL: https://personal.utdallas.edu/~scortes/ochem/OChem_Lab1/recit_notes/ir_presentation.pdf.

[84] J. CAÑAVATE et al. "STUDY OF THE CURING PROCESS OF AN EPOXY RESIN BY FTIR SPECTROSCOPY". In: *Polymer-Plastics Technology and Engineering* 39.5 (Nov. 2000), pp. 937–943. ISSN: 0360-2559. DOI: 10.1081/PPT-100101414.

[85] Jerry R. Mohrig, Christina Noring Hammond, and Paul F. Schatz. *Techniques in Organic Chemistry*. New York, 2010. URL: http://orga.blog.unq.edu.ar/wp-content/uploads/sites/72/2016/08/Techniky-organickej-chemie.pdf.

[86] Amalina Ahmad et al. "A FLUORESCENCE PHOSPHATE SENSOR BASED ON POLY(GLYCIDYL METHACRYLATE) MICROSPHERES WITH ALUMINIUM-MORIN". In: *Malaysian Journal of Analytical Sciences* 20.4 (2016), pp. 704–712. ISSN: 13942506. DOI: 10.17576/mjas-2016-2004-02.

[87] Phil Beauchamp. *Lecture 2. IR spectroscopy*. 2016. URL: http://www.cpp.edu/~psbeauchamp/pdf_videos/lecture_2_IR.pdf.

[88] W. N. E. van Dijk-Wolthuis et al. "Synthesis, Characterization, and Polymerization of Glycidyl Methacrylate Derivatized Dextran". In: *Macromolecules* 28.18 (Aug. 1995), pp. 6317–6322. ISSN: 0024-9297. DOI: 10.1021/ma00122a044.

[89] António H. S. Delgado and Anne M. Young. "Methacrylate peak determination and selection recommendations using ATR-FTIR to investigate polymerisation of dental methacrylate mixtures". In: *PLOS ONE* 16.6 (June 2021), e0252999. ISSN: 1932-6203. DOI: 10.1371/journal.pone.0252999.

[90] Mettler Toledo. *Thermal Analysis : Dynamic Mechanical Analysis*. Schwerzenbach, Sept. 2006.

[91] V. Mouillet, F. Farcas, and E. Chailleux. “Physico-chemical techniques for analysing the ageing of polymer modified bitumen”. In: *Polymer Modified Bitumen*. Elsevier, 2011, pp. 366–395. DOI: 10.1533/9780857093721.2.366.

[92] Michael Kelly. *Simplified model for rubber friction to study the effect of diract and indirect DMA test results*. Tech. rep. 2021.

[93] “Complex modulus (complex dynamic modulus)”. In: *Encyclopedic Dictionary of Polymers*. New York, NY: Springer New York, 2007, pp. 215–215. DOI: 10.1007/978-0-387-30160-0{_}2690.

[94] Ayman M. Atta et al. “Epoxy resins from rosin acids: Synthesis and characterization”. In: *Polymers for Advanced Technologies* 15.9 (Sept. 2004), pp. 514–522. ISSN: 10427147. DOI: 10.1002/pat.507.

[95] Levente Kárpáti et al. “One-Pot Depolymerization and Polycondensation of PET Based Random Oligo- and Polyesters”. In: *Journal of Polymers and the Environment* 27.10 (Oct. 2019), pp. 2167–2181. ISSN: 1566-2543. DOI: 10.1007/s10924-019-01490-3.

[96] S. Zulfiqar et al. “Thermal degradation of poly(glycidyl methacrylate)”. In: *Polymer Degradation and Stability* 30.2 (Jan. 1990), pp. 195–203. ISSN: 01413910. DOI: 10.1016/0141-3910(90)90075-I.

[97] Yuuki Hagiwara et al. “Experimental variable effects on laser heating of inclusions during Raman spectroscopic analysis”. In: *Chemical Geology* 559 (Jan. 2021), p. 119928. ISSN: 00092541. DOI: 10.1016/j.chemgeo.2020.119928.

[98] Yvonne J. West. “Study of Sample Heating Effects Arising During Laser Raman ”. In: *International Journal of Vibrational Spectroscopy (IJVS)* 1.1 (1996).

[99] Francisco Fraga et al. “Curing kinetics of the epoxy system diglycidyl ether of bisphenol A/isophoronediamine by Fourier transform infrared spectroscopy”. In: *Polymers for Advanced Technologies* (2008), n/a–n/a. ISSN: 10427147. DOI: 10.1002/pat.1178.

[100] Tracy M. Jr Patrick. *Process for the preparation of saturated oxonitriles*. 1950.

[101] Yueqi Shen et al. “Thermal decomposition of solid benzoyl peroxide using Advanced Reactive System Screening Tool: Effect of concentration, confinement and selected acids and bases”. In: *Journal of Loss Prevention in the Process Industries* 60 (July 2019), pp. 28–34. ISSN: 09504230. DOI: 10.1016/j.jlp.2019.04.001.

[102] Andrey Krauklis and Andreas Echtermeyer. “Mechanism of Yellowing: Carbonyl Formation during Hygrothermal Aging in a Common Amine Epoxy”. In: *Polymers* 10.9 (Sept. 2018), p. 1017. ISSN: 2073-4360. DOI: 10.3390/polym10091017.

Appendix

A Experiments

A.1 Depolymerisation of PET

Figure 4.1: Slurring with methanol

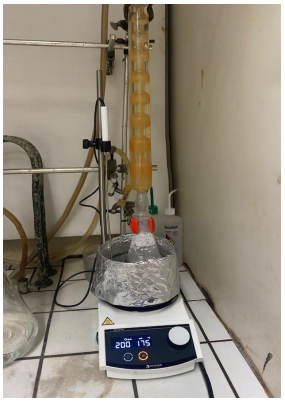

Figure 4.2: Glycolysis of PET and PD

Figure 4.3: Grinding of depolymerised PET

Figure 4.4: Solubilisation of BHET in hot water.

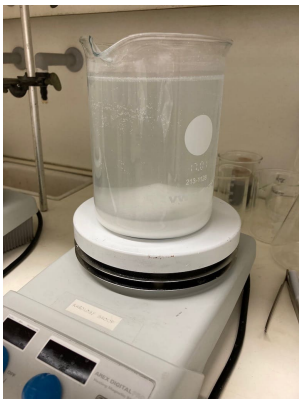

Figure 4.5: Decantation of GPET.

Figure 4.6: Filtration of BHET.

A.2 Repolymerization of GPET into UP

Figure 4.7: Polycondensation reaction with CA and PD.

Figure 4.8: Solubilisation in dichloromethane.

Figure 4.9: Precipitation in methanol.

A.3 Cured resins

A.3.1 Use of dichloromethane as solvant for curing

Figure 4.10: Curing of resin with 40% of UP, 60% of GMA and 0.2% of BPO as initiator

A.4 SEM images of GMA and UP/GMA resins with UPsc and UPam

A.4.1 GMA resin

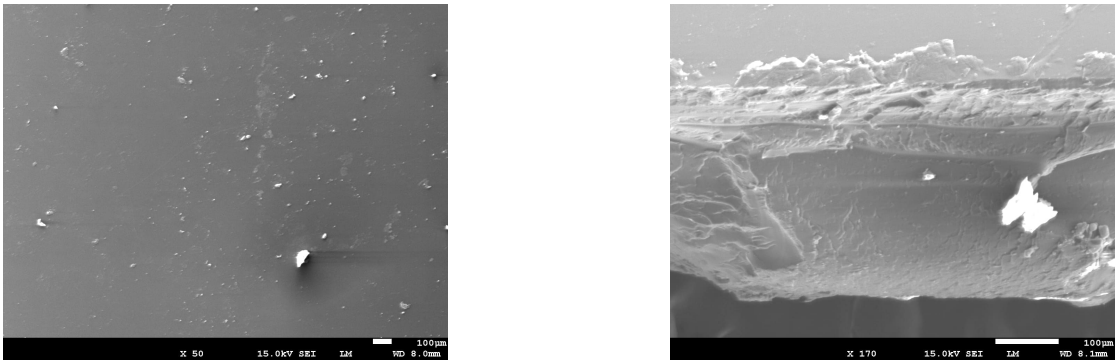

(a) **(b)**

Figure 4.11: Images obtained from SEM analysis on GMA samples. (a) sample surface (polished) (b) side of the sample (non-polished)

A.4.2 Resin with UPsc

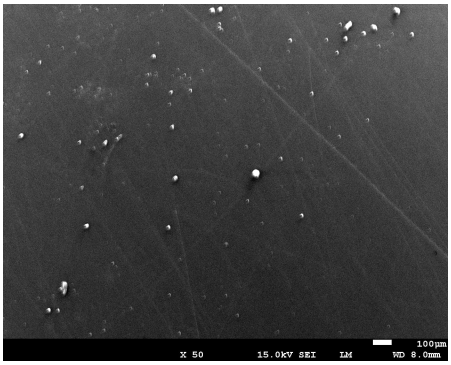

(a)

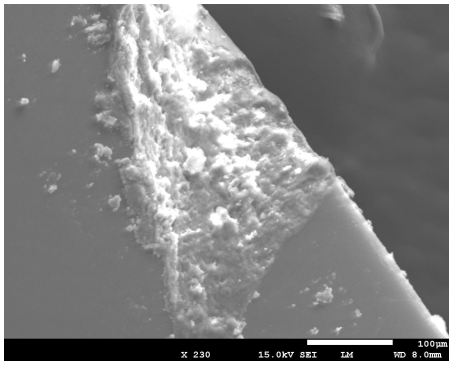

(b)

Figure 4.12: Images obtained from SEM analysis on UP/GMA samples. (a) 5 wt% UPsc (b) 10 wt% UPsc.

A.4.3 Resin with UPam

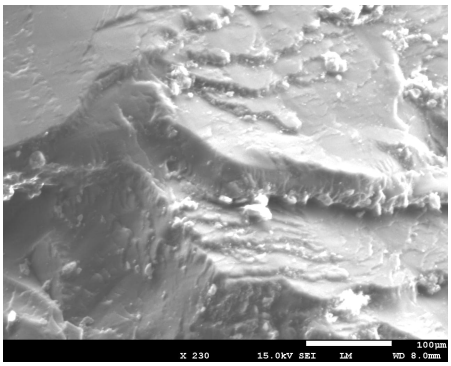

(a)

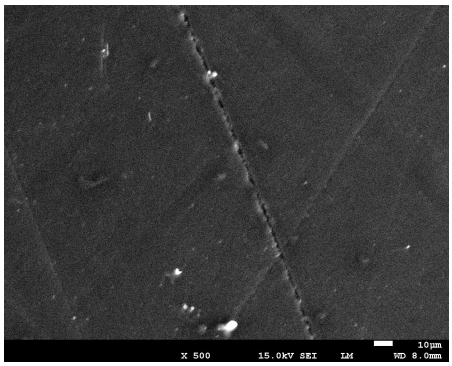

(b)

Figure 4.13: Images obtained from SEM analysis on resin samples with 5 wt% of UPam. (a) sample surface (polished) (b) side of the sample (non-polished)

UNIVERSITÉ CATHOLIQUE DE LOUVAIN
École polytechnique de Louvain
Rue Archimède, 1 bte L6.11.01, 1348 Louvain-la-Neuve, Belgique | **www.uclouvain.be/epl**